POLITECNICO DI TORINO

Master's Degree in Electrical Engineering

Politecnico
di Torino

Master's Degree Thesis

Management Of Renewable Energy Sources Under Grid Fault Conditions

Supervisors

Prof. Radu BOJOI

Fabio MANDRILE

Candidate

Antonino PELLEGRINO

March 2022

Summary

In this study are presented five current control techniques to enhance the reliability and stability of the Grid-connected inverter during unbalanced grid fault conditions. The analyzed control strategies simultaneously achieve multiple objectives during grid faults; eliminating both active–reactive power oscillations and the DC- link voltage oscillations. Reducing active power oscillations ensure an adjustable control for the DC-link voltage oscillations. In addition, for four current controls, an algorithm to limit the grid-side currents was entirely implemented, developed and validated by the author. All the techniques are based on the injection of positive and negative sequence of currents, which references are strictly correlated to power reference and voltages sequences during fault occurrence. For that reason, to implement an algorithm to extract the direct and inverse sequences of the grid voltages was fundamental. Once the voltage sequences have been extracted, the study continue with the implementation of the five currents control methods, whose have been validated through software simulations and experimental validations.

Acknowledgements

Vorrei ringraziare, in primis, Fabio Mandrile, che mi ha seguito nei sei mesi di sviluppo e stesura della tesi. Persona capace, affidabile, disponibile al dialogo, sia per questioni riguardanti la tesi ma soprattutto extracurricolari. Una vera e propria guida al perfezionamento professionale.

Ringrazio i miei genitori e mio fratello per essere la colonna a cui appoggiarsi nei momenti di stanchezza e stress psicologico. Una nave che mi ha permesso di superare quello che sembrava l'oceano di cinque anni al Politecnico, permettendomi di attraccare alla fine di questo percorso. Nave che è pronta a ripartire per accompagnarmi a ciò che il futuro mi riserva...

Alla mia ragazza, che in questi due anni e mezzo mi ha dato forza, leggerezza e coraggio... "*ad maiora*".

Ai miei colleghi, nonché amici, Nick, Simo, Matti, Matte, Giova, Gabri, Rick, Franci, che hanno reso lo studio un divertimento e il divertimento follia.

Un grosso bacio ai miei nonni che, insieme a miei genitori, hanno definito la persona che sono oggi.

"Se fai solo quello che sai fare non sarai mai più di quello che sei ora."
Shifu, Kung Fu Panda 3

Table of Contents

List of Figures

Acronyms

PR

Proportional Resonant

IARC

Instantaneous Active Reactive Control

BPSC

Balanced Positive Sequence Control

AARC

Average Active Reactive Control

PNSC

Positive and Negative Sequence Control

FPNSC

Flexible Positive and Negative Sequence Control

IPT

Inverter Protection Triggering

Chapter 1

Introduction

During the recent last years the demand and presence of distributed energy sources, such as PV(Photovoltaic) and WT(Wind Turbine) has rapidly increased, as also reported in Fig.1.1. Together to demand of distributed energy sources, grid codes refers to LVRT (Low Voltage Ride Through), HVRT (High Voltage Ride Through) and injection of reactive current, have been defined, as also reported in Fig.1.2.

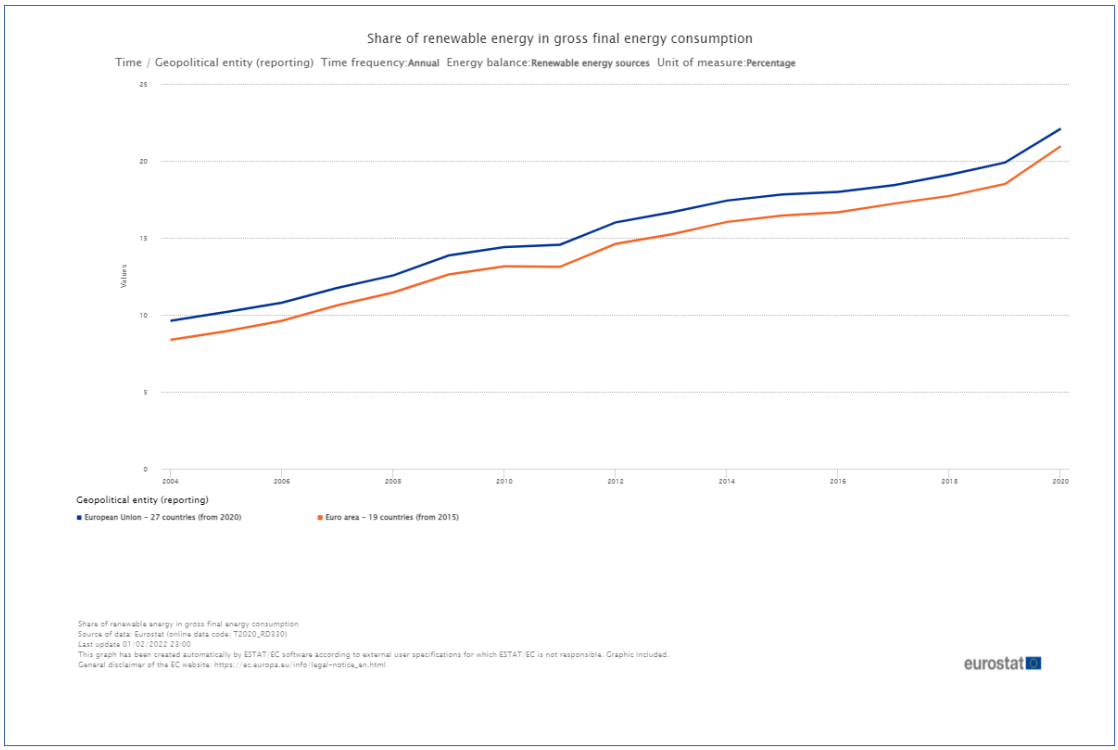

Figure 1.1: Annual renewable energy sources, percentage. Image extracted from Eurostat.

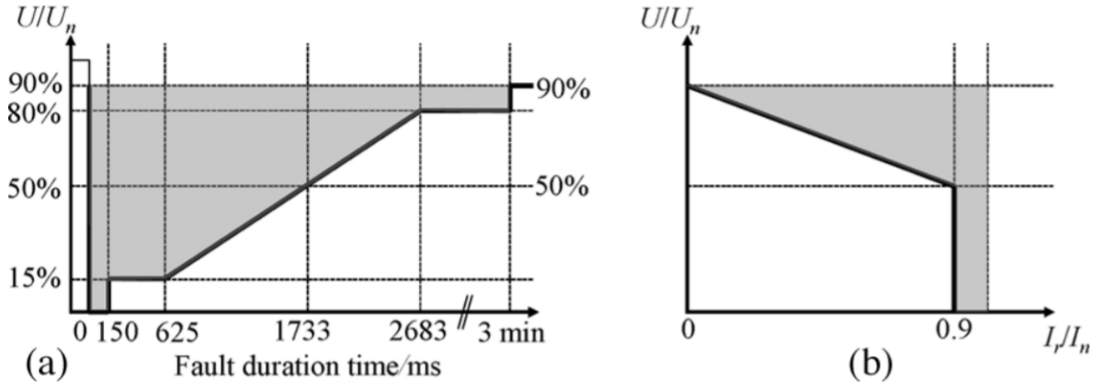

Figure 1.2: LVRT and reactive current to inject during the fault. Image extrapolated from[1].

For that reason, developing control techniques for interfacing AC/DC grid converters has become an important challenge to guarantee the reliability and continuity of service for grid interfaced distributed energy sources, even during fault conditions.

For that reason, in this thesis will be analyzed the control of an AC/DC grid interfaced converter during grid fault conditions. The types of faults that can occur are reported in Fig.1.3.

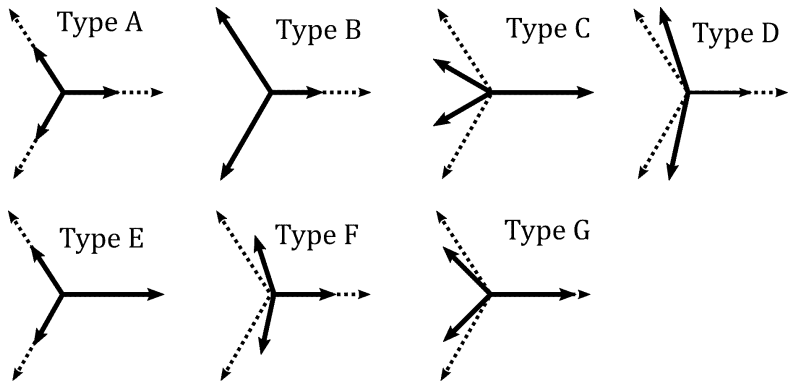

Figure 1.3: Types of voltage sags, image extrapolated from [2].

As it is possible to notice, there are seven type of sags: A,B,C,D,E,F,G. However, in this thesis, just one voltage sags will be experimentally tested, the E type. The reason for this choice is that this kind of faults are common, bringing into play either the positive and the negative sequence.

During faults, grid voltages and currents can be seen as the sum of three terms [3], according to Fortescue transform: the positive sequence, the negative sequence,

and the omopolar sequence (see Fig.1.4).

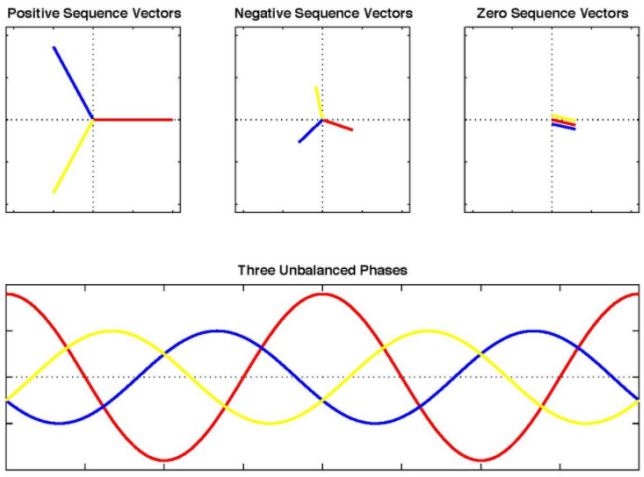

Figure 1.4: Phasors interpretation of positive, negative and omopolar sequence. Image extrapolated from Wikiwand.

Regardless, a three wire line will be analyzed, so the omopolar current component can be neglected.

1.1 Output Powers During Fault Conditions

The active and reactive power can be calculated respectively as the dot and cross product between voltages and currents, as reported in (1.1).

$$\mathbf{p} = \mathbf{v} \cdot \mathbf{i}; \quad \mathbf{q} = \mathbf{v} \times \mathbf{i}; \tag{1.1}$$

Modifying (1.1) through positive and negative sequence, we obtain:

$$\mathbf{p} = (\mathbf{v}^+ + \mathbf{v}^-) \cdot (\mathbf{i}^+ + \mathbf{i}^-); \quad \mathbf{q} = (\mathbf{v}^+ + \mathbf{v}^-) \times (\mathbf{i}^+ + \mathbf{i}^-) \tag{1.2}$$

$$\mathbf{p} = \mathbf{v}^+\mathbf{i}^+ + \mathbf{v}^-\mathbf{i}^- + \mathbf{v}^+\mathbf{i}^- + \mathbf{v}^-\mathbf{i}^+; \quad \mathbf{q} = \mathbf{v}^+ \times \mathbf{i}^+ + \mathbf{v}^- \times \mathbf{i}^- + \mathbf{v}^+ \times \mathbf{i}^- + \mathbf{v}^- \times \mathbf{i}^+ \tag{1.3}$$

According to [3], the product between the positive and negative sequence gives rise to an oscillation at the double of the fundamental frequency, as reported in (1.4) and (1.5) .

$$p = P_0 + P_{c2}cos(2\omega t) + P_{s2}sin(2\omega t) \tag{1.4}$$

$$q = Q_0 + Q_{c2}cos(2\omega t) + Q_{s2}sin(2\omega t) \tag{1.5}$$

where P_0 and Q_0 are the average values of the instantaneous output powers and P_{c2},P_{s2},Q_{c2},Q_{s2}. are the overlapped oscillations. These power oscillations, directly influence the performance of the power converter during the fault, generating a DC-link voltage oscillation if the converter interfaces a load to the grid, or a source current oscillation if the converter interfaces the grid to a generator, as reported in Fig.1.5 and Fig.1.6

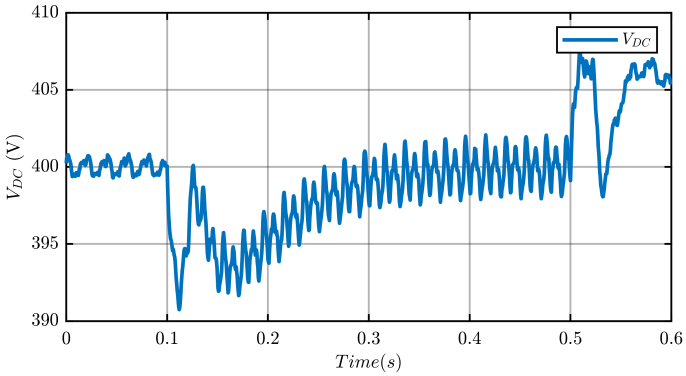

Figure 1.5: Effect of power oscillations on DC-link voltage during a fault for an AC/DC converter interfaces the grid to a load.

In Fig.1.5 absorbing power oscillations could be a problem in terms of stresses on the DC-link capacitors because of the RMS value of the current ripple and the ESR resistor in series to the capacitor incrementing power losses.

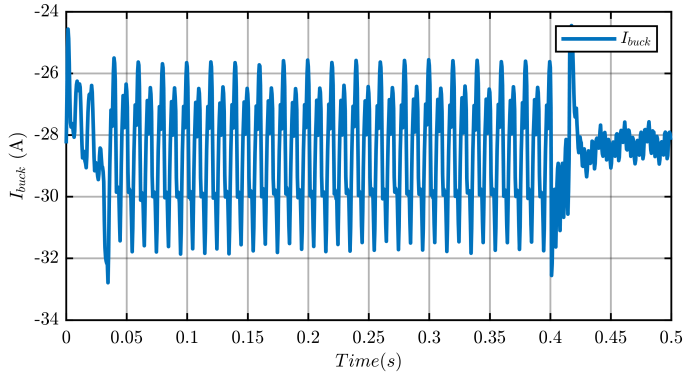

Figure 1.6: Effect of power oscillations on source current, I_{buck}, during a fault for an AC/DC converter interfaces the grid to a generator.

In Fig.1.6 these oscillations contribute to a larger stress on the DC source. This is for example an issue when interfacing battery storage systems (stress on batteries) or solar production plants, where an oscillating power at the output also means a stress on the MPPT algorithms of the PV system.

1.1.1 Setup Scheme and Control

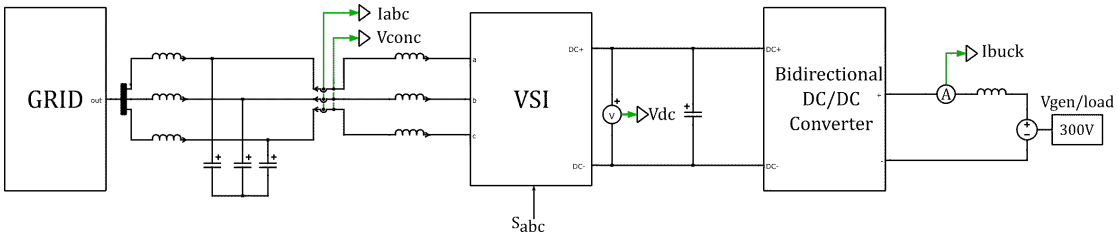

Figure 1.7: Setup scheme and control.

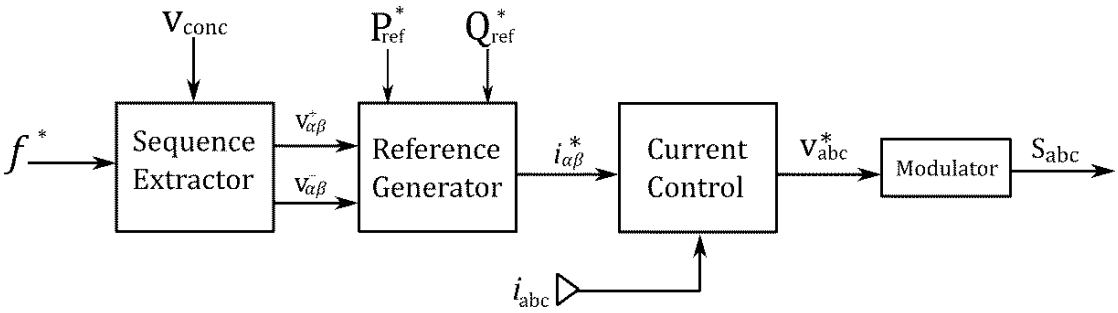

Figure 1.8: Control blocks scheme.

The considered conversion system is shown in Fig.1.7 and it consists of low voltage grid, an LCL filter and the voltage source inverter. A bidirectional DC/DC converter interfaces the DC side to a load or a generator. The control consists of four blocks: the sequence extractor to track the positive and negative voltage sequences, the reference generator, the current control to generate the voltage reference and the modulator to impulse the inverter legs, as shown in Fig.1.8. The variables sent to the sequence extractor, are the grid voltages, V_{conc}. For the current control loop, a PR (Proportional Resonant) regulator was chosen. The reason behind this choice is that in this application, it is necessary to track current references both in positive and negative sequence. A traditional PI regulator in the rotating dq reference frame synchronous with the grid voltage would not suffice, as it would only track the positive sequence (DC values in dq) but not the negative one (AC at double grid frequency in dq). The input of the reference generator

are the voltage sequences, $v^{+}_{\alpha\beta}$ and $v^{-}_{\alpha\beta}$, the power references, P^{*}_{ref} and Q^{*}_{ref}. The input to the PR regulator are the reference currents and the output are the voltage references, V_{abc}, for the modulator to impulse the inverter leg. All the developed techniques works through injecting positive and negative currents sequences, with the goal to cancel the power ripple. The currents depend on the direct and inverse voltage sequences. For this reason, the first step was to implement the sequence extractor to track the direct and inverse voltage sequence. The control technique must be chosen according to the application. In general, the goals are cancelling AC power oscillations, limiting DC-link voltage oscillations and source current oscillations. In this study, the control techniques reported are five:

- IARC (Instantaneous Active Reactive Control)
- BPSC (Balanced Positive Negative Control)
- PNSC (Positive Negative Sequence Control)
- AARC (Average Active Reactive Control)
- FPNSC (Flexible Positive Negative Sequence Control)

Each of the techniques has its own peculiarities.

Chapter 2

Control of grid converters under grid fault

This section describes a current control technique based on PR (Proportional Resonant) regulators of a grid converter under grid fault condition. The PR has been chosen because, compared to the PI regulator, the introduced PR control can overcome two drawbacks of PI control: inability to track a sinusoidal reference with zero steady-state error and poor disturbance rejection capability. Due to an infinite gain at the fundamental frequency, here set at the grid frequency, the PR controller can achieve the high performance in both the sinusoidal reference tracking and the disturbance rejection. The input to the PR regulator is the error between the reference current and the measured current. The proportional and integral gains, K_p and K_i, are the same used for a PI regulator. The output of the PR regulator is the reference voltages in $\alpha\beta$ axis, then applying the inverse Clarke transformation the three-phase reference voltages are obtained. Finally, the reference three-phase voltages are used to calculate the reference duty cycles of the three-phase leg inverter, as shown in Fig.2.1.

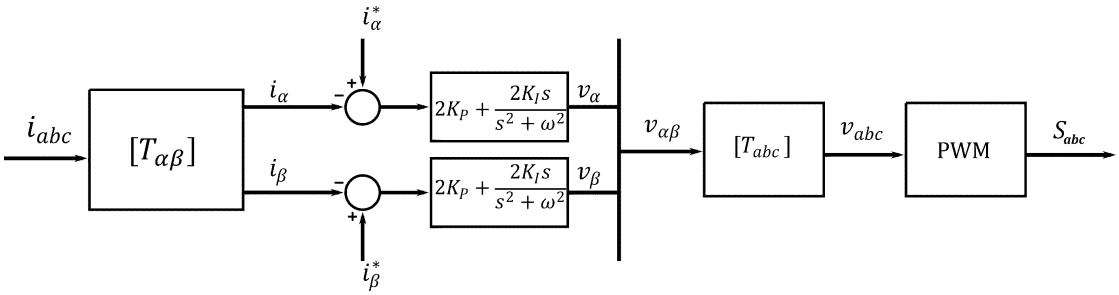

Figure 2.1: Proportional resonant regulator to generate voltage references.

2.1 Computation of Symmetrical Components of an Unbalanced Three Phase System

The computation of the symmetrical components is deeply important to calculate the correct reference currents to inject into the grid, obtaining the desired performance such as no-power (active/reactive) oscillation or symmetrical and balanced grid currents. Several techniques are presented in literature[3, 4], but all of these can be grouped in two: those which operate with the grid angle estimation and those which operate with the grid frequency estimation. The main difference between them is the fact that the frequency is more stable of the grid angle, and a frequency-based control features a smoother response during the fault transient.

2.1.1 The Double Second Order Generalized Integrator (DSOGI)

The DSOGI is a kind of frequency-based sequences' extractor. By starting from an unbalanced three-phase voltage phasors applying the Fortescue transformation is possible to extract the positive and negative sequence (the omopolar has been ignored because a three wire system connection has been considered).

$$\begin{bmatrix} v_a^+ \\ v_b^+ \\ v_c^+ \end{bmatrix} = \frac{1}{3} \begin{bmatrix} 1 & a & a^2 \\ a^2 & 1 & a \\ a & a^2 & 1 \end{bmatrix} \begin{bmatrix} v_a \\ v_b \\ v_c \end{bmatrix} \tag{2.1}$$

$$\begin{bmatrix} v_a^- \\ v_b^- \\ v_c^- \end{bmatrix} = \frac{1}{3} \begin{bmatrix} 1 & a^2 & a \\ a & 1 & a^2 \\ a^2 & a & 1 \end{bmatrix} \begin{bmatrix} v_a \\ v_b \\ v_c \end{bmatrix} \tag{2.2}$$

Then working on the stationary reference frame, $\alpha\beta$, we obtain 1.3 and 1.4:

$$v_{\alpha\beta}^+ = \left[T_{\alpha\beta}\right] \left[T_+\right] \left[T_{\alpha\beta}\right]^{-1} v_{\alpha\beta} \tag{2.3}$$

$$v_{\alpha\beta}^- = \left[T_{\alpha\beta}\right] \left[T_-\right] \left[T_{\alpha\beta}\right]^{-1} v_{\alpha\beta} \tag{2.4}$$

were $[T_+]$ and $[T_-]$ are respectively the Fortescue matrix of 1.1 and 1.2 and $[T_{\alpha\beta}]$ and $[T_{\alpha\beta}]^{-1}$ are the Clarke and inverse-Clarke matrix. In conclusion, after these operations we obtain the following results:

$$v_{\alpha\beta}^+ = [T_{\alpha\beta}^+] v_{\alpha\beta} \; ; \; [T_{\alpha\beta}^+] = \frac{1}{2} \begin{bmatrix} 1 & -q \\ q & 1 \end{bmatrix} \tag{2.5}$$

$$v_{\alpha\beta}^{-} = [T_{\alpha\beta}^{-}]v_{\alpha\beta} \; ; \; [T_{\alpha\beta}^{-}] = \frac{1}{2}\begin{bmatrix} 1 & q \\ -q & 1 \end{bmatrix} \tag{2.6}$$

where $q = e^{-j\frac{\pi}{2}}$ is a 90° lagging phase shifting operator.
The structure of the DSOGI and the sequence calculator are shown in Fig.2.2:

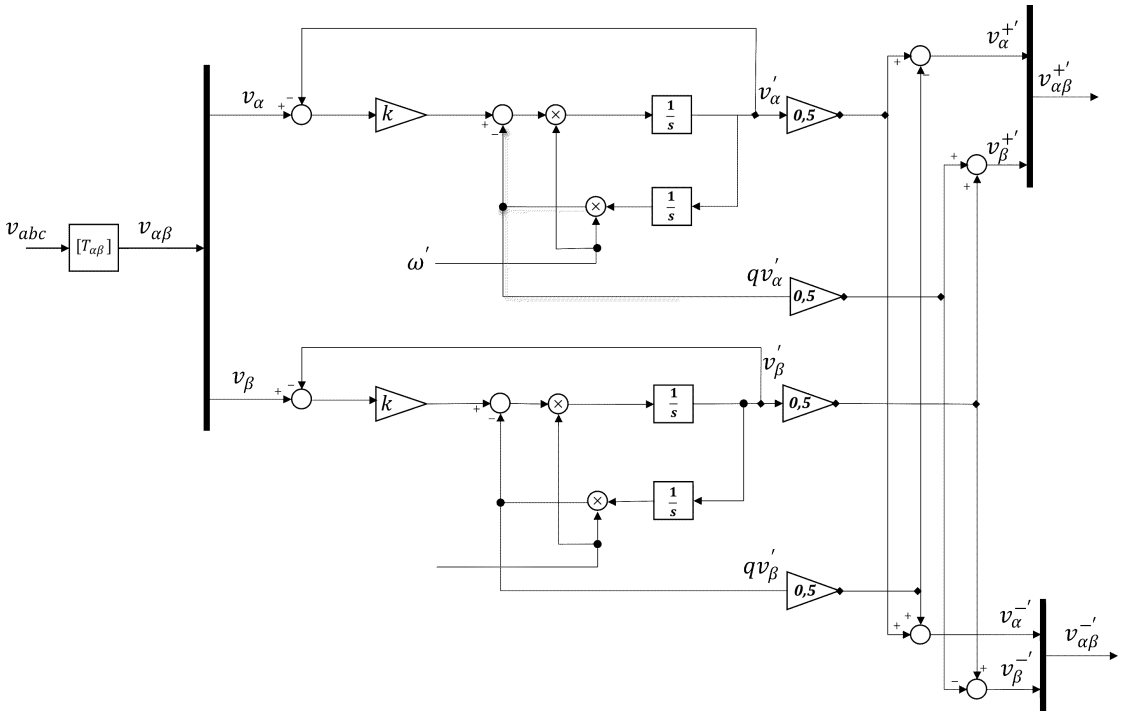

Figure 2.2: Structure of DSOGI and Positive Negative Sequence calculator.

As we can notice, from Fig.(2.3), the DSOGI is a powerful tool both for filtering higher harmonics and extracting the positive and negative sequences.

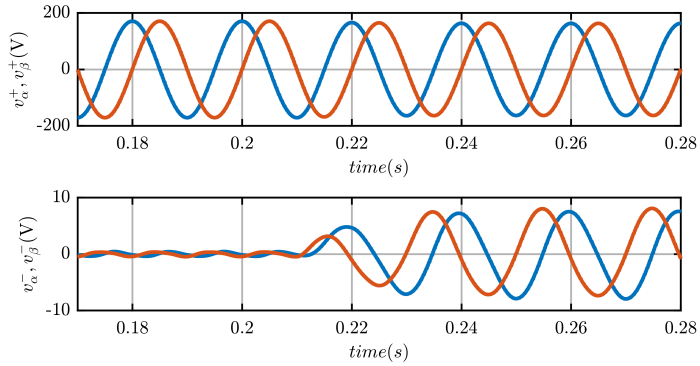

Figure 2.3: Extraction of direct-inverse sequence in $\alpha\beta$ axis during a bi-phase fault occurrence.

Fig.2.3 shows a plot of a simulation of a bi-phase fault occurrence and the extraction of the positive and negative sequence of the voltages components in $\alpha\beta$ axis.

2.2 Generation Of The Current Reference.

As already mentioned in section 2.1, the generation of an appropriate current reference is important to achieve no power oscillation or balanced symmetrical current. In our case a power oscillation means variation of the DC-bus voltage, that for a renewable energy source's connection must be avoided.
Five techniques are presented: IARC, PNSC, AARC, BPSC, FPNSC.

- Instantaneous Active Reactive Control (IARC)
- Positive Negative Sequence control (PNSC)
- Average Active Reactive Control (AARC)
- Balanced Positive Sequence Control (BPSC)
- Flexible Positive Negative Sequence Control (FPNSC)

2.2.1 Instantaneous Active-Reactive Control (IARC).

The output power (active/reactive) can be expressed as the dot product between the grid voltages **v** and the grid currents **i**, while the reactive power can be expressed as the cross product between the grid voltages **v** and the grid currents **i**:

$$P = \mathbf{v} \cdot \mathbf{i} \tag{2.7}$$

$$Q = |\mathbf{v} \times \mathbf{i}| = \mathbf{v}_\perp \cdot \mathbf{i} \tag{2.8}$$

According to (2.7),(2.8) is possible to express the current as the contribution of two parts $\mathbf{i}_{p^*}$ and $\mathbf{i}_{q^*}$ account for generating active and reactive power respectively.

$$\mathbf{i}_{p^*} = g\ \mathbf{v} \tag{2.9}$$

$$\mathbf{i}_{q^*} = b\ \mathbf{v}_\perp \tag{2.10}$$

where $\mathbf{v}_\perp$ is equal to

$$\mathbf{v}_\perp = \begin{bmatrix} v_{\alpha\perp} \\ v_{\beta\perp} \end{bmatrix} = \begin{bmatrix} 0 & -1 \\ 1 & 0 \end{bmatrix} \begin{bmatrix} v_\alpha \\ v_\beta \end{bmatrix} \tag{2.11}$$

The parameters g and b are the instantaneous conductance and susceptance calculated as [3]:

$$g = \frac{P}{|\mathbf{v}^2|} \tag{2.12}$$

$$b = \frac{Q}{|\mathbf{v}^2|} \tag{2.13}$$

$$|\mathbf{v}^2| = 1.5 \cdot (v_a^2 + v_b^2 + v_c^2) = 1.5 \cdot (v_\alpha^2 + v_\beta^2) = 1.5 \cdot (v_d^2 + v_q^2); \tag{2.14}$$

so by setting the active power P and the reactive power, Q the current reference will be calculated accordingly. The parameter of (2.14) is constant when the voltage vectors are symmetrical and balanced but during faults an oscillation at twice the fundamental appears according to 2.15:

$$|\mathbf{v}^2| = |\mathbf{v}^+|^2 + |\mathbf{v}^-|^2 + 2|\mathbf{v}^+||\mathbf{v}^-|cos(2\omega t + \phi^+ + \phi-) \tag{2.15}$$

Here it is shown the variation of $|v^2|$ before and after a fault occurrence (Fig.2.4)

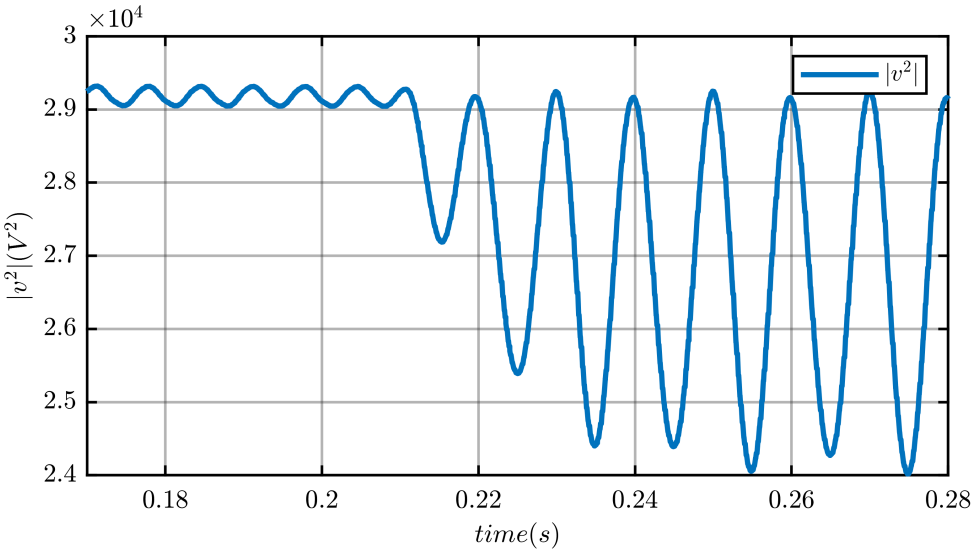

Figure 2.4: Variation of $|v^2|$ parameter before and during the fault occurrence.

The expected output active and reactive power can be calculated as follows, considering 2.7 and 2.8:

$$P = g \cdot v^2 = \frac{P^*}{|v^2|} \cdot |v^2| = P^*;$$

$$Q = b \cdot v^2 = \frac{Q^*}{|v^2|} \cdot |v_\perp^2| = Q^*;$$

where P^* is the active power reference and Q^* the reactive power reference. Considering the previous result, no power oscillations will occur, Fig.2.5.

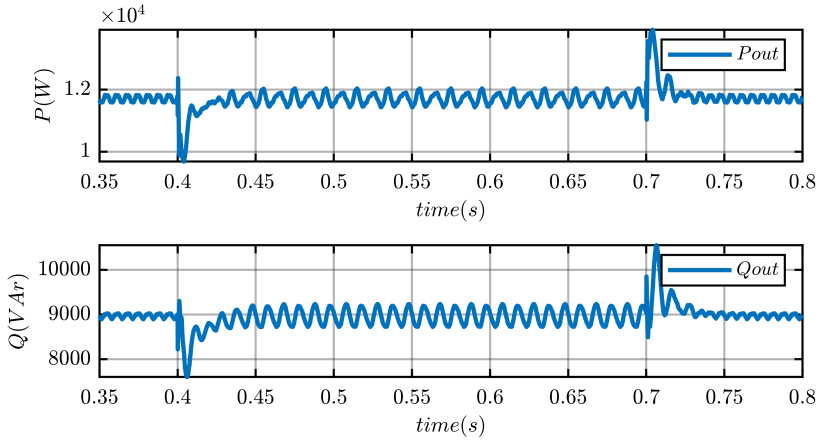

Figure 2.5: PLECs simulations of the instantaneous active and reactive power before and during a fault occurrence using IARC control technique.

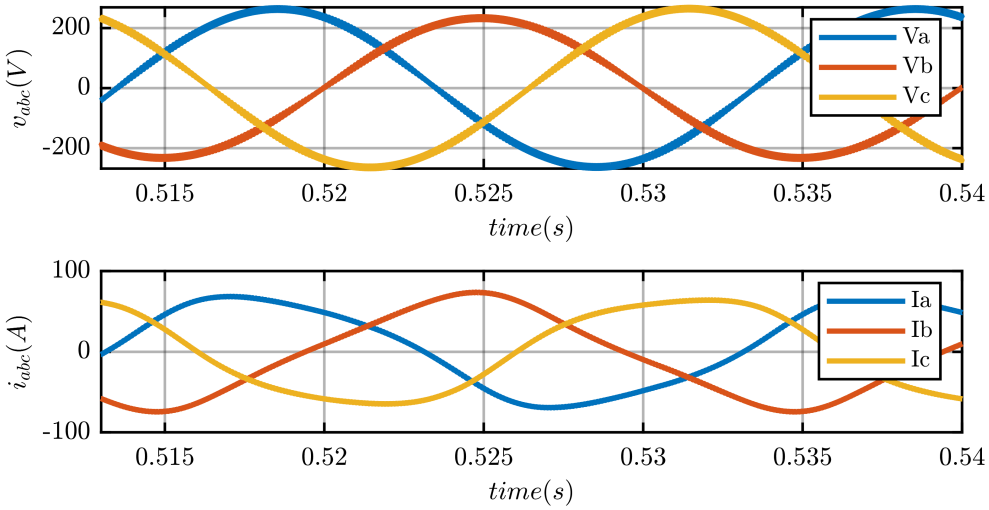

Figure 2.6: Output currents generated through IARC technique

looking at the previous figures (Fig.2.5)(Fig.2.6), IARC technique allows having no power oscillation during the fault, but it generates dissymmetrical and unbalanced currents because of the variable value of g and b.

2.2.2 Balanced Positive Sequence Control (BPSC).

The following technique is based on injecting to the grid a set of balanced symmetrical currents with only the positive sequence. For this reason, $\mathbf{i}_p^*$ and $\mathbf{i}_q^*$ are defined differently respect to the IARC.

$$\mathbf{i}_p^* = G^+ \cdot \mathbf{v}^+; \quad G^+ = \frac{P}{|\mathbf{v}^+|^2} \tag{2.16}$$

$$\mathbf{i}_q^* = B^+ \cdot \mathbf{v}^+; \quad B^+ = \frac{Q}{|\mathbf{v}^+|^2} \tag{2.17}$$

were $|\mathbf{v}^+|^2$ is the same parameter of (2.15) considering only the contribution of the direct sequence (see Fig.2.7).The parameter keeps constant also during the fault because only the positive sequence is considered, so $|v|^2$ in equation 2.15 is equal to the squared amplitude of the voltage positive sequence.

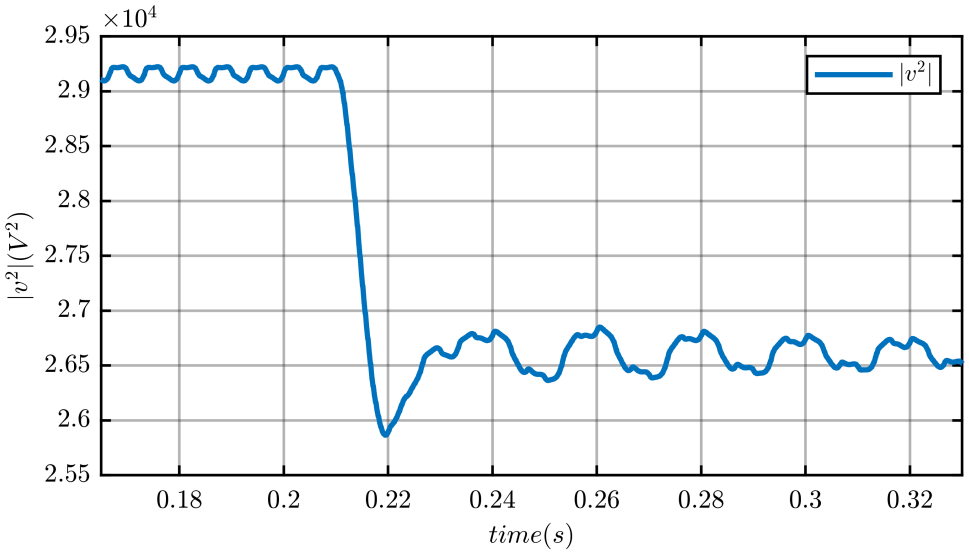

Figure 2.7: Variation of $|v^+|^2$ before, during and after the fault. The oscillations during the fault are caused by tiny errors in the extrapolation of the negative sequence.

This means that through the BPSC the reference currents are a set of balanced positive sequence sinusoidal waveforms (see Fig.2.8).

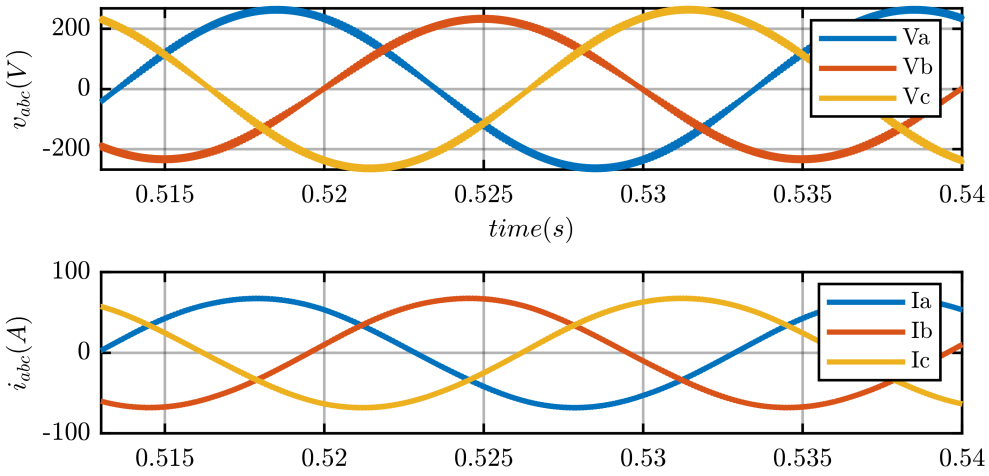

Figure 2.8: Output currents during a fault occurrence.

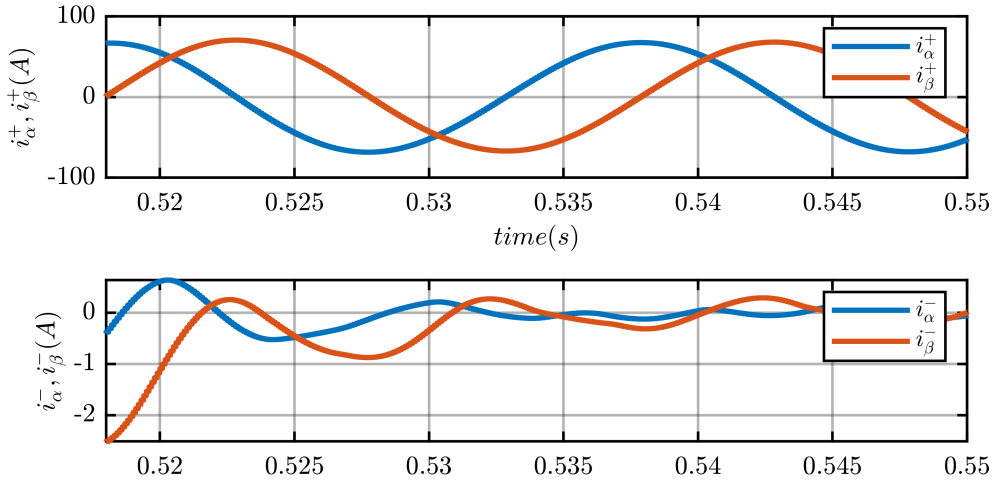

Figure 2.9: Positive and negative current references generated during grid fault conditions in $\alpha\beta$ axis.

Anyway, through this kind of current reference generation, the output power differ from those set in (2.16), (2.17), because of the cross effect between the direct and negative sequence.

$$p = \mathbf{v} \cdot \mathbf{i}_p^* = \mathbf{v}^+ \cdot \mathbf{i}_p^* + \mathbf{v}^- \cdot \mathbf{i}_p^* \tag{2.18}$$

$$q = \mathbf{v}_\perp \cdot \mathbf{i}_q^* = \mathbf{v}_\perp^+ \cdot \mathbf{i}_q^* + \mathbf{v}_\perp^- \cdot \mathbf{i}_q^* \tag{2.19}$$

The output powers, as noticed in (2.18), (2.19), present a constant value, derived from the product of the positive sequence components of voltages and currents, and an overlapped sinusoidal signal caused by the cross effect between negative sequence voltages set and positive sequence currents set.
In the figure below (Fig.2.10) the active power is set at 12kW and reactive at 9kVar.

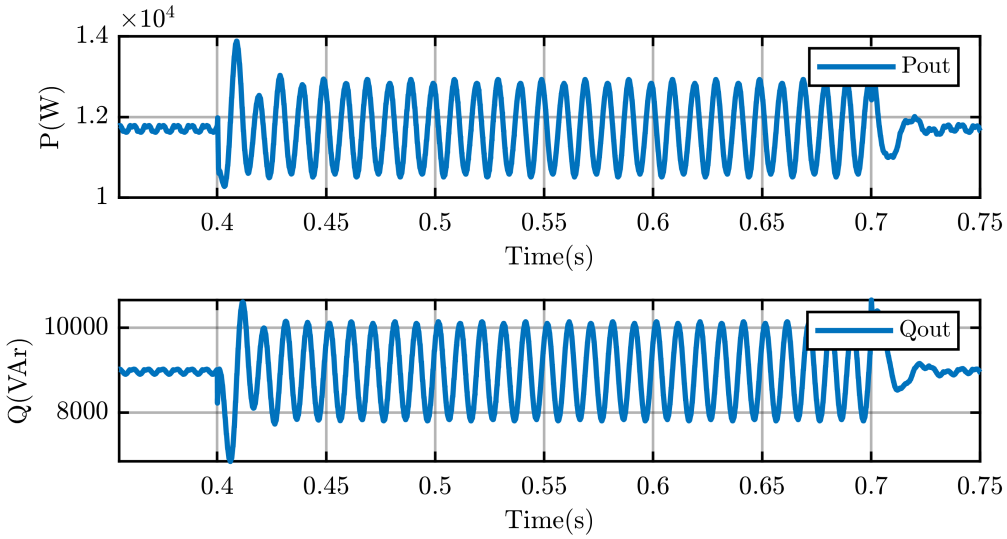

Figure 2.10: Output powers and sinusoidal signal overlapped, caused by the cross effect of positive and negative sequence during a fault occurrence at 0,4s.

2.2.3 Positive Negative Sequence Control (PNSC).

The PNSC consists on injecting a proper set of positive and negative sequence currents in to the grid as shown in (2.20):

$$\mathbf{i}^{*} = \mathbf{i}^{*+} + \mathbf{i}^{*-} \tag{2.20}$$

where $\mathbf{i}^{*+}$ and $\mathbf{i}^{*-}$ are the positive and negative currents components respectively. The reference current can be calculated considering generating only active power free of oscillation, obtaining (2.21):

$$\mathbf{v}^{+} \cdot \mathbf{i}_p^{*+} + \mathbf{v}^{-} \cdot \mathbf{i}_p^{*-} = P \tag{2.21}$$

$$\mathbf{v}^{+} \cdot \mathbf{i}_p^{*-} + \mathbf{v}^{-} \cdot \mathbf{i}_p^{*+} = 0 \tag{2.22}$$

from (2.22) is possible to obtain an expression of $\mathbf{i}_p^{*-}$ in function of $\mathbf{i}_p^{*+}$, which can be substituted in (2.21) to obtain:

$$\mathbf{v}^{+} \cdot \mathbf{i}_p^{*-} = -\mathbf{i}_p^{*+} \cdot \mathbf{v}^{-} \implies |\mathbf{v}^{+}|^2 \cdot \mathbf{i}_p^{*-} = -\mathbf{v}^{+} \cdot \mathbf{i}_p^{*+} \cdot \mathbf{v}^{-} \implies \mathbf{i}_p^{*-} = \frac{\mathbf{v}^{+} \cdot \mathbf{i}_p^{*+}}{|\mathbf{v}^{+}|^2} \cdot \mathbf{v}^{-} \tag{2.23}$$

Therefore the active power P can be calculated as:

$$P = \mathbf{v}^{+} \cdot \mathbf{i}_p^{*+} \left(1 - \frac{|\mathbf{v}^{-}|^2}{|\mathbf{v}^{+}|^2}\right) \tag{2.24}$$

Then, multiplying (2.24) for $\mathbf{v}^+$ we obtain:

$$\mathbf{i}_p^{*+} = \frac{P}{|\mathbf{v}^+|^2 - |\mathbf{v}^-|^2} \cdot \mathbf{v}^+ \tag{2.25}$$

Finally, adding (2.23) and (2.25), the reference for the active current is given by:

$$\mathbf{i}_p^* = g^{\pm}(\mathbf{v}^+ - \mathbf{v}^-); \qquad g^{\pm} = \frac{P}{|\mathbf{v}^+|^2 - |\mathbf{v}^-|^2} \tag{2.26}$$

Similar constraints used in (2.21) and (2.22) can be imposed to determine the current reactive power reference Q

$$\mathbf{i}_q^* = b^{\pm}(v_\perp^+ - v_\perp^-); \qquad b^{\pm} = \frac{Q}{|\mathbf{v}^+|^2 - |\mathbf{v}^-|^2} \tag{2.27}$$

referring to (2.20), current reference can be also written as follows in order to study the performance of the instantaneous powers.

$$\mathbf{i}^+ = \mathbf{i}_p^{*+} + \mathbf{i}_q^{*+} \tag{2.28}$$

$$\mathbf{i}^- = \mathbf{i}_p^{*-} + \mathbf{i}_q^{*-} \tag{2.29}$$

Where the instantaneous power delivered is given by:

$$p = \mathbf{v}^+ \cdot \mathbf{i}_p^+ + \mathbf{v}^- \cdot \mathbf{i}_p^- + \underbrace{\mathbf{v}^+ \cdot \mathbf{i}_q^+ + \mathbf{v}^- \cdot \mathbf{i}_q^-}_{0} + \underbrace{\mathbf{v}^+ \cdot \mathbf{i}_p^- + \mathbf{v}^- \cdot \mathbf{i}_p^+}_{0} + \underbrace{\mathbf{v}^+ \cdot \mathbf{i}_q^- + \mathbf{v}^- \cdot \mathbf{i}_q^+}_{\tilde{p}} \tag{2.30}$$

$$q = \mathbf{v}_\perp^+ \cdot \mathbf{i}_q^+ + \mathbf{v}_\perp^- \cdot \mathbf{i}_q^- + \underbrace{\mathbf{v}_\perp^+ \cdot \mathbf{i}_p^+ + \mathbf{v}_\perp^- \cdot \mathbf{i}_p^-}_{0} + \underbrace{\mathbf{v}_\perp^+ \cdot \mathbf{i}_q^- + \mathbf{v}_\perp^- \cdot \mathbf{i}_q^+}_{0} + \underbrace{\mathbf{v}_\perp^+ \cdot \mathbf{i}_p^- + \mathbf{v}_\perp^- \cdot \mathbf{i}_p^+}_{\tilde{q}} \tag{2.31}$$

In both the expressions the instantaneous delivered powers present a constant output power (P, Q) plus an overlapped ripple $(\tilde{p}, \tilde{q})$.The third and fourth terms are cancelled out from the previous equation, as the dot product between two components with the same sequence but 90° shifted is null. Anyway, it is possible to cancel the overlapped ripple by eliminating $\mathbf{i}_p^*$ or $\mathbf{i}_q^*$ from the equations, by setting the reference power P or Q, respectively in equations (2.26), (2.27), to zero.
It means that the only way for having a constant active power to the output is to set the reactive power to zero.

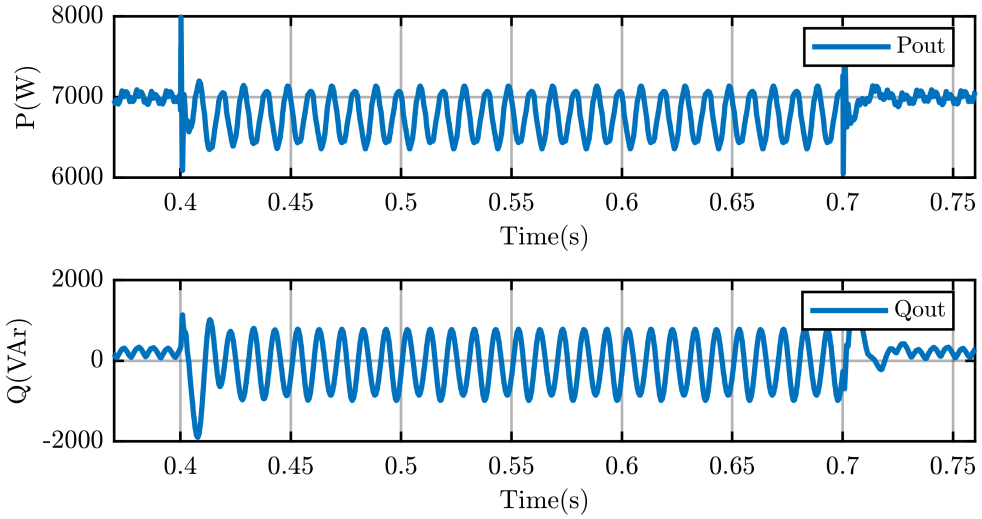

Figure 2.11: Instantaneous active and reactive power.

In the previous figure, Fig.2.11, it is important to notice the reactive power reference, Q, is set to zero to obtain a constant instantaneous active power. The small oscillation in reactive power before the fault occurrence (time $<$ 0.4s), and in the active power after fault occurrence (time $>$ 0.4s) is caused by small tracking error on the extraction of negative voltage sequence. Anyway, this oscillation is tiny compared to power inject in the grid, for this reason can be neglected.

2.2.4 Average Active-Reactive Control (AARC).

AARC control can be considered a middle way between IARC and PNSC, contrary to the IARC, where the output currents feature harmonics caused by the variable value of g and b in equations (2.12)(2.13), AARC's conductance and suscettance are calculated as follows

$$\mathbf{i}_p^* = G\mathbf{v}; \qquad G = \frac{P}{V_\Sigma^2} \tag{2.32}$$

$$\mathbf{i}_q^* = B\mathbf{v}; \qquad B = \frac{Q}{V_\Sigma^2} \tag{2.33}$$

where V_Σ^2 is the collective rms value of the grid voltage, defined as

$$V_\Sigma = \sqrt{\frac{1}{T}\int_0^T |\mathbf{v}^2| dt} = \sqrt{|\mathbf{v}^+|^2 + |\mathbf{v}^-|^2} \tag{2.34}$$

Equation (2.34) shows that conductance and suscettance in (2.32), (2.33) are constants, so the reference currents are proportional to the grid voltage.
The instantaneous output powers are calculated as

$$p = \mathbf{i}_p^* \cdot \mathbf{v} = \frac{|\mathbf{v}|^2}{V_\Sigma^2} \cdot P = \mathbf{P} + \tilde{p} \tag{2.35}$$

$$p = P\left(1 + \frac{2|\mathbf{v}^+||\mathbf{v}^-|}{|\mathbf{v}^+|^2 + |\mathbf{v}^-|^2} cos(2\omega t + \phi^+ + \phi^-)\right) \tag{2.36}$$

where ϕ^+ and ϕ^- are the phase angle of the positive and negative sequences voltages vector components. At the same way, the instantaneous reactive power can be calculated as

$$q = \mathbf{v}_\perp \cdot \mathbf{i}_q^* = \frac{|\mathbf{v}^2|}{V_\Sigma^2} Q = \mathbf{Q} + \tilde{q} \tag{2.37}$$

$$q = Q\left(1 + \frac{2|\mathbf{v}^+||\mathbf{v}^-|}{|\mathbf{v}^+|^2 + |\mathbf{v}^-|^2} cos(2\omega t + \phi^+ + \phi^-)\right) \tag{2.38}$$

As equations (2.36), (2.38) shown, if the active power is set to zero, the instantaneous active power will be zero without any oscillation. The same consideration can be done if just the reactive power, in this case the reactive power will be zero and free of oscillations.

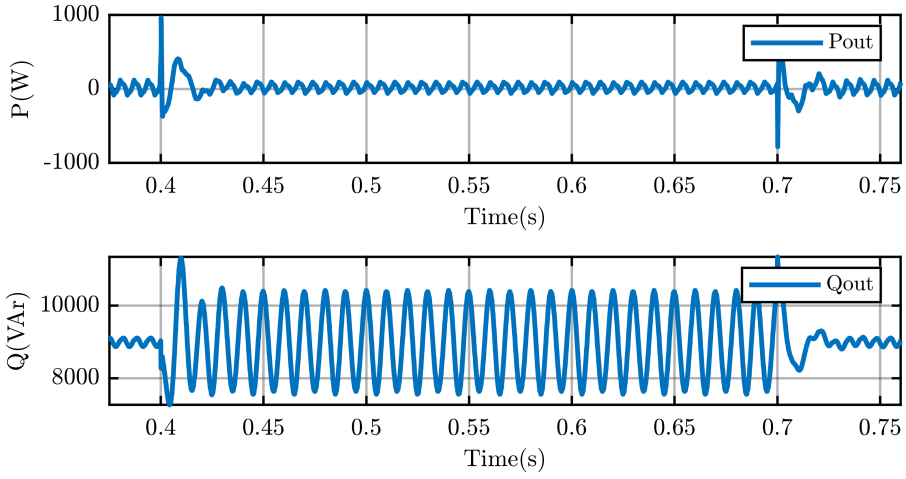

Figure 2.12: Instantaneous active and reactive power using AARC.

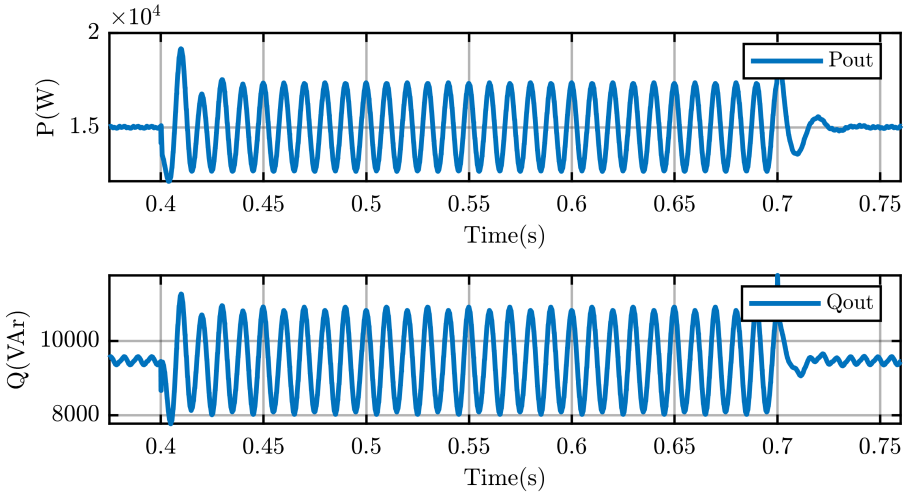

Figure 2.13: Instantaneous active and reactive power using AARC.

Fig.(2.12) shows that the only way to keep constant the instantaneous active power during the fault is setting the power reference, P, equal to zero. Also without power delivering a constant value of the active power means no oscillations at the DC-bus. Otherwise, setting an active power reference different to zero generate an instantaneous active power oscillation, as shown in Fig.(2.13).

2.2.5 Flexible Positive and Negative Sequence Control (FPNSC).

FPNSC implements a more flexible technique for generating the current reference, adjusting two parameters, k_1 and k_2, in order to deliver a certain amount of active/reactive power. The current reference is calculated as follows,

$$\mathbf{i}_p^* = k1G^+\mathbf{v}^+ + (1-k1)G^-\mathbf{v}^- \tag{2.39}$$

$$\mathbf{i}_q^* = k2B^+\mathbf{v}_\perp^+ + (1-k2)B^-\mathbf{v}_\perp^- \tag{2.40}$$

where G^+ and G^- are

$$G^+ = \frac{P}{|v^+|^2}; \qquad G^- = \frac{P}{|v^-|^2} \tag{2.41}$$

and B^+ and B^- are

$$B^+ = \frac{Q}{|v^+|^2}; \qquad B^- = \frac{Q}{|v^-|^2} \tag{2.42}$$

Finally by summing (2.39) and (2.40) the current reference to provide to the current controller is obtained.

$$\mathbf{i}^* = P\Big(\frac{k1}{|v^+|^2}\cdot\mathbf{v}^+ + \frac{(1-k1)}{|v^-|^2}\cdot\mathbf{v}^-\Big) + Q\Big(\frac{k2}{|v^+|^2}\cdot\mathbf{v}_\perp^+ + \frac{(1-k2)}{|v^-|^2}\cdot\mathbf{v}_\perp^-\Big) \tag{2.43}$$

Equation (2.43) shows how by setting $k1$ and $k2$ it is possible to choose the amount of active or reactive power to deliver to the grid. Now it is important how to choose these two parameters for having certain performance such as no active power oscillation, P, or reactive, Q.
The following equation shows the instantaneous active power delivered to the grid, equal to:

$$p = \mathbf{P} + \tilde{p} \tag{2.44}$$

where $\mathbf{P}$ is the average value and $\tilde{p}$ is the overlapped oscillation.

$$\mathbf{P} = \frac{Pk1}{|v^+|^2}\cdot\mathbf{v}^+\cdot\mathbf{v}^+ + \frac{P(1-k1)}{|v^-|^2}\cdot\mathbf{v}^-\cdot\mathbf{v}^- \tag{2.45}$$

$$\tilde{p} = \left(\frac{Pk1}{|v^+|^2} + \frac{P(1-k1)}{|v^-|^2}\right)\cdot\mathbf{v}^+\cdot\mathbf{v}^- + \left(\frac{Qk2}{|v^+|^2} - \frac{Q(1-k2)}{|v^-|^2}\right)\cdot\mathbf{v}_\perp^+\cdot\mathbf{v}^- \tag{2.46}$$

The same equations can be obtained for the reactive power.

$$q = \mathbf{Q} + \tilde{q} \tag{2.47}$$

where $\mathbf{Q}$ is the average value and $\tilde{q}$ is the overlapped oscillation.

$$\mathbf{Q} = \frac{Qk2}{|v^+|^2}\cdot\mathbf{v}_\perp^+\cdot\mathbf{v}_\perp^+ + \frac{Q(1-k2)}{|v^-|^2}\cdot\mathbf{v}_\perp^-\cdot\mathbf{v}_\perp^- \tag{2.48}$$

$$\tilde{q} = \left(\frac{Pk1}{|v^+|^2} + \frac{P(1-k1)}{|v^-|^2}\right)\cdot\mathbf{v}_\perp^+\cdot\mathbf{v}^- + \left(\frac{Qk2}{|v^+|^2} - \frac{Q(1-k2)}{|v^-|^2}\right)\cdot\mathbf{v}_\perp^+\cdot\mathbf{v}_\perp^- \tag{2.49}$$

Anyway, (2.46) shows that it is possible to calculate a specific value of $k1$ and $k2$ to cancel out the active power oscillation (2.50) by imposing (2.46) equal to zero.

$$k1 = \frac{|\mathbf{v}^+|^2}{|\mathbf{v}^+|^2 - |\mathbf{v}^-|^2} \geq 1 \tag{2.50}$$

The same consideration to cancel the second active power ripple term (2.51) can be done.

$$\left(\frac{Qk2}{|v^+|^2} - \frac{Q(1-k2)}{|v^-|^2}\right)\cdot\mathbf{v}_\perp^+\cdot\mathbf{v}_\perp^- = 0 \tag{2.51}$$

Then, we obtain (2.52).

$$k2 = \frac{|\mathbf{v}^+|^2}{|\mathbf{v}^+|^2 + |\mathbf{v}^-|^2} \leq 1 \tag{2.52}$$

This feature is interesting because allows to have instantaneous active output power free of oscillation. Using the coefficients value calculated in (2.50) and (2.52) means that FPNSC behave as the PNSC with an important difference: one of the reference powers P or Q must not be necessarily set to zero for not having overlapped power oscillations (see Fig.2.14).

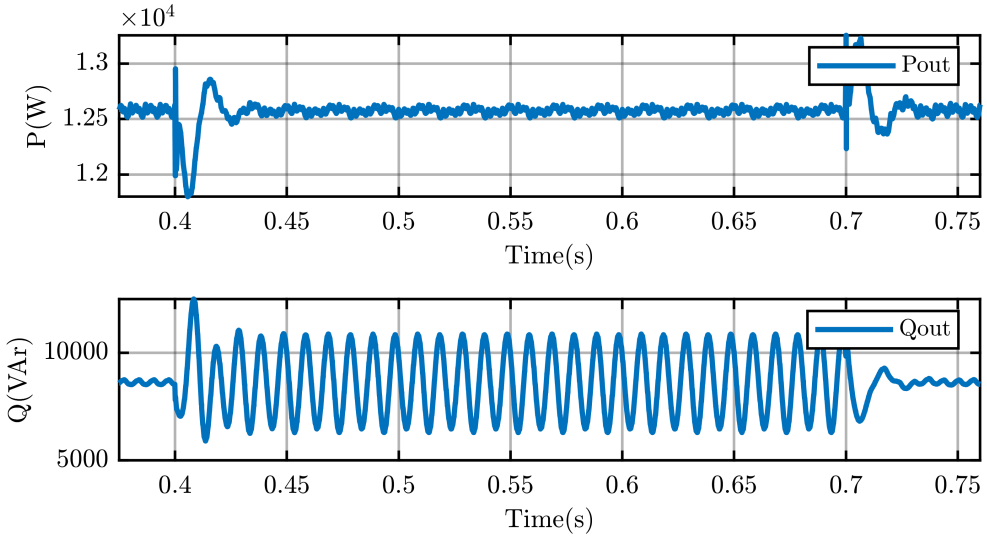

Figure 2.14: Instantaneous active and reactive power using FPNSC

Chapter 3

Current Control Algorithm With Current Limitation

Every of these techniques take as input the active power P and the reactive power Q, this means that, during the fault, while the voltage decreases, the current goes up as the power reference if fixed. For the reason just explained, to implement a control algorithm to re-calculate the power reference P and Q during the fault to avoid the the inverter protections triggering (IPT) is fundamental. Five control techniques will be presented, in which four are developed by the author, while FPNSC current control limit technique can be found in literature[3].

3.1 IARC Current Limitation Control

Starting from the definition of the current reference, it is possible to obtain a formulation of the maximum reactive power reference by setting the current reference and the power reference.

$$\mathbf{i}^* = g\mathbf{v} + b\mathbf{v}_\perp$$

where

$$g = \frac{P}{|v|^2}; \quad b = \frac{Q}{|v|^2}$$

Then, writing currents in $\alpha\beta$ axis, we obtain:

$$i_\alpha = \frac{P}{|v|^2} \cdot v_\alpha - \frac{Q}{|v|^2} \cdot v_\beta \tag{3.1}$$

$$i_\beta = \frac{P}{|v|^2} \cdot v_\beta + \frac{Q}{|v|^2} \cdot v_\alpha \tag{3.2}$$

Then

$$\hat{I}^2 = i_\alpha^2 + i_\beta^2 \tag{3.3}$$

$$i_\alpha^2 + i_\beta^2 \leq \hat{I}^2 \tag{3.4}$$

by substituting (3.1) and (3.2) in (3.4), is possible to obtain:

$$Q \leq \sqrt{|v|^2 \hat{I}^2 - P^2} \tag{3.5}$$

Equation (3.5) shows that the power P must be limited to avoid the generation of negative square root argument. So:

$$P \leq \sqrt{|v|^2 \hat{I}^2} \tag{3.6}$$

In (3.6) the maximum power reference P is oscillating, according to the value of $|v|^2$ during the fault, but every control technique (IARC,BPSC,PNSC,AARC,FPNSC) need as input a constant power reference P. What just discussed means to develop an algorithm to extract the constant minimum value of P in (3.6), for avoiding a negative rooting in (3.5). Supposing to have found a way to extrapolate P_{min}, also Q in (3.5) depends on $|v|^2$, this means that also the maximum reactive power reference will be oscillating, but what is needed is a constant reactive power reference.
This procedure starts by filtering the input signal by using a Resonant Filter,whose block diagram is shown in Fig(3.1).

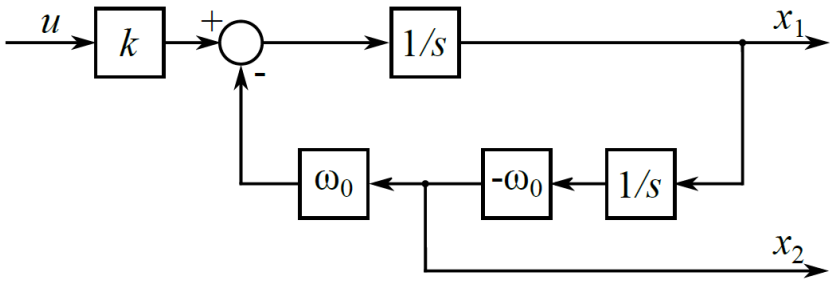

Figure 3.1: Resonant Filter.

3.1.1 Online Power Reference Computation

Accordingly with said in section 3.1, it is important to compute the minimum value of P in (3.6) to generate a constant power reference and avoiding negative rooting and then compute the minimum value of Q in (3.5) to feature maximum output

phase currents avoiding IPT.
What just introduced has been reported through a block scheme, Fig.3.2.

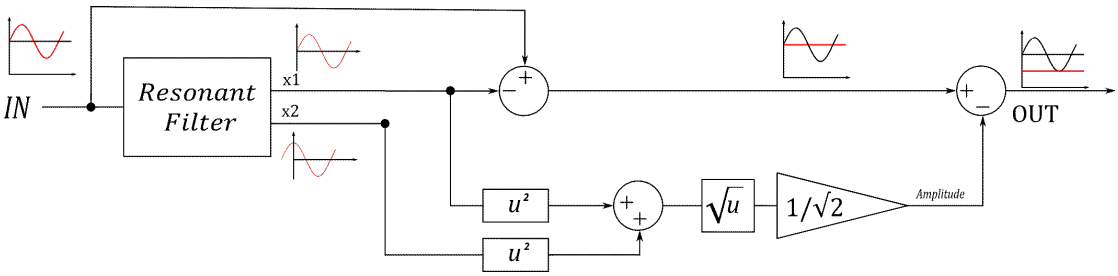

Figure 3.2: Minimum output power reference extractor block scheme

The RF gives at the output the sinusoidal waveform without the mean value ($x1$) and a quadrature signal ($x2$) then used to compute the amplitude of a sinusoidal wave. The mean value will be the difference between the input and the output ($x1$).

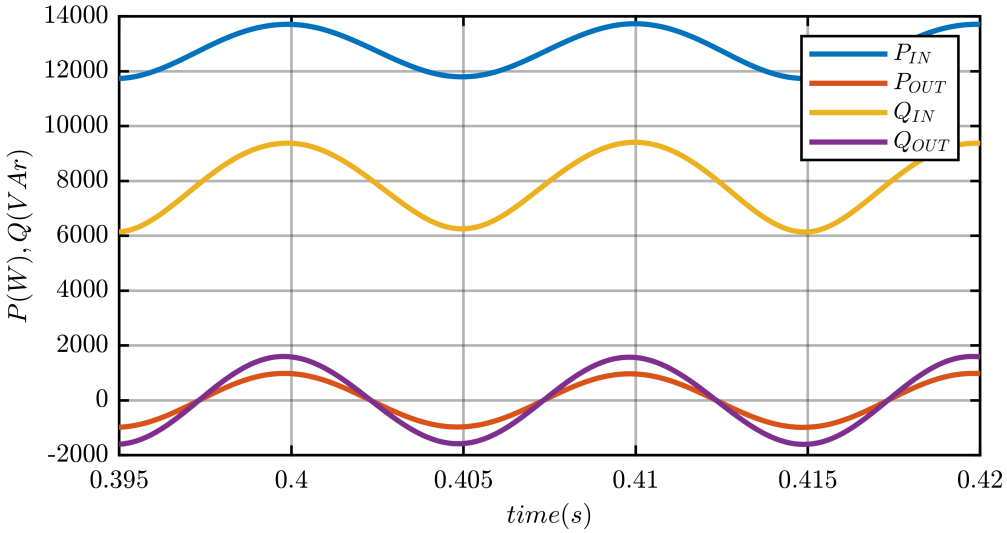

Figure 3.3: Input powers (blue line, yellow line) feature mean value and ripple and output filtered powers (red line, violet line) without mean value.

Once obtained the DC value of power reference, it is necessary to subtract the amplitude of the sinusoidal wave to calculate the minimum. To do that, the quadrature signal of the RF is used. The quadrature signal $\mathbf{qP}_{ripple}$ keeps 90° shifted in respect to the sinusoidal signal $\mathbf{P}_{ripple}$ during the time; the amplitude of the two signals, $\mathbf{qP}_{ripple}$ and $\mathbf{P}_{ripple}$ is equal, so by imaging the two signals as two

phasors the amplitude is given by:

$$P_{amp} = \frac{\sqrt{\mathbf{P}^2_{ripple} + \mathbf{qP}^2_{ripple}}}{\sqrt{2}}; \qquad q = e^{-j\frac{\pi}{2}} \tag{3.7}$$

Fig(3.4) gives a graphic interpretation of what happen: also if the instantaneous value of $\mathbf{qP}_{ripple}$ and $\mathbf{P}_{ripple}$ is variable the relation in (3.7) is fixed in the time, as the two signals are the same but 90° shifted. So $\mathbf{P}_{amp}$ will be the diagonal of a square divided $\sqrt{2}$. The final value of the powers reference, P and Q, given as input to the control will be the minimum value of the oscillating powers, as shown in Fig.3.5.

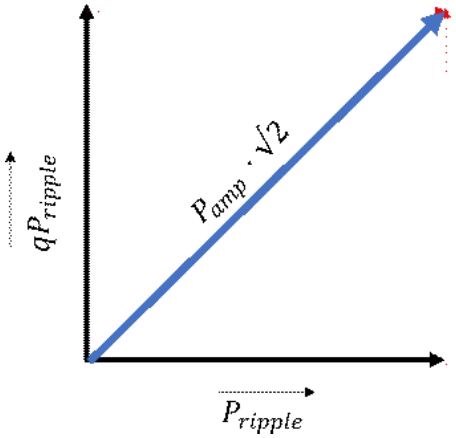

Figure 3.4: Graphic interpretation of (3.7).

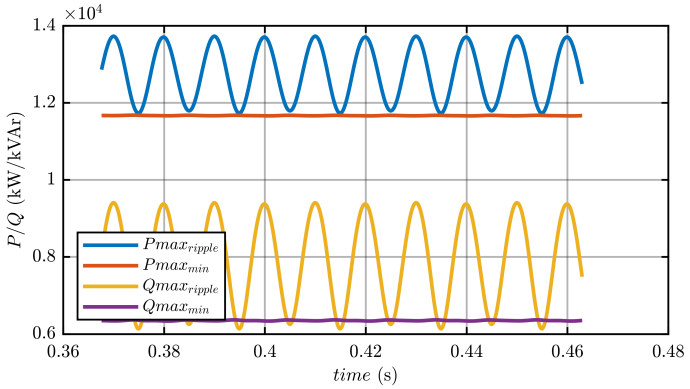

Figure 3.5: Oscillating power reference and computation of the minimum constant value of P and Q to avoid inverter protection triggering.

This strategy will be implemented in every control except the FPNSC, that will feature a dedicated control strategy.

3.2 BPSC With Current Limitation Control

The theoretical base to develop a strategy to limit the current is the same for every control (IARC,BPSC,PNSC,AARC,FPNSC). Starting from the $i^*_{\alpha\beta}$ current reference, the output power is calculated to maximize the reactive power injected to the grid to support it during faults conditions.

$$\mathbf{i}^* = g\mathbf{v} + b\mathbf{v}_\perp$$

where

$$g = \frac{P}{|v^+|^2}; \quad b = \frac{Q}{|v^+|^2}$$

Then, writing currents in $\alpha\beta$ axis, we obtain:

$$i_\alpha = \frac{P}{|v^+|^2} \cdot v_\alpha - \frac{Q}{|v^+|^2} \cdot v_\beta \tag{3.8}$$

$$i_\beta = \frac{P}{|v^+|^2} \cdot v_\beta + \frac{Q}{|v^+|^2} \cdot v_\alpha \tag{3.9}$$

Then

$$i_\alpha^2 + i_\beta^2 \leq \hat{I}^2 \tag{3.10}$$

by substituting (3.8) and (3.9) in (3.10), is possible to obtain:

$$Q \leq \sqrt{|v^+|^2\hat{I}^2 - P^2} \tag{3.11}$$

Equation (3.11) shows that the power P must be limited to avoid the generation of negative rooting. So:

$$P \leq \sqrt{|v^+|^2\hat{I}^2} \tag{3.12}$$

Differently from the IARC, $|v^+|^2$ is a constant value so, for BPSC current limitation, filtering the power through an RF is unnecessary.

$$P_{max} = |v^+| \cdot \hat{I} \tag{3.13}$$

$$Q_{max} = \sqrt{|v^+|^2 \cdot \hat{I}^2 - P^2} \tag{3.14}$$

As a direct consequence of (3.14), if the power reference P before the fault is greater than P_{max}, the reactive power reference will be set to zero, as shown in Fig.3.6.

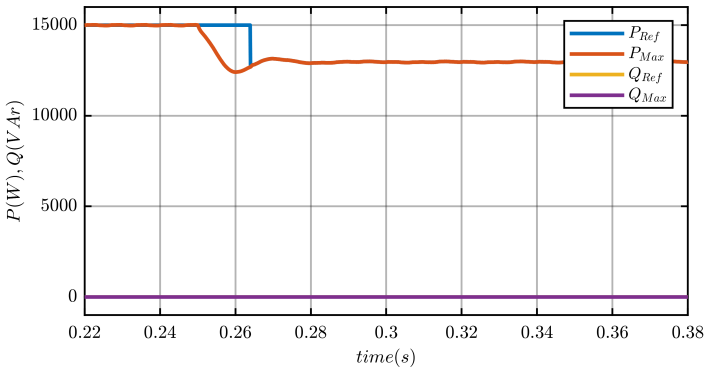

Figure 3.6: Maximum power reference computation for BPSC control.

The previous figure, Fig.3.6, shows that the reactive power is set to zero because before the fault the active power reference P_{ref} is set higher than the maximum settable value P_{max}; according to (3.14) there is no margin for the reactive power Q_{ref}, for being settable greater than zero.

The result is different for the figure below, Fig.3.7, where the power reference P_{ref} is lower than the maximum settable value P_{max}. For what just said, the reactive power reference Q_{ref} has margin to be settable greater than zero, exactly to his maximum value Q_{max} to avoid inverter protection triggering.

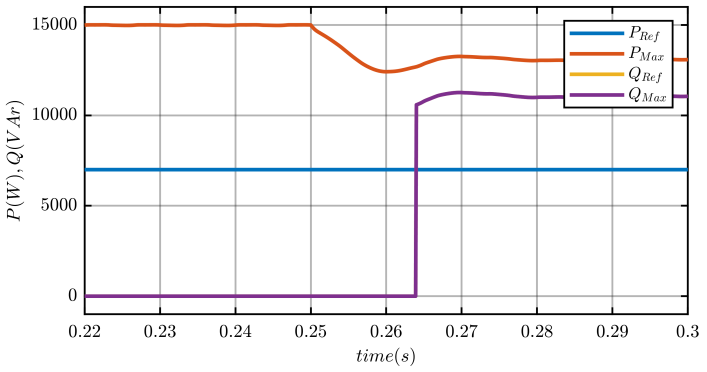

Figure 3.7: Maximum power reference computation for BPSC control.

In Fig.3.7, the fault starts at $t = 0.25s$. The reason why the reactive power Q_{ref} is zero until $t = 0.263s$ is due to the fact that P_{ref} computation has a transient in

which the rooting of (3.14) is negative and to avoid this problem Q_{ref} is saturated at zero.

3.3 PNSC with Current Limitation Control

As already said, the formulation starts from the current reference. For PNSC the current reference is given by:

$$i_\alpha = \frac{P}{|v^+|^2 - |v^-|^2} \cdot (v_\alpha^+ - v_\alpha^-) + \frac{Q}{|v^+|^2 - |v^-|^2} \cdot (-v_\beta^+ + v_\beta^-) \tag{3.15}$$

$$i_\beta = \frac{P}{|v^+|^2 - |v^-|^2} \cdot (v_\beta^+ - v_\beta^-) + \frac{Q}{|v^+|^2 - |v^-|^2} \cdot (v_\alpha^+ - v_\alpha^-) \tag{3.16}$$

Then

$$i_\alpha^2 + i_\beta^2 \leq \hat{I}^2 \tag{3.17}$$

by substituting (3.15) and (3.16) in (3.17), is possible to obtain:

$$Q \leq \sqrt{\frac{(|v^+|^2 - |v^-|^2)^2}{|v^+|^2 + |v^-|^2 - 2v_\alpha^+ v_\alpha^- - 2v_\beta^+ v_\beta^-} \hat{I}^2 - P^2} \tag{3.18}$$

Equation (3.18) shows that the power P must be limited to avoid the generation of negative rooting. So:

$$P \leq \sqrt{\frac{(|v^+|^2 - |v^-|^2)^2}{|v^+|^2 + |v^-|^2 - 2v_\alpha^+ v_\alpha^- - 2v_\beta^+ v_\beta^-} \hat{I}^2} \tag{3.19}$$

The figure below, Fig.3.8, shows P_{max} and Q_{max} waveform and the computation of their minimum value Q_{ref} and P_{ref}.

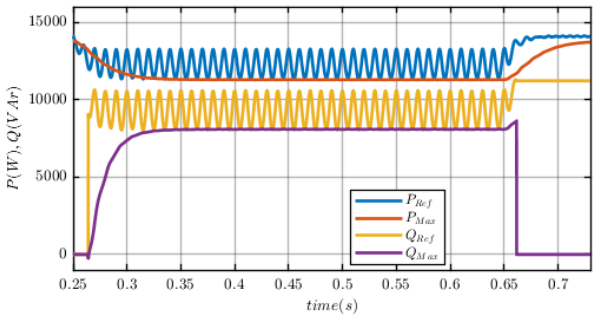

Figure 3.8: Maximum power reference computation for PNSC strategy, during and after the fault.

The previous figure, Fig.3.8, shows an improper use of the PNSC control strategy; one of the power reference P or Q should be set to zero. In case Q is null, the active power will be free of oscillation, at the same way if P is null, the reactive power will be constant.

3.4 AARC With Current Limitation Control

In AARC control technique, currents references are defined as:

$$i_\alpha = \frac{P}{|v^+|^2 + |v^-|^2} \cdot v_\alpha - \frac{Q}{|v^+|^2 + |v^-|^2} \cdot v_\beta \tag{3.20}$$

$$i_\beta = \frac{P}{|v^+|^2 + |v^-|^2} \cdot v_\beta + \frac{Q}{|v^+|^2 + |v^-|^2} \cdot v_\alpha \tag{3.21}$$

Then,

$$i_\alpha^2 + i_\beta^2 \leq \hat{I}^2 \tag{3.22}$$

by substituting (3.20) and (3.21) in (3.22), is possible to obtain:

$$Q \leq \sqrt{\frac{(|v^+|^2 + |v^-|^2)^2}{v_\alpha^2 + v_\beta^2}\hat{I}^2 - P^2} \tag{3.23}$$

Equation (3.23) shows that the power P must be limited to avoid the generation of negative rooting. So:

$$P \leq \sqrt{\frac{(|v^+|^2 + |v^-|^2)^2}{v_\alpha^2 + v_\beta^2}\hat{I}^2} \tag{3.24}$$

The maximum power references waveform are the same of Fig.3.8. Even for the AARC, the control strategy is to set one of the power references, P or Q, to zero. The one set to zero performs no oscillation, while the other one features oscillations overlapped to the reference value.

3.5 FPNSC With Current Limitation Control

This current limitation control is different from the previous ones and can be found in literature[3]. Starting from the equation of the reference current, it is possible to demonstrate that the reference moves around an ellipse [3], as in Fig.3.9.

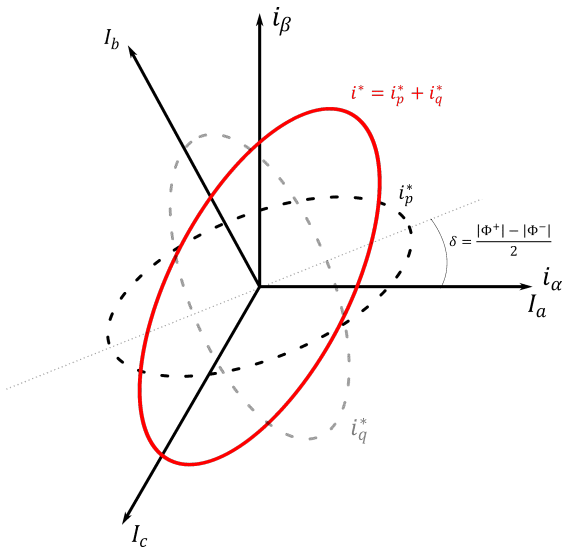

Figure 3.9: Loci of i^*,i_p^*,i_q^* for a given Φ^+ and Φ^-.

So, defining the projection in three-phase axis is possible to estimate the maximum peak phase current (Fig.3.10).

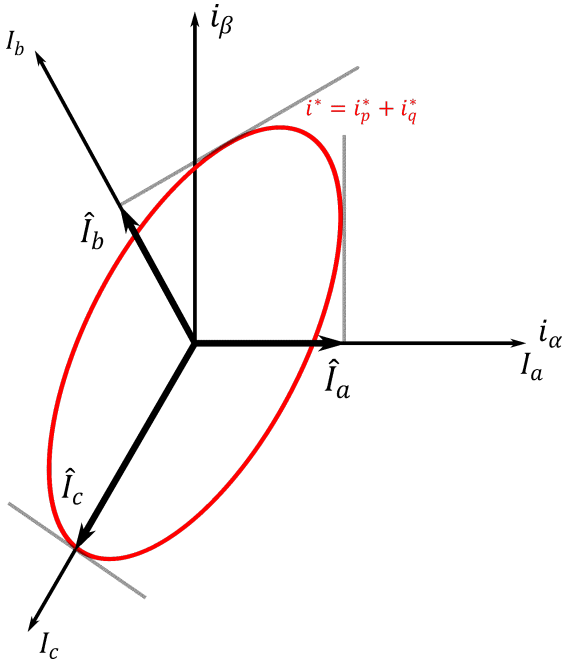

Figure 3.10: Maximum peak phase currents in three-phase axis.

which phase angle are defined in the table below.

Phase	γ
$\hat{I}_a$	$\gamma = \frac{\lvert\Phi^+\rvert - \lvert\Phi^-\rvert}{2} + 0$
$\hat{I}_b$	$\gamma = \frac{\lvert\Phi^+\rvert - \lvert\Phi^-\rvert}{2} + \frac{\pi}{3}$
$\hat{I}_c$	$\gamma = \frac{\lvert\Phi^+\rvert - \lvert\Phi^-\rvert}{2} - \frac{\pi}{3}$

Anyway, defining the equation to estimate the peak phase currents is out of our analysis and can be found in literature[3]. What is important to know is the physical meaning of δ, then used to define the phase angle of the three-phase currents γ. In our analysis will be analyzed the way to inject the maximum reactive power reference to the grid for a given set point of active power and maximum peak current supported by the converter. Essentially, starting from the current reference $\mathbf{i}^*$, it is possible to write an equation for a given maximum current amplitude and an active power reference.

$$\begin{aligned} 0 =& Q^2[k_2^2 \cdot |\mathbf{v}^-|^2 + (1-k_2)^2 \cdot |\mathbf{v}^+|^2 - 2k_2(1-k_2)cos(2\gamma) \cdot |\mathbf{v}^+| \cdot |\mathbf{v}^-|] \\ & - PQ[(2k_1 + 2k_2 - 4k_1k_2) \cdot |\mathbf{v}^+| \cdot |\mathbf{v}^-|sin(2\gamma)] \\ & + P^2[k_1^2 \cdot |\mathbf{v}^-|^2 + (1-k_1)^2 \cdot |\mathbf{v}^+|^2 + 2k_1(1-k_1)cos(2\gamma) \cdot |\mathbf{v}^+| \cdot |\mathbf{v}^-|] \\ & - \hat{I}^2 \cdot |\mathbf{v}^+|^2 \cdot |\mathbf{v}^-|^2 \end{aligned} \tag{3.25}$$

The value of $|\Phi^+|$ and $|\Phi^-|$ are the positive and negative sequence phase angle of the voltage. From equation (3.25) is possible to obtain

$$0 = aQ^2 + bQ + c \tag{3.26}$$

Equation (3.26) gives rise to three solutions because γ can have three different value as seen in the previous table. Between the three values of the reactive power, the minimum one must be selected for a given set point of active power and maximum peak current, e.g. $(Q = Q_{min}(\hat{I}, P^*))$.

Chapter 4

Simulations

4.1 Plecs Simulations

All the theoretical analysis has been validated using the software simulation PLECS. Basically, the simulation is made up of three blocks that represent the grid, the converter and load/generator. The grid block function is to generate a set of three-phase grid voltages, implementing also the possibility to generate the grid faults to test the various current control techniques. The block scheme is shown in Fig.(4.1).

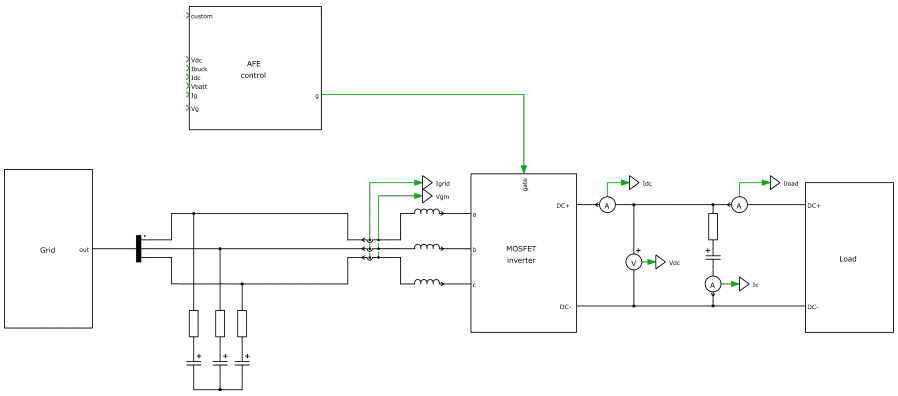

Figure 4.1: Plecs simulation block scheme.

The grid block generates the grid voltages before and during the fault. AFE control block scheme contains the C-Script block to implement the digital control to generate the current reference for the various techniques (IARC, BPSC, PNSC, AARC, FPNSC) and then modulating the inverter's legs. Load block scheme is essentially made up by a bidirectional buck/boost converter connected to a load/generator seen as a constant voltage generator (Fig.4.2).

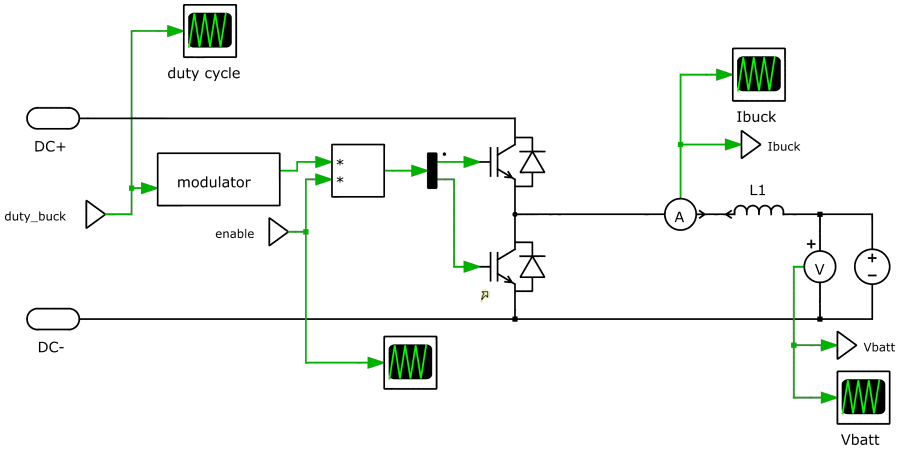

Figure 4.2: Load block.

The "modulator" block in Fig.4.2 takes as input the signal to compare with the triangular wave to trigger the three legs of the inverter and it is generated by the digital control inside the C-script function in AFE control block of Fig.4.1.

4.1.1 DC/DC Control Loop for a Grid Connected to a Generator

The control loop of the DC/DC converter changes if the grid is connected to a generator or to a load. In the case to be connected to a generator, it is made up by the voltage loop and the current loop, as in Fig.4.3.

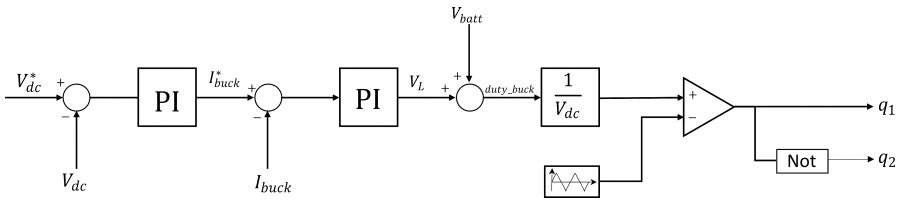

Figure 4.3: Voltage and current loop DC/DC side generator connected.

Fig.4.3 in terms of C-code can be implemented as follows:

```
Vdc_link_vars.fbk = Vdc;
PIReg(&Vdc_link_pars,&Vdc_link_vars);
Ibuck_ref = -Vdc_link_vars.out;// * Vdc/Vbatt;
Iload_vars.ref = Ibuck_ref;
Iload_pars.lim = Vdc;
Iload_vars.fbk = Ibuck;
```

```
Iload_vars.fwd = Vbatt;
PIReg(&Iload_pars,&Iload_vars);
duty_buck = (Iload_vars.out/Vdc);
```

4.1.2 DC/DC Control Loop for a Grid Connected to a Load

The control loop is different in case to be connected to a load because the DC-link capacitor is charged from the grid side, so the control for the buck/boost presents only the DC current loop Fig.4.4.

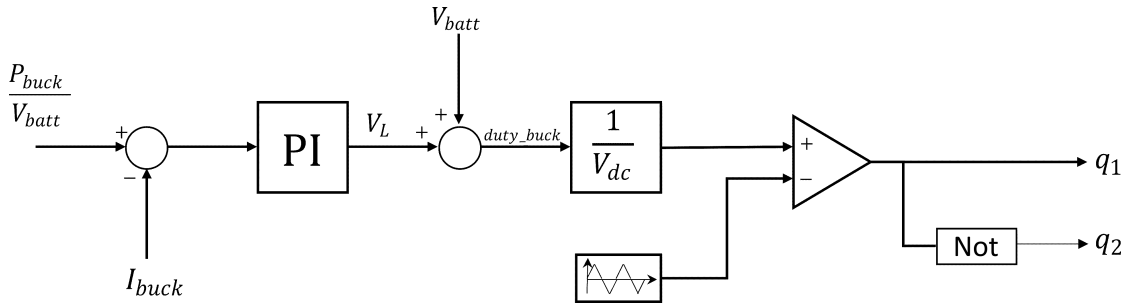

Figure 4.4: Current control DC side load connected.

Fig.4.4 in terms of C-code can be translated as follows:

```
Iinverter_ref = Pbuck/300.0;
Iload_vars.ref = Iinverter_ref;
Iload_pars.kp = 500.0 * double_pi * 10e-3;
Iload_pars.ki = 0.2* 500.0 * double_pi * Iload_pars.kp * Ts;
Iload_pars.lim = Vdc;
Iload_vars.fbk = Ibuck;
Iload_vars.fwd = Vbatt;;
PIReg(&Iload_pars,&Iload_vars);
duty_buck = Iload_vars.out/Vdc;
```

For what just said, the DC-link voltage control loop will be inside the control of the inverter rather than the DC/DC side. In this case the V_{dc} control loop generates as output a DC current reference, I^*_{dc}, that multiplied for the DC voltage reference V^*_{dc} generate the power reference P, then used in the grid current control techniques.

The DC-link voltage control loop in case to be connected to a load is shown in Fig.4.5.

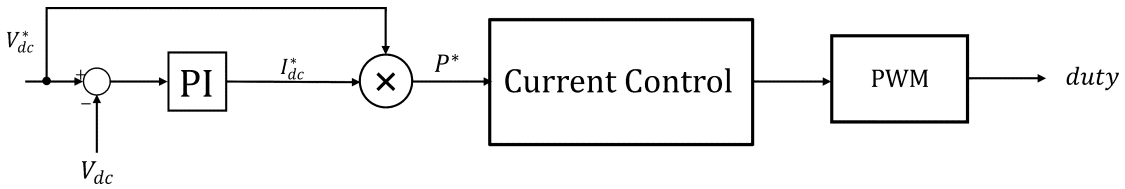

Figure 4.5: DC-link voltage control, load case.

Fig.4.5 in terms of C-code can be translated as follows:

```
Vdc_par.kp=wv_band*C_cond;
Vdc_par.ki=0.2*wv_band*Vdc_par.kp*Ts;
Vdc_var.ref = Vdc_ref;
Vdc_var.fbk = Vdc;
PIReg(&Vdc_par,&Vdc_var);
I_ref = Vdc_var.out;
P = I_ref * Vdc_ref;
```

4.2 Simulation Results (Case Generator)

How to use the power reference P and maximize the reactive power Q has been already discussed in the previous sections, so once how to control the DC/DC side has been defined, it is possible to simulate a fault and test the various techniques. The parameters chosen for the simulation are reported in the next page.

GRID	L_{grid}	$120\mu H$
	$V_{abc\,,rms}$	120V
	C_{filter}	$22\mu F$
DC-SIDE	C_{DC}	$1.8mF$
	L_{buck}	$10mH$
	V_{batt}	300V
	$V_{DC,link}$	400V
INVERTER	Dead Time	$3\mu s$
	f_{sw}	10kHz
	$f_{i,band}$	500Hz
	$f_{v,band}$	30Hz
	$k_{p,i}$	$2\pi f_{i,band} \cdot L_{grid}$
	$k_{p,v}$	$2\pi f_{v,band} \cdot C_{DC}$
	$k_{i,i}$	$0.2 \cdot \omega_{i,band} \cdot k_{p,i}$
	$k_{i,v}$	$0.2 \cdot \omega_{v,band} \cdot k_{p,v}$
BUCK/BOOST	Dead Time	$3\mu s$
	f_{sw}	10kHz
	$f_{i,band}$	500Hz
	$f_{v,band}$	30Hz
	$k_{p,i}$	$2\pi f_{i,band} \cdot L_{buck}$
	$k_{p,v}$	$2\pi f_{v,band} \cdot C_{DC}$
	$k_{i,i}$	$0.2 \cdot \omega_{i,band} \cdot k_{p,i}$
	$k_{i,v}$	$0.2 \cdot \omega_{v,band} \cdot k_{p,v}$

Figure 4.6: Parameters used in the simulations

All the simulations were tested for a voltage dip in which $V_a = 1pu$, $V_b = 0.85pu$ and $V_c = 0.85pu$, as shown in (Fig.4.7).

In the next section, the simulation results for every technique (IARC, BPSC, PNSC, AARC, FPNSC) are shown and discussed.

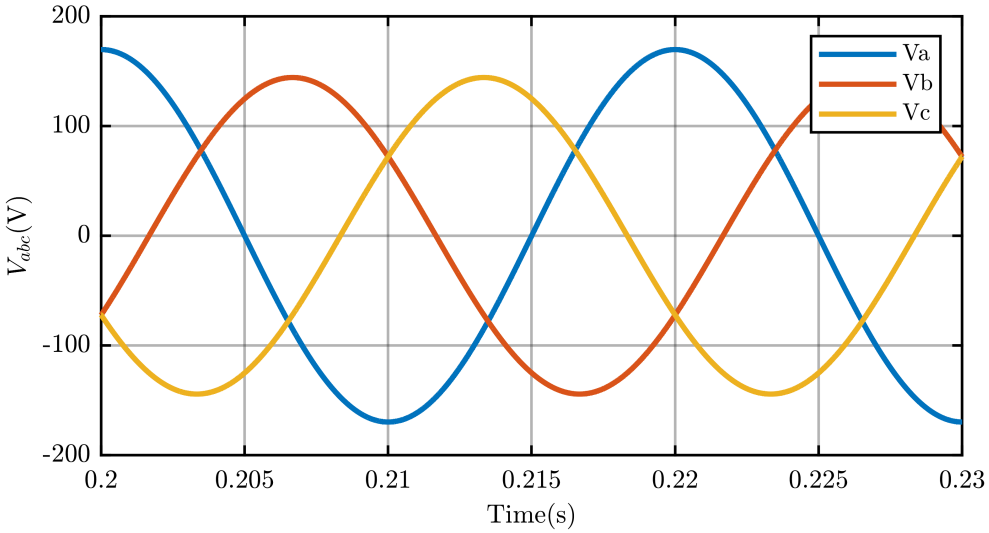

Figure 4.7: Voltage dip.

4.2.1 Simulation Results for IARC

The results of the simulation for IARC technique are shown in the following figures.

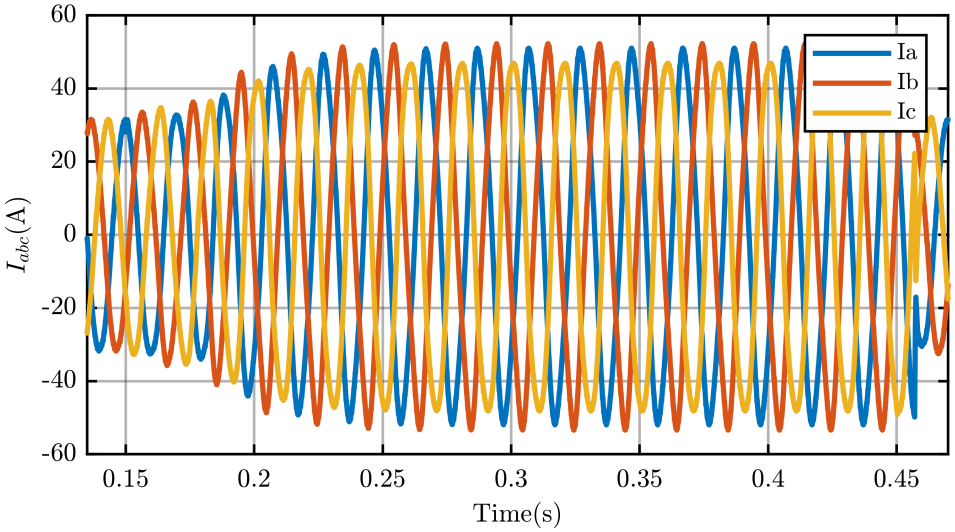

Figure 4.8: Phase currents during fault conditions.

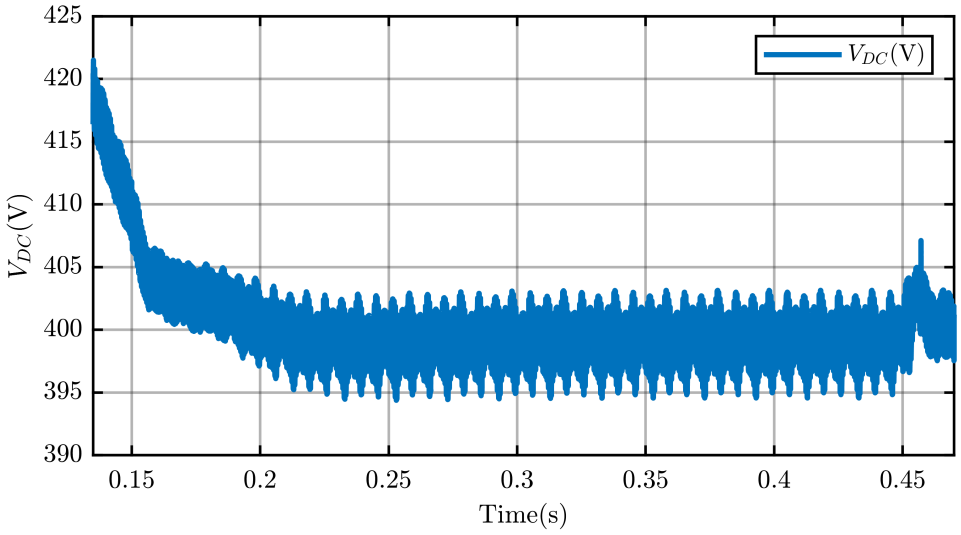

Figure 4.9: DC-link voltage during fault conditions.

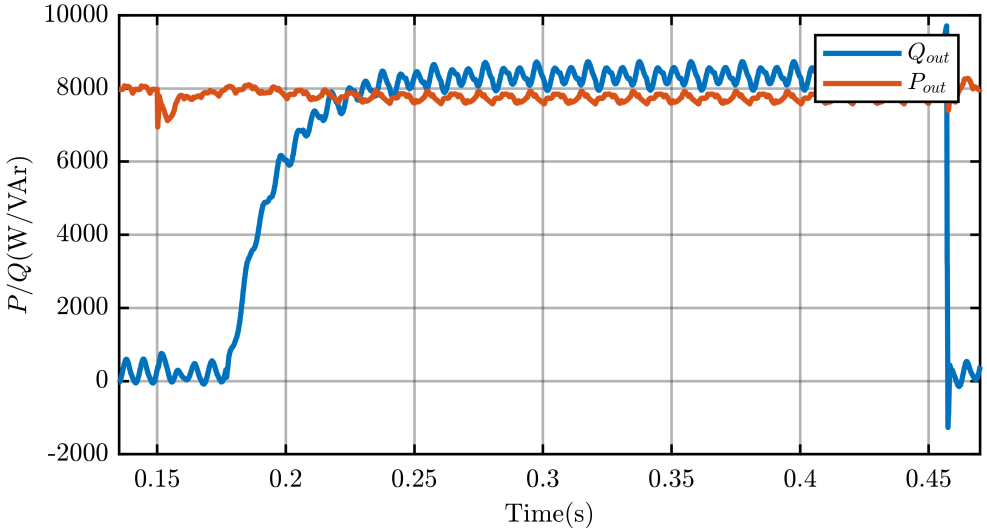

Figure 4.10: Active and reactive power during fault conditions.

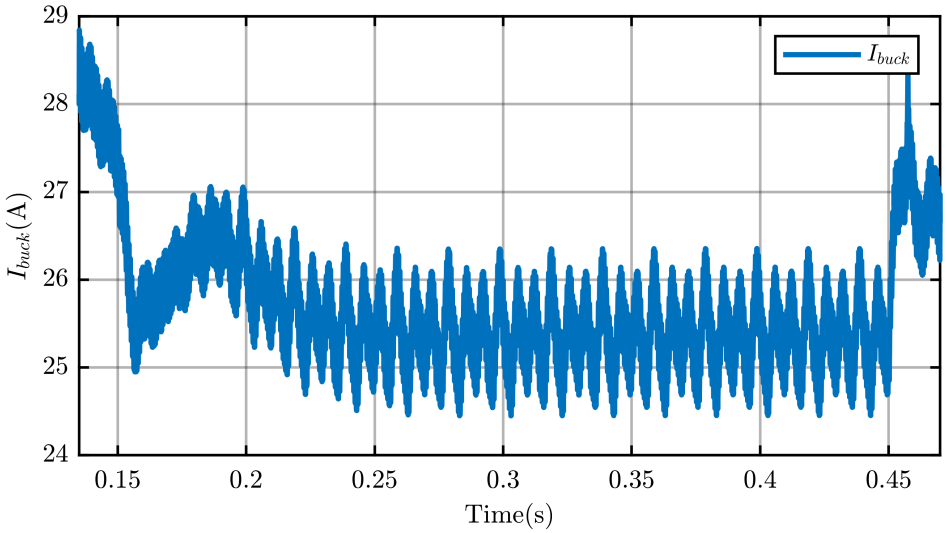

Figure 4.11: Buck current during fault conditions.

As anticipated from the theory, currents (Fig.4.8) features a high harmonics content, powers are constant, and the buck current oscillation is very limited due to power waveforms. The reactive power is maximized, and this feature can be seen in the peak value of the currents (55A circa).

4.2.2 Simulation Results for BPSC

The results of the simulation for BPSC technique are shown in the following figures.

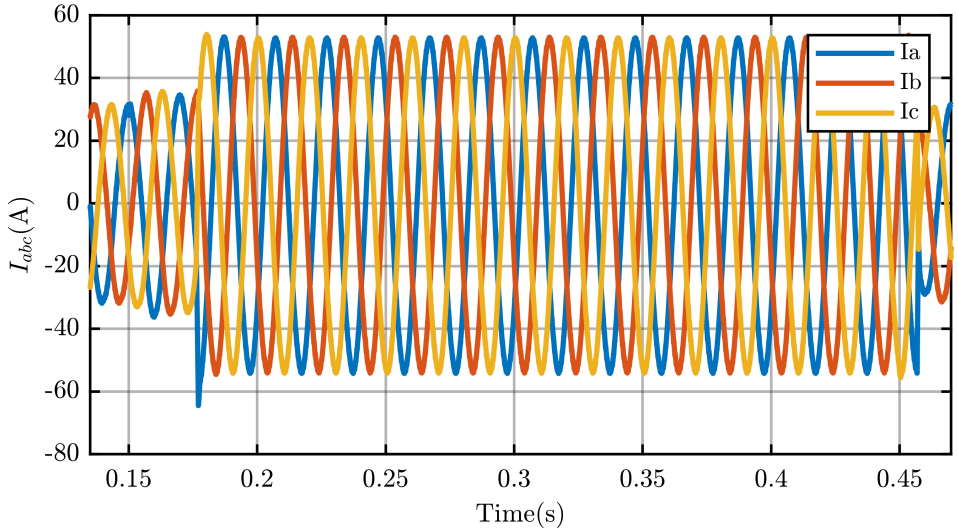

Figure 4.12: Phase currents during fault conditions.

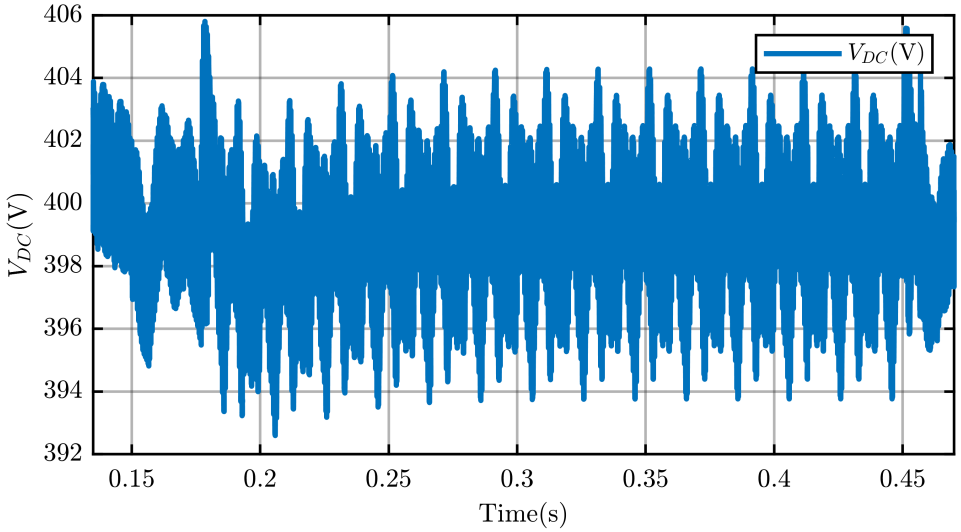

Figure 4.13: DC-link voltage during fault conditions.

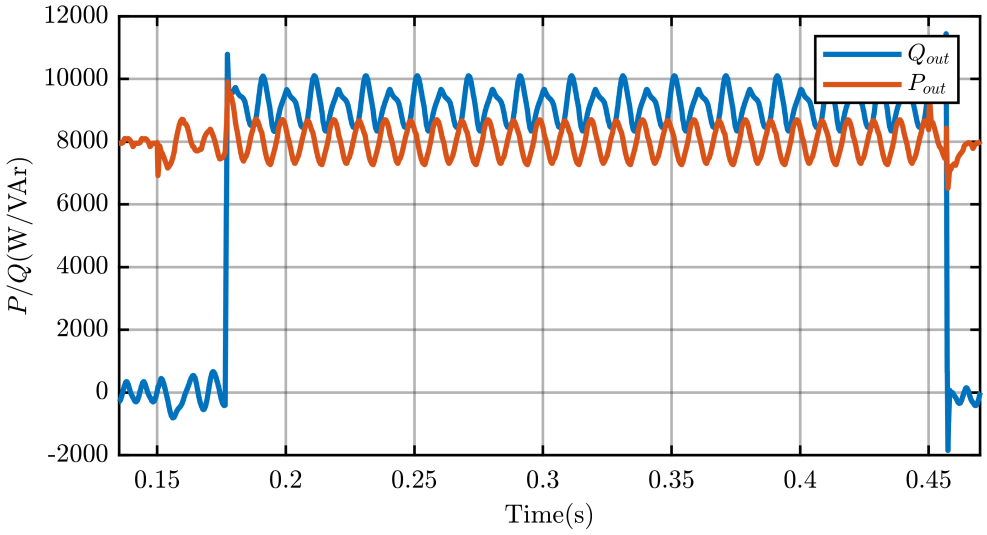

Figure 4.14: Active and reactive power during fault conditions.

As already seen in theory, BPSC inject a set of balanced currents during the faults. Contrary to the IARC, either the powers injected to the grid are oscillating, influencing the current injected from the buck converter. This can be a problem in case the generator was a battery, because oscillating current could stress the battery or the latter could not be able to give that current at the output.

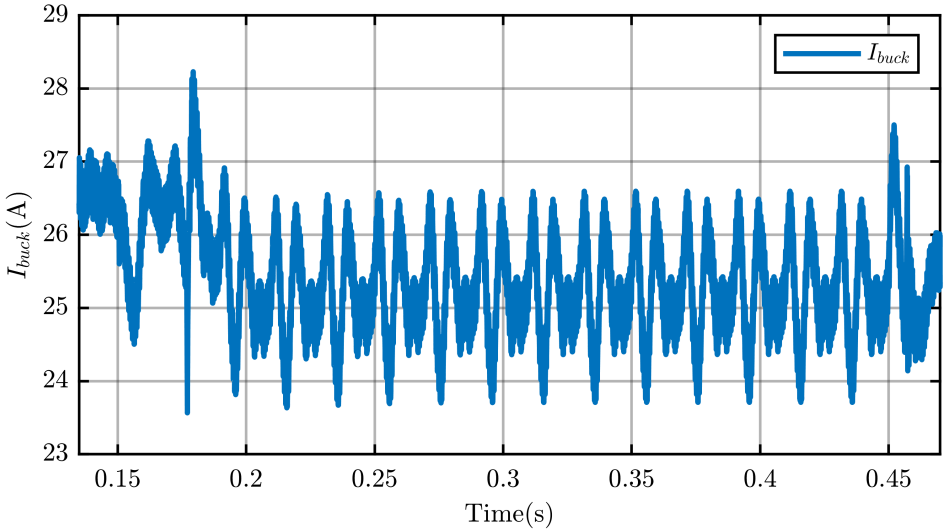

Figure 4.15: Buck current during fault conditions.

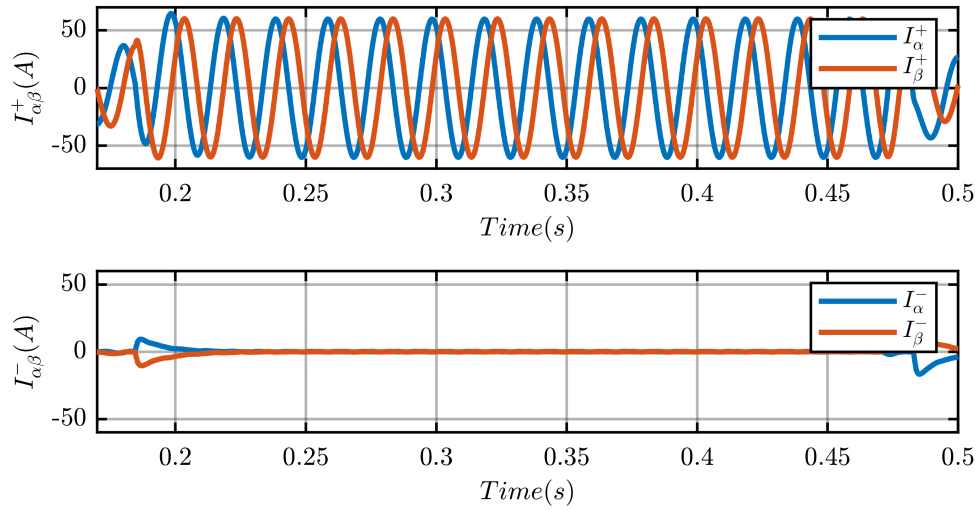

Figure 4.16: Currents sequences during a fault.

4.2.3 Simulation Results for PNSC

For PNSC technique, the simulation results are developed in more test than one, because it is useful to see how the technique works in three different conditions.

- Injecting Active power P only.
- Injecting Reactive Power Q only.
- Injecting Active and Reactive power.

Starting from injecting only Active power, we obtain the following results.

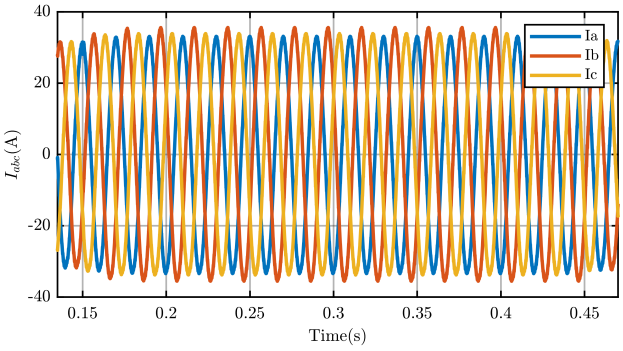

Figure 4.17: Phase currents during fault conditions.

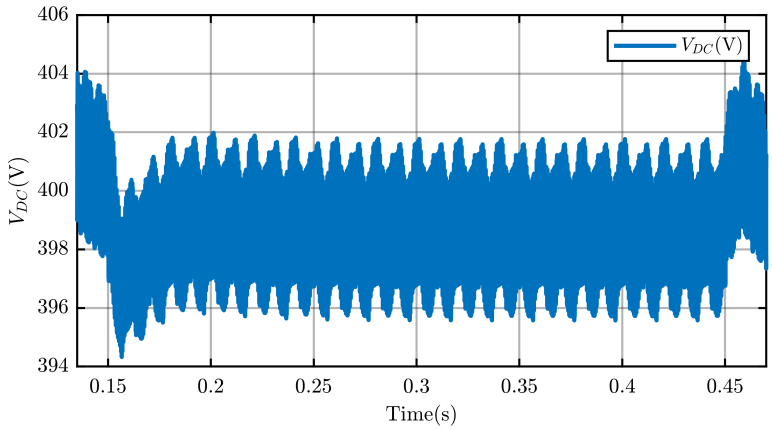

(a) DC-link voltage during fault conditions.

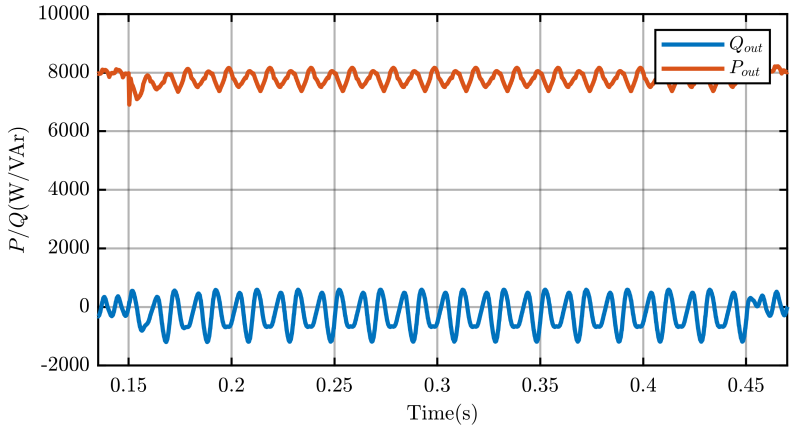

(b) Active and reactive power during fault conditions.

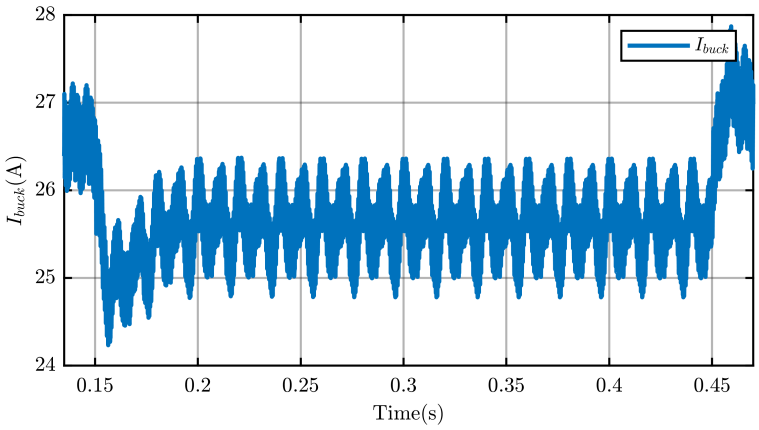

(c) Source current during fault conditions.

Figure 4.18: DC-link voltage (4.18a), active and reactive power(4.18b), source current, I_{buck}(4.18c), during grid fault conditions.

Injecting Reactive Power Q only

As already discussed in theory, setting the Reactive power reference to zero performs the cancellation of the ripple term in the output instantaneous active power, but performing a ripple in the instantaneous output reactive power. The consequence of this is that the buck current is constant as the Vdc, but avoiding supporting the grid during the fault, risking being isolated during the fault.
The symmetrical result can be obtained, setting the active power reference to zero, cancelling the reactive power ripple. The simulations result injecting only the reactive power are shown in the following figures.

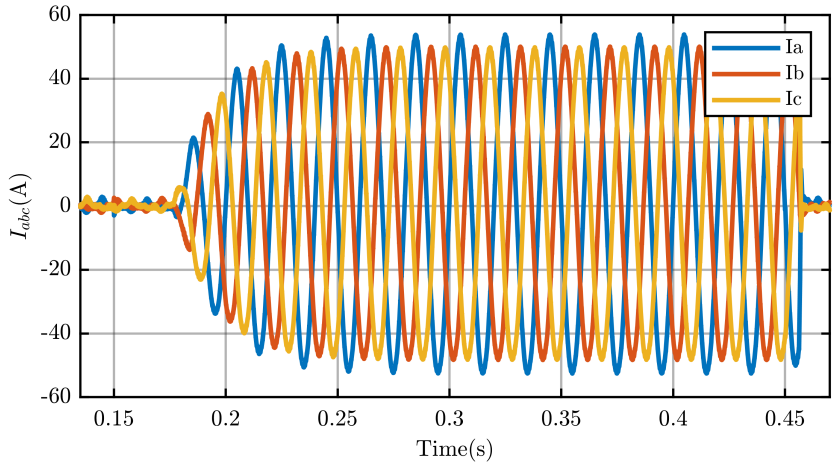

Figure 4.19: Phase currents during fault conditions.

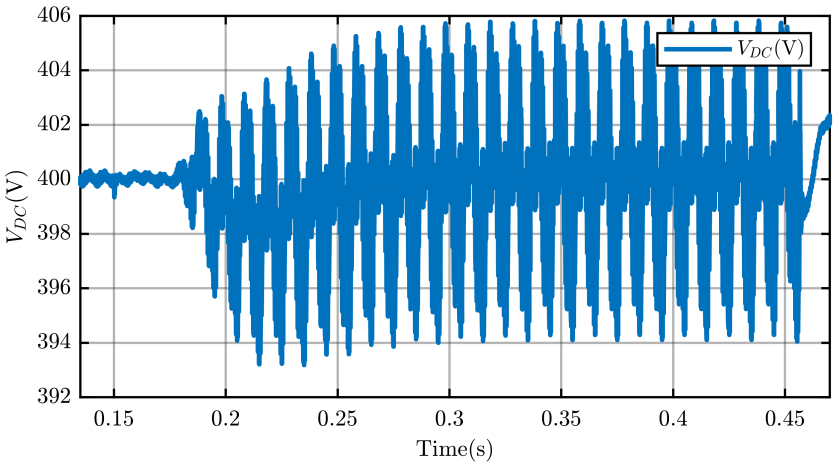

Figure 4.20: DC-link voltage during fault conditions.

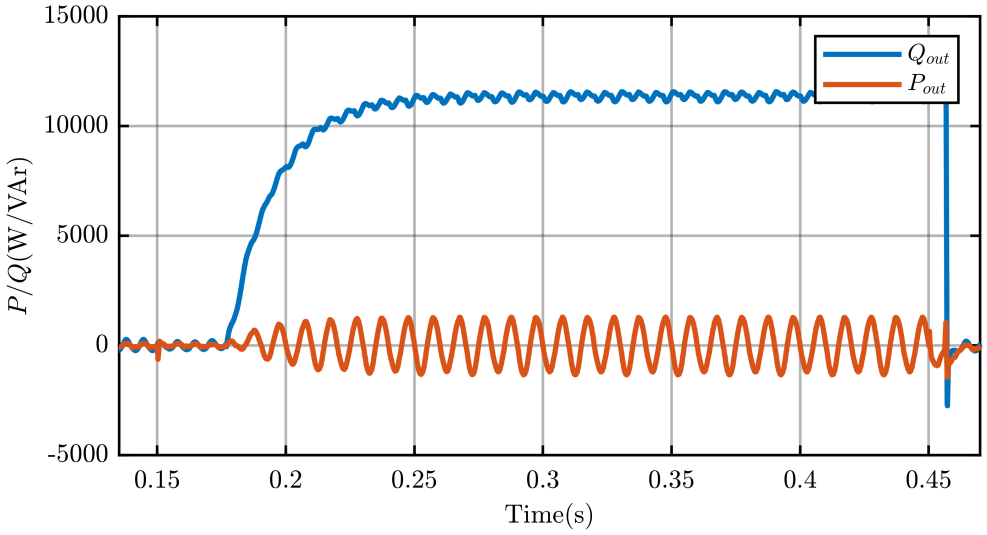

Figure 4.21: Active and reactive power during fault conditions.

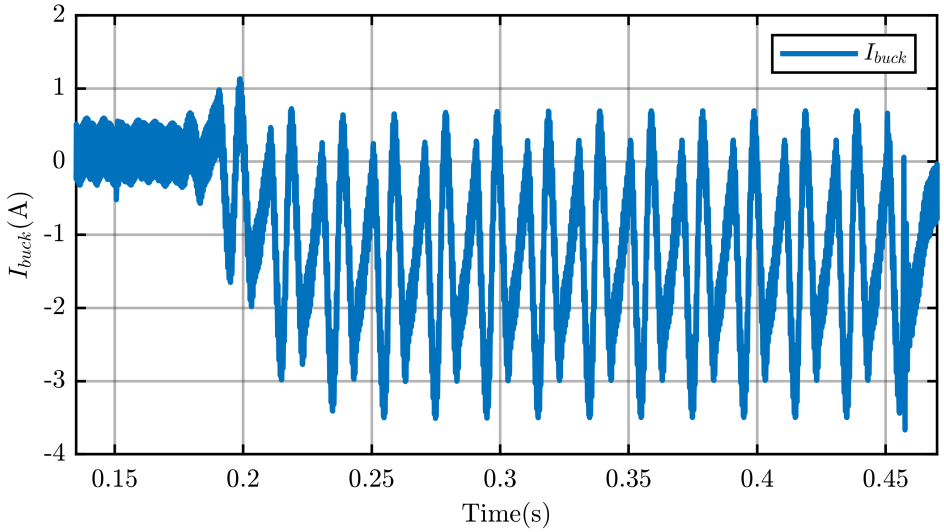

Figure 4.22: Buck current during fault conditions.

In this case the reactive power is maximized, fully supporting the grid during the fault but the active power generation is wasted.

Injecting Active and Reactive power

The last simulation represents an improper use of the PNSC technique, because it does not exploit the mathematical strategy to cancel the power oscillations, based on setting one of the two power reference to zero, as just seen. The simulation results injecting either the active power and the reactive one are shown in the following figures.

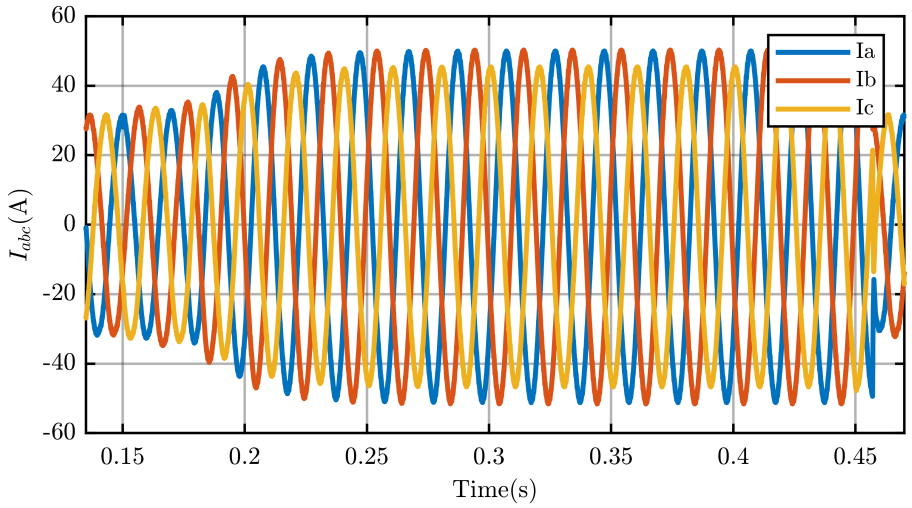

Figure 4.23: Phase currents during fault conditions.

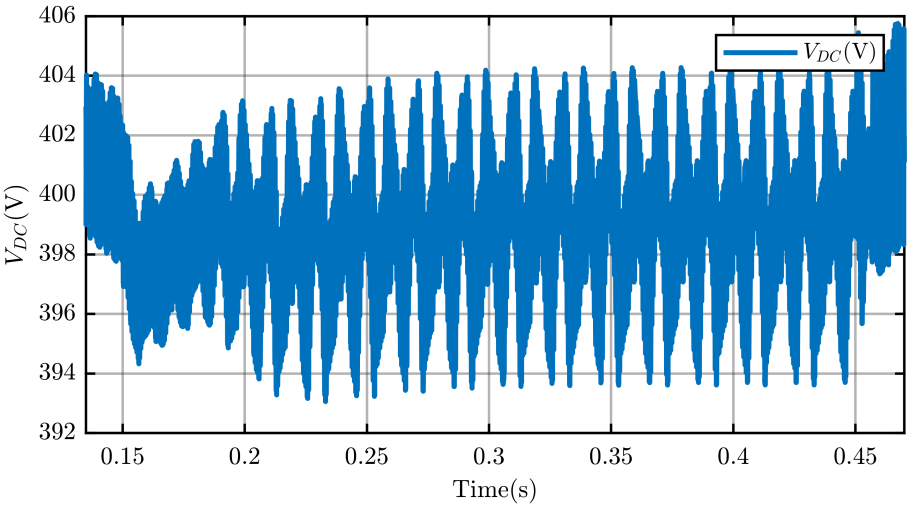

Figure 4.24: DC-link voltage during fault conditions.

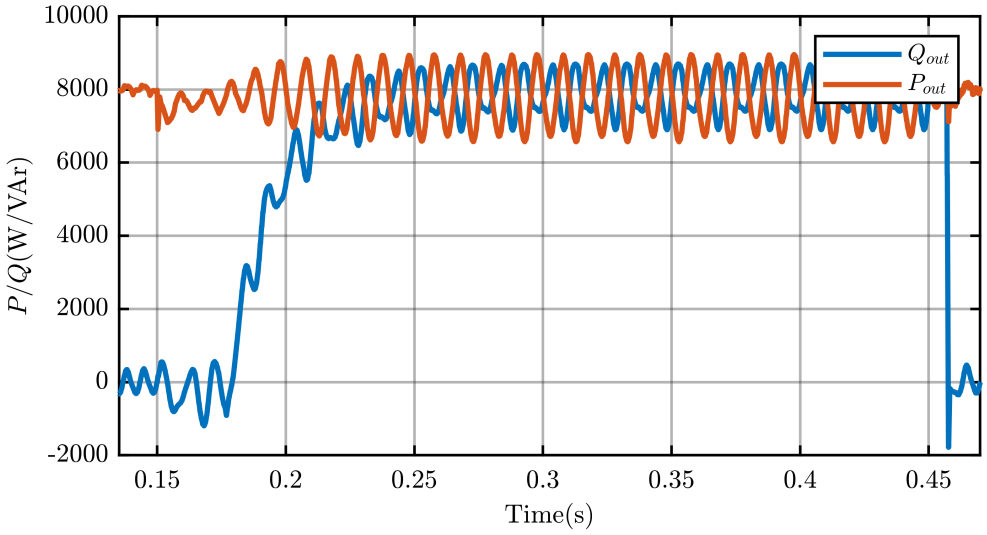

Figure 4.25: Active and reactive power during fault conditions.

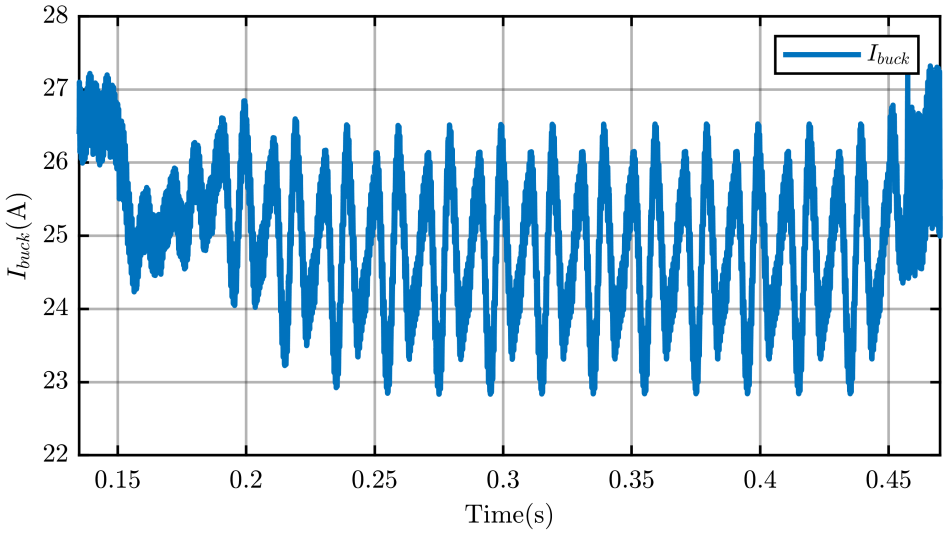

Figure 4.26: Buck current during fault conditions.

4.2.4 Simulation Results for AARC

For AARC technique, the simulation results are developed in more test than one, because it is useful to see how the technique works in three different conditions.

- Injecting Active power P only.
- Injecting Reactive Power Q only.
- Injecting Active and Reactive power.

As already discussed in theory, the only way to cancel the power oscillation is to set the power reference to zero. The power reference between the two (P or Q) set to zero performs no oscillations. Starting from injecting only Active power, we obtain the following results.

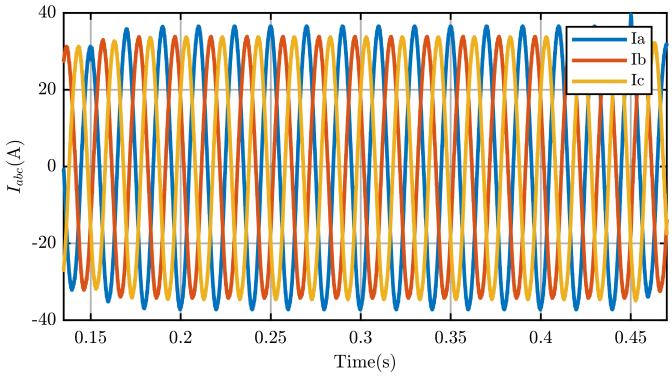

Figure 4.27: Phase currents during fault conditions.

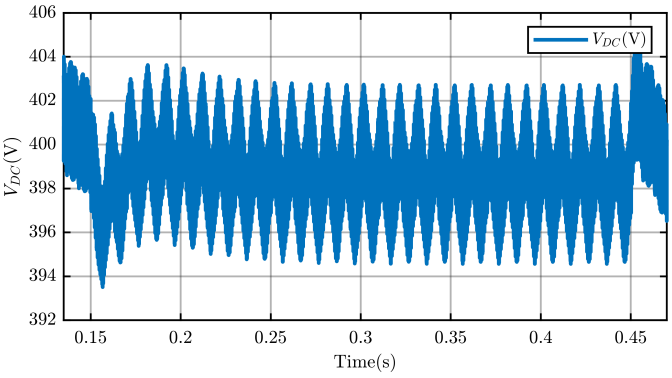

Figure 4.28: DC-link voltage during fault conditions.

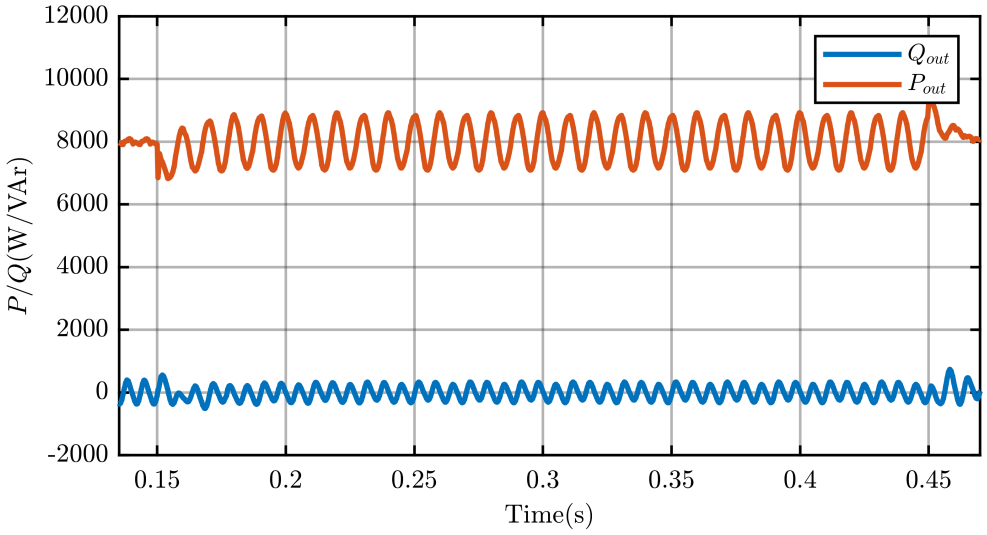

Figure 4.29: Active and reactive power during fault conditions.

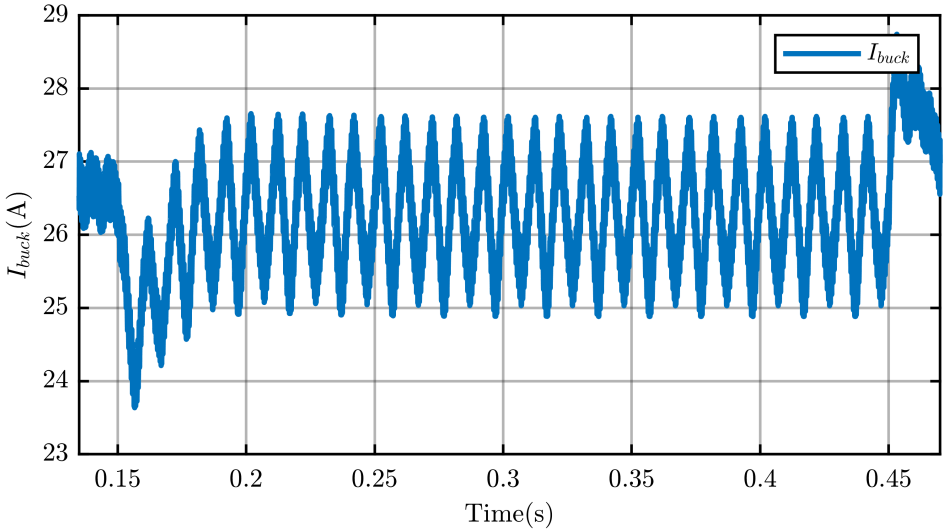

Figure 4.30: Buck current during fault conditions.

As we can see, Q is set to zero, and it keeps constant in time while P performs oscillations.

Injecting Reactive Power Q only

In the following figures, instead, we can see the results of setting the active power reference to zero.

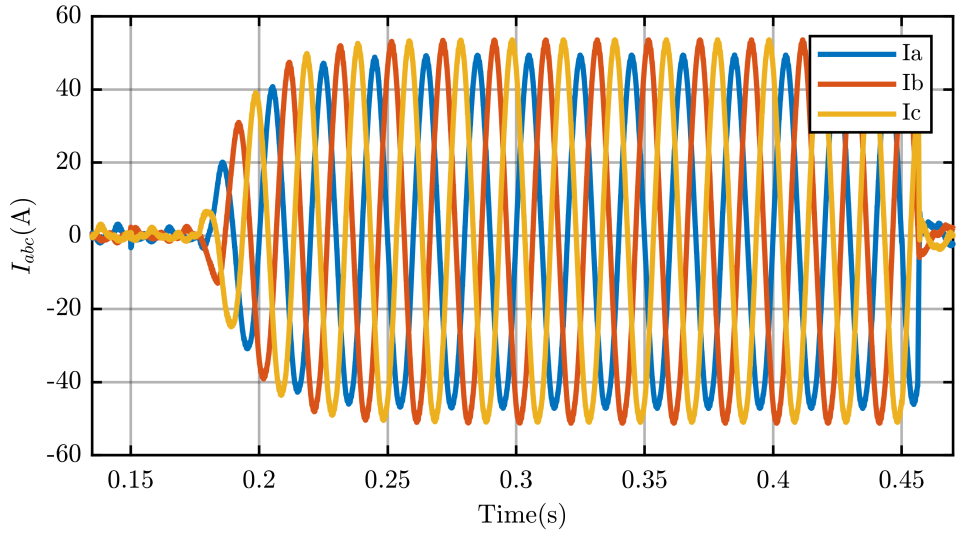

Figure 4.31: Phase currents during fault conditions.

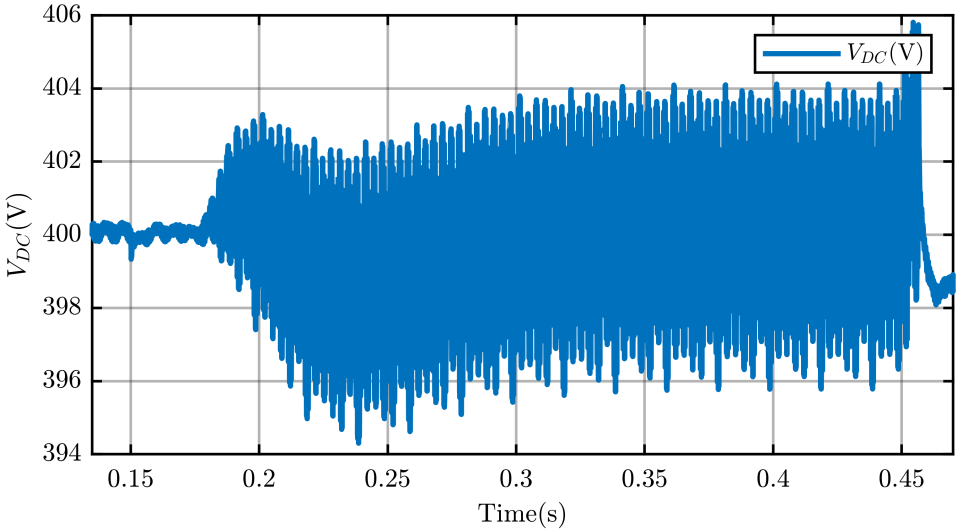

Figure 4.32: DC-link voltage during fault conditions.

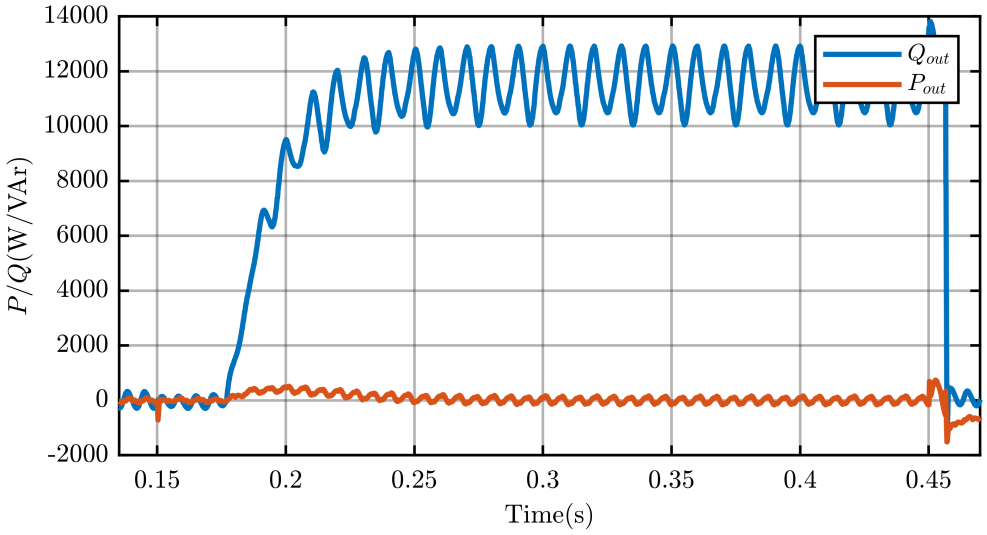

Figure 4.33: Active and reactive power during fault conditions.

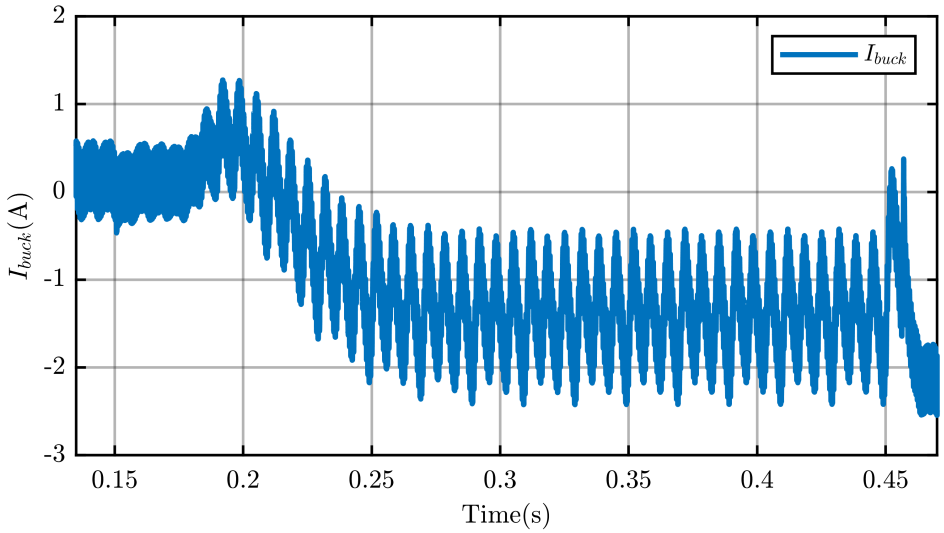

Figure 4.34: Buck current during fault conditions.

In this case, the reactive power is maximized but oscillating in respect to the PNSC, but the active power generation is wasted also if constant in time.

Injecting Active and Reactive power

The last simulation represents an improper use of the AARC technique, because it does not exploit the mathematical strategy to cancel the power oscillations, based on o set one of the two power reference to zero, as just seen.
The simulation results in injecting either the active power and the reactive one are shown in the following figures.

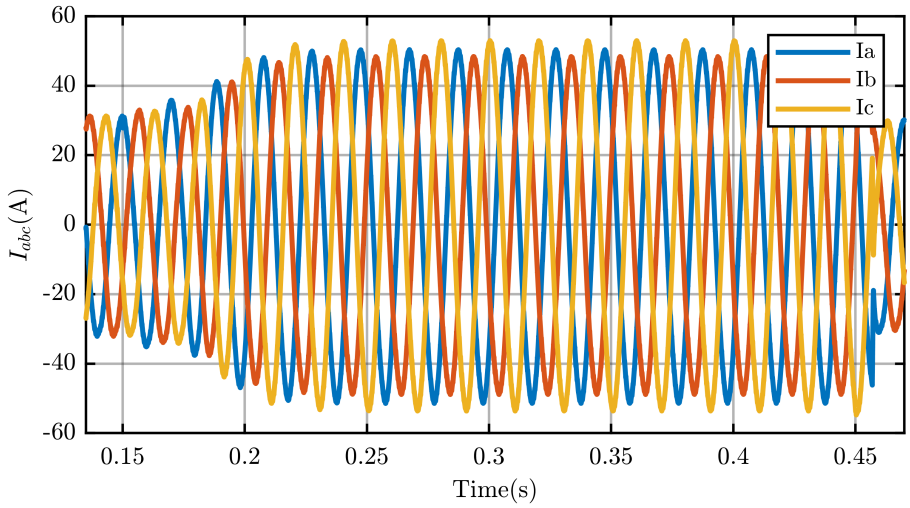

Figure 4.35: Phase currents during fault conditions.

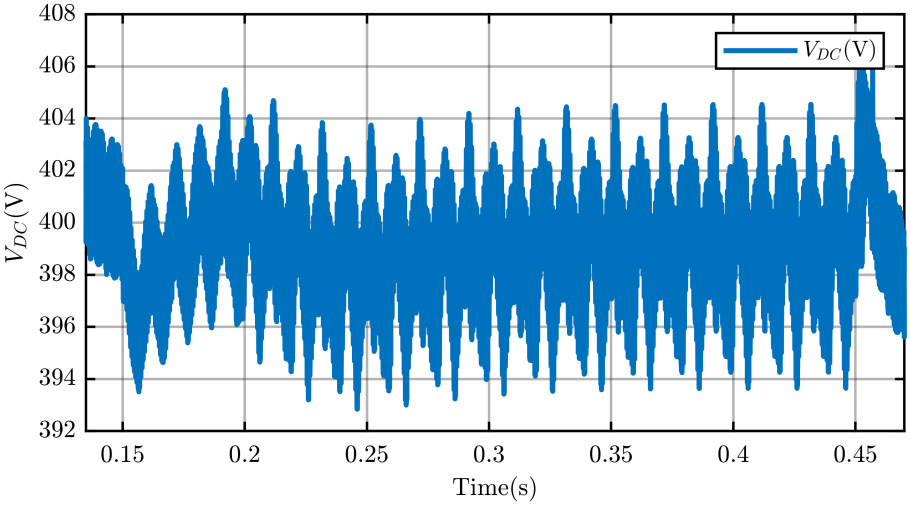

Figure 4.36: DC-link voltage during fault conditions.

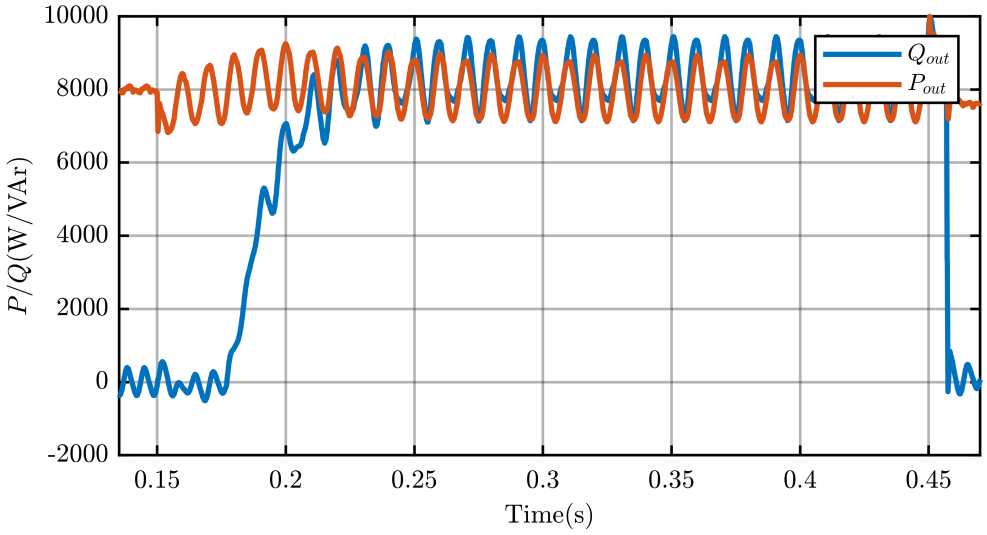

Figure 4.37: Active and reactive power during fault conditions.

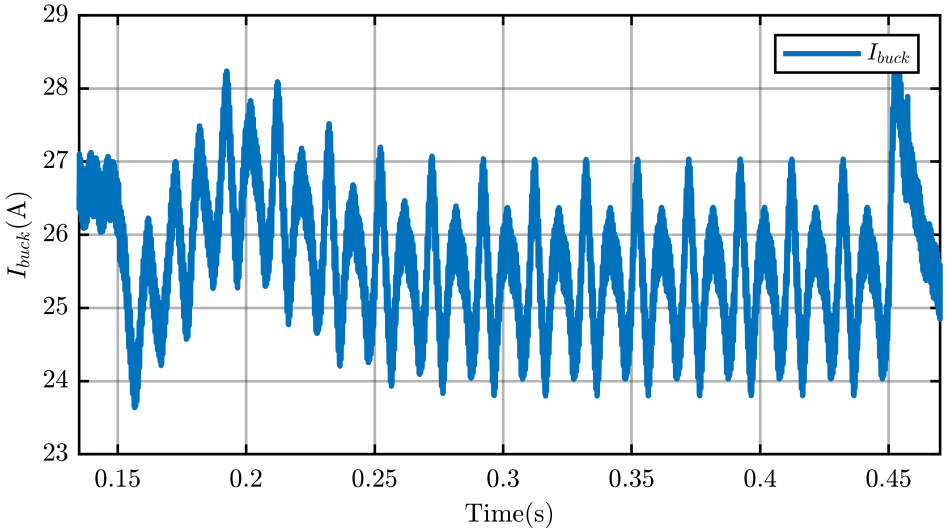

Figure 4.38: Buck current during fault conditions.

As we can see, the oscillations in power reference generates oscillations in the source current, I_{buck}.

4.2.5 Simulation Results for FPNSC

As already said, FPNSC is the more flexible technique, because by setting k_1 and k_2 is possible to performs no active power oscillations and supporting the grid with the maximum amount of reactive power.
The result for k_1 and k_2 set to avoid instantaneous active power oscillation is shown in the following figures.

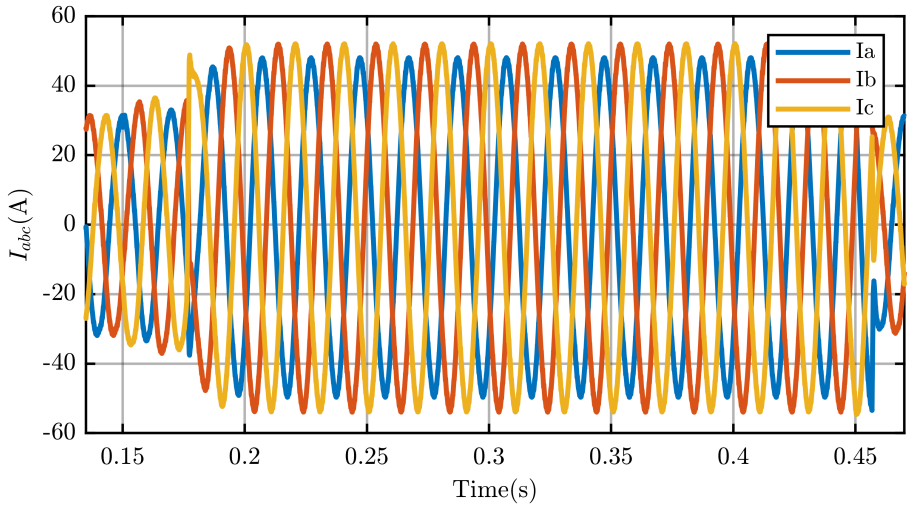

Figure 4.39: Phase currents during fault conditions.

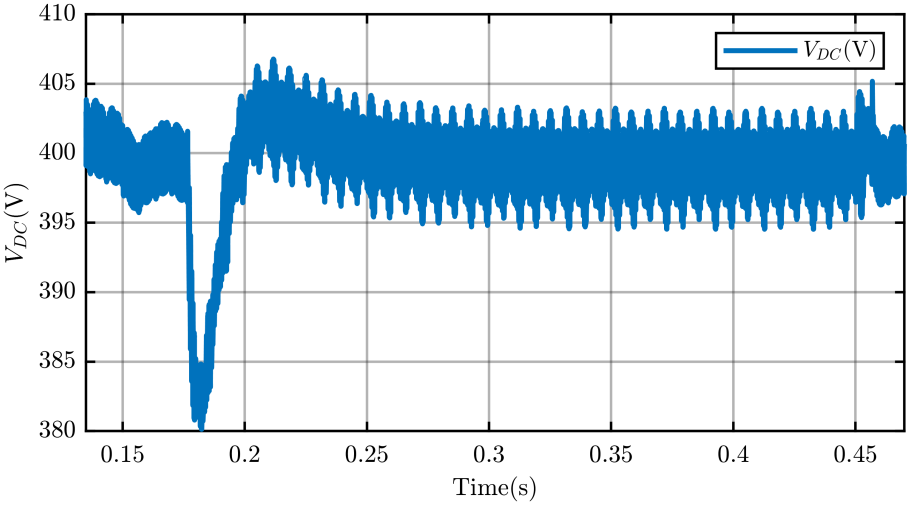

Figure 4.40: DC-link voltage during fault conditions.

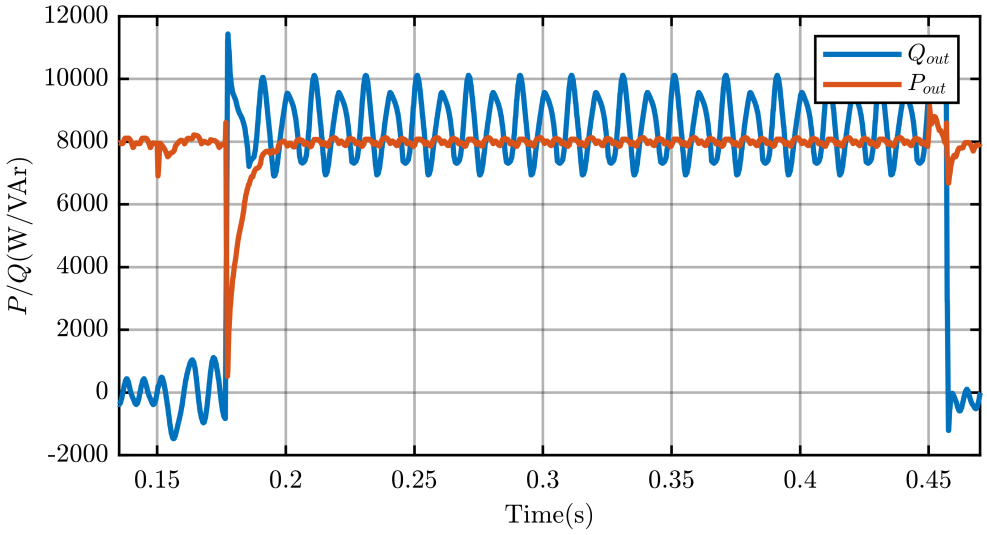

Figure 4.41: Active and reactive power during fault conditions.

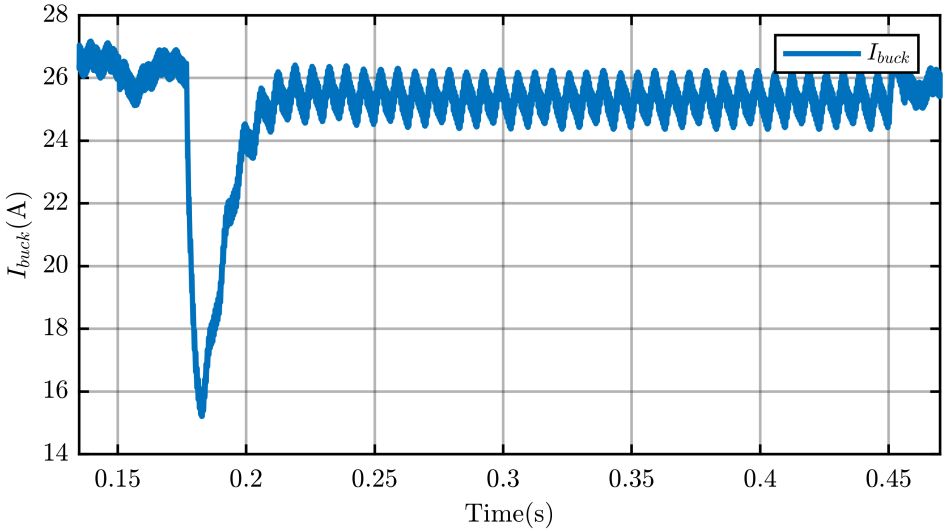

Figure 4.42: Buck current during fault conditions.

It is also possible to set k_1 and k_2 to obtain the symmetrical result for the reactive power. In this case, the active power is oscillating.

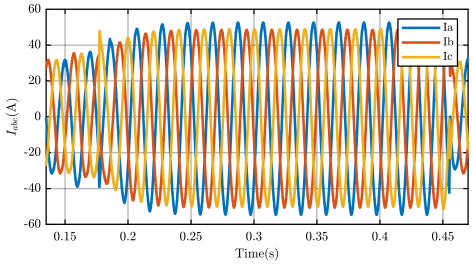

(a) Phase currents during fault conditions.

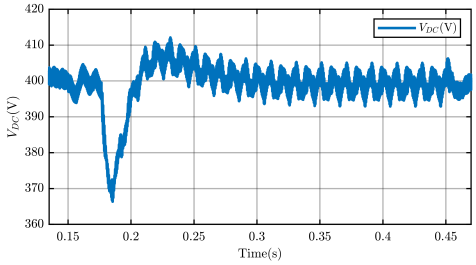

(b) DC-link voltage during fault conditions.

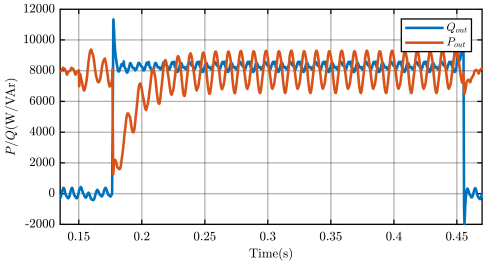

(c) Active and reactive power during fault conditions.

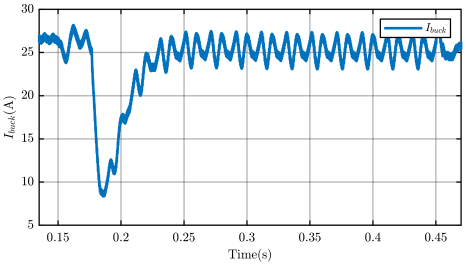

(d) Buck current during fault conditions.

Figure 4.43: FPNSC simulation with k_1 and k_2 set to generate constant reactive power.

4.3 Simulation Results (Case Load)

In this case, the grid is connected to a load. For what already explained, the DC-link voltage control loop is managed by the grid control; it means that the power oscillations are absorbed by the DC-link capacitor. Absorbing power oscillations could be a problem in terms of stresses on the DC-link capacitors because of the RMS value of the current ripple and the ESR resistor in series to the capacitor incrementing power losses. The relation between the voltage ripple and current is reported in (4.1). So, if the amplitude of the voltage ripple increase by a factor of 2, also the current absorbed will be double.

$$I_{pk} = j\omega C \cdot V_{dc,pk}; \tag{4.1}$$

The ESR value is not constant and depends on the frequency and the temperature, as reported in Fig.4.44. It is important to notice how at 100Hz the ESR assumes heavy values, incrementing also the power losses, as reported in (4.2)

$$P_{losses} = 0.5 \cdot ESR \cdot I_{pk}^2 \tag{4.2}$$

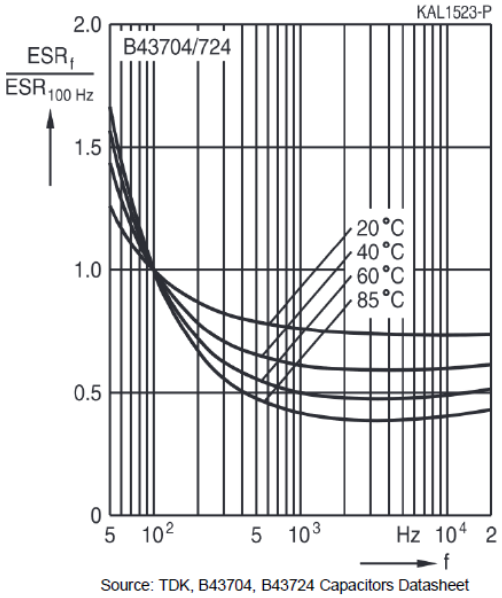

Figure 4.44: ESR capacitor value.

The following subsections are going to shows the results of the simulations in case to be connected to a load, showing the same results for the generator case except for the power oscillations that in this case influence the DC-link voltage and not the buck current.

4.3.1 Simulation Results for IARC

The simulation results for the load case are the following.

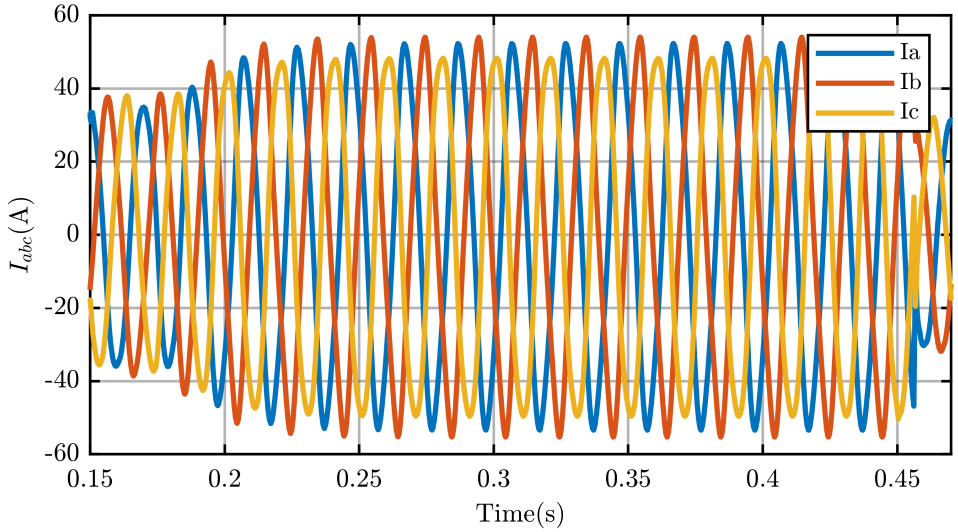

Figure 4.45: Phase currents during fault conditions.

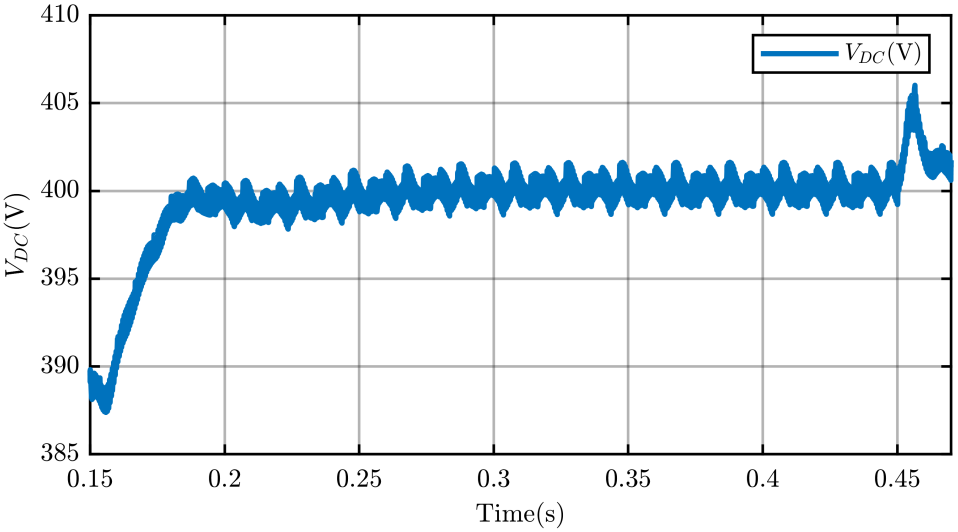

Figure 4.46: DC-link voltage during fault conditions.

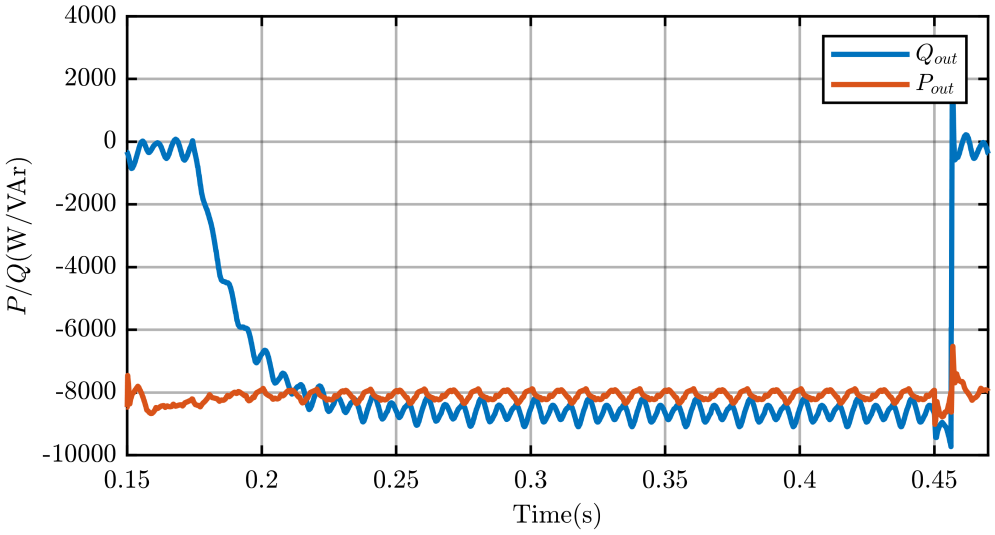

Figure 4.47: Active and reactive power during fault conditions.

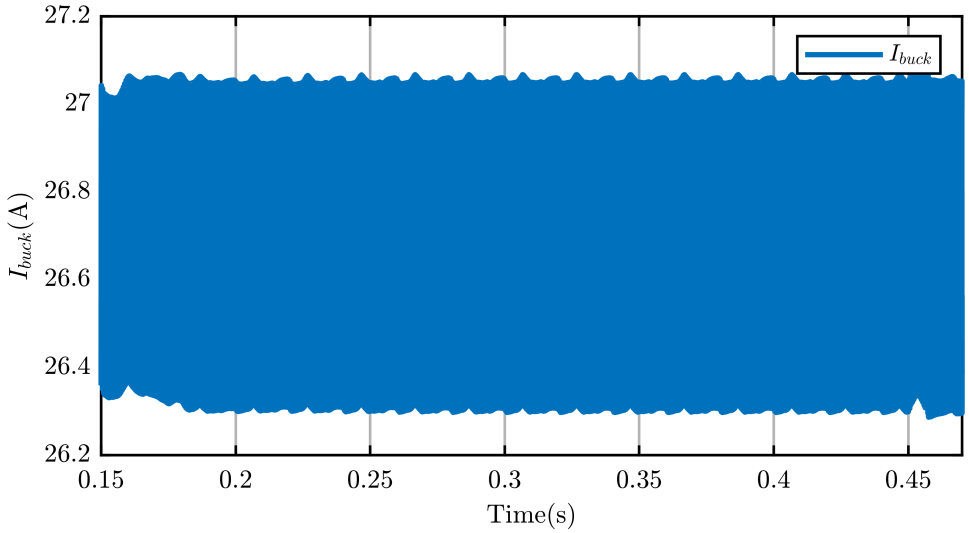

Figure 4.48: Buck current during fault conditions.

4.3.2 Simulation Results for BPSC

The simulation results for the load case are the following.

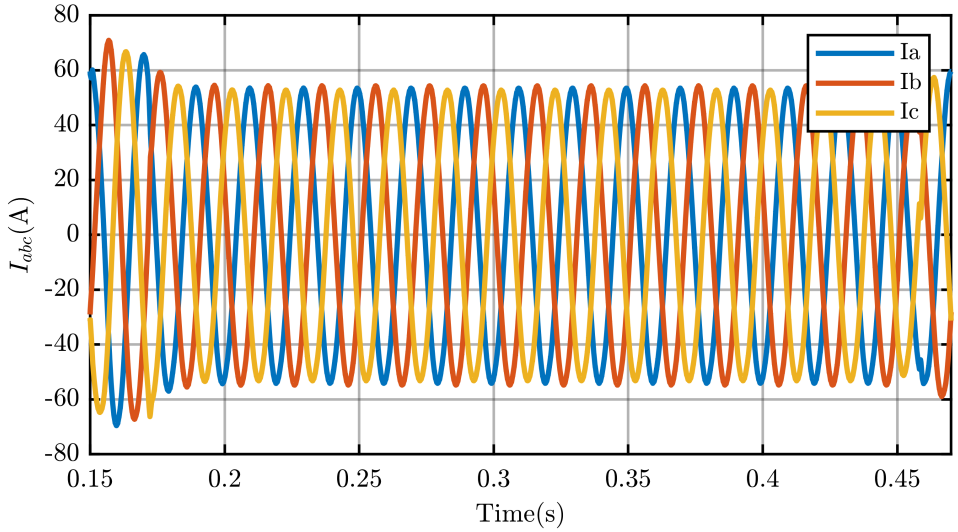

Figure 4.49: Phase currents during fault conditions.

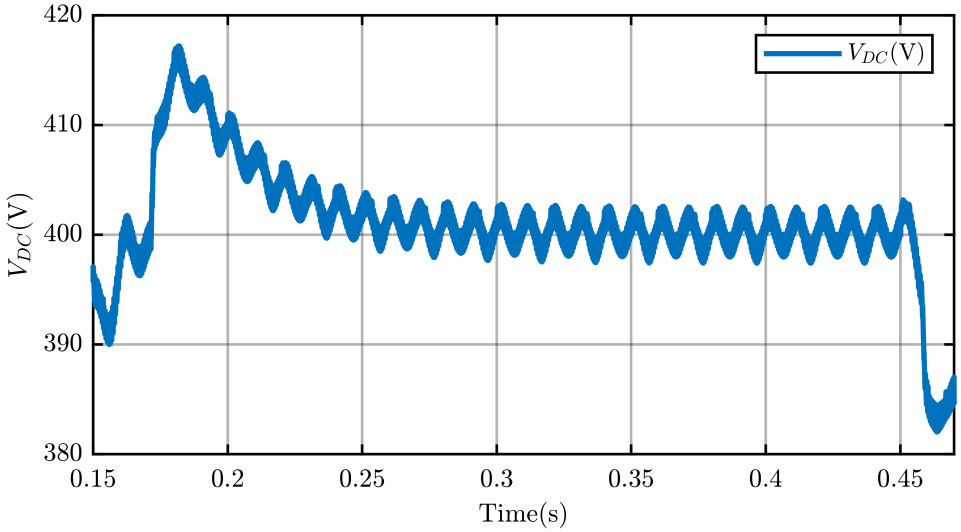

Figure 4.50: DC-link voltage during fault conditions.

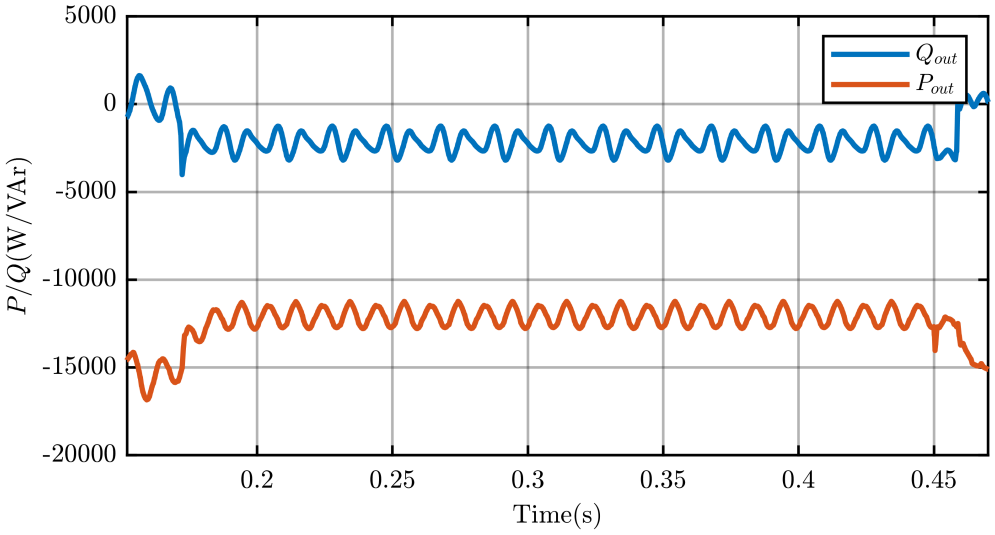

Figure 4.51: Active and reactive power during fault conditions.

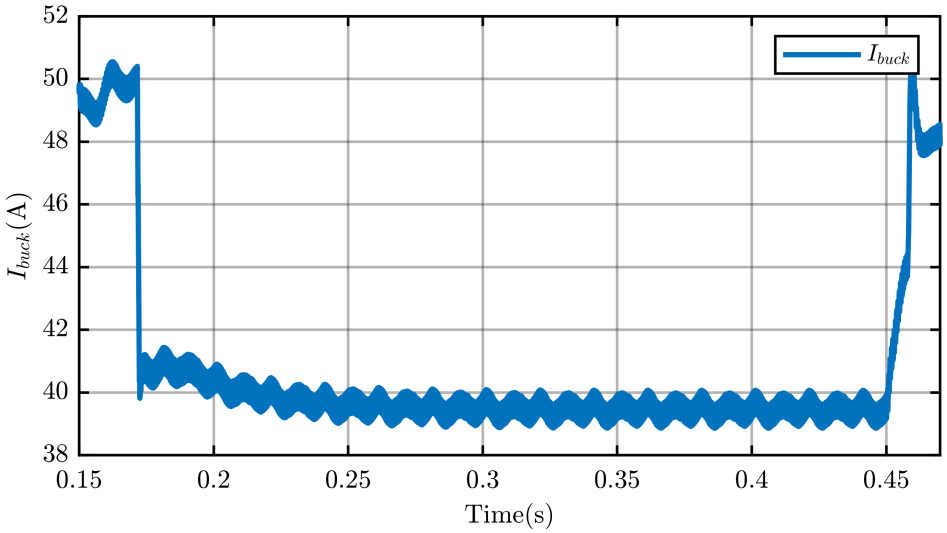

Figure 4.52: Buck current during fault conditions.

4.3.3 Simulation Results for PNSC

As for the case generator, the PNSC technique is tested in three different ways. The simulation results for the load case are the following.Starting from absorbing only Active power, we obtain the following results.

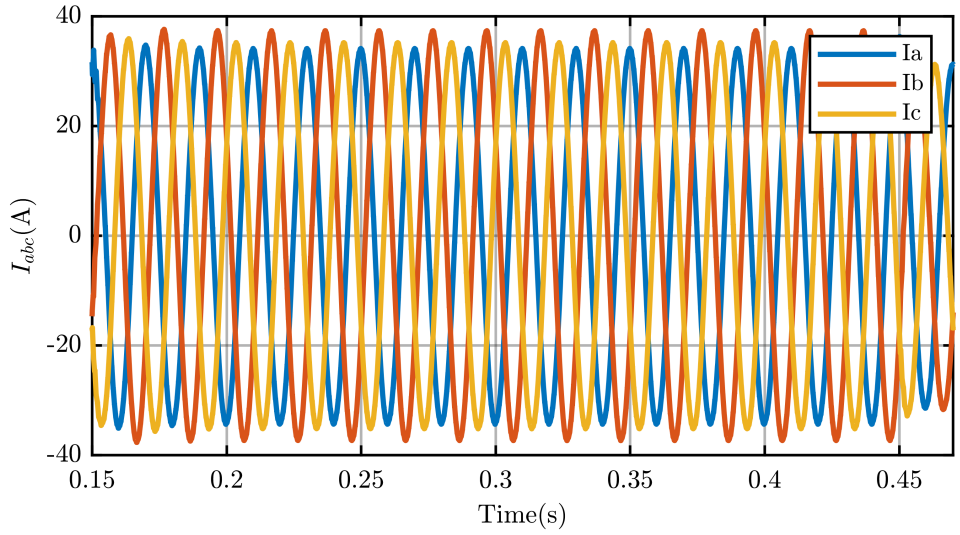

Figure 4.53: Phase currents during fault conditions.

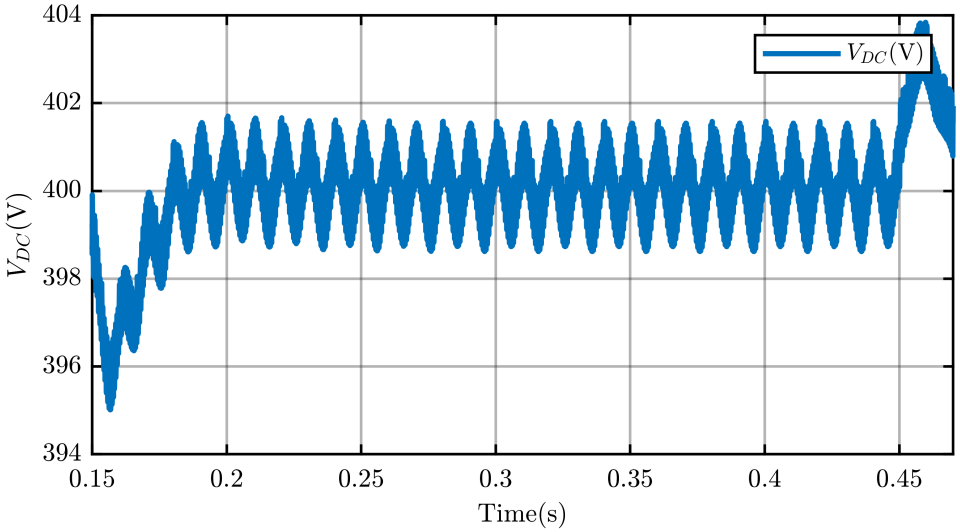

Figure 4.54: DC-link voltage during fault conditions.

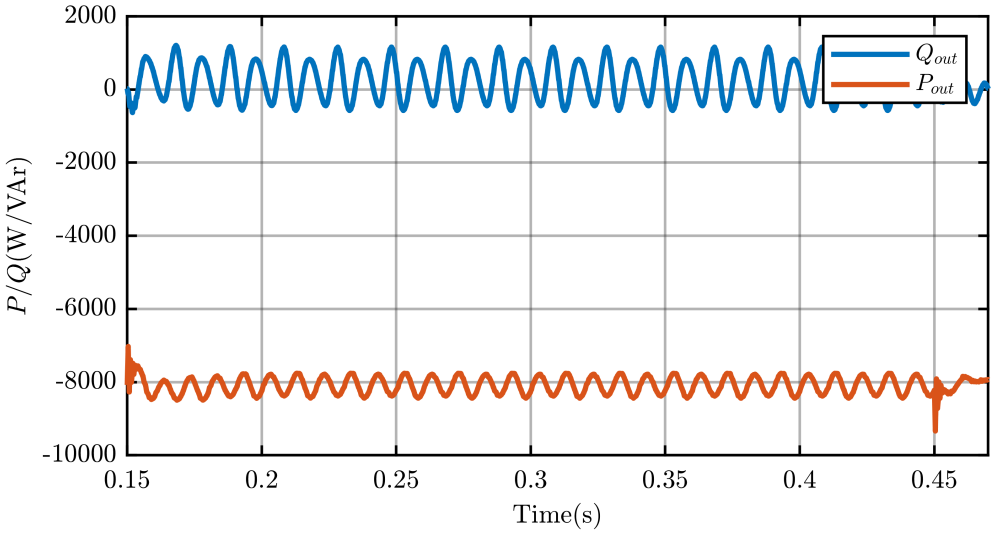

Figure 4.55: Active and reactive power during fault conditions.

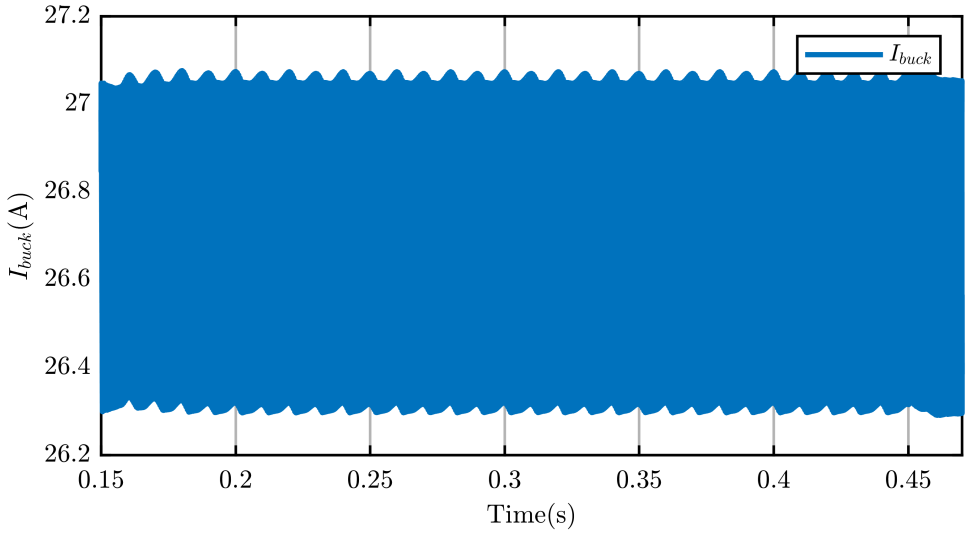

Figure 4.56: Buck current during fault conditions.

The symmetrical result can be obtained, setting the active power reference to zero, cancelling the reactive power ripple. The simulations result absorbing only the reactive power are shown in the following figures.

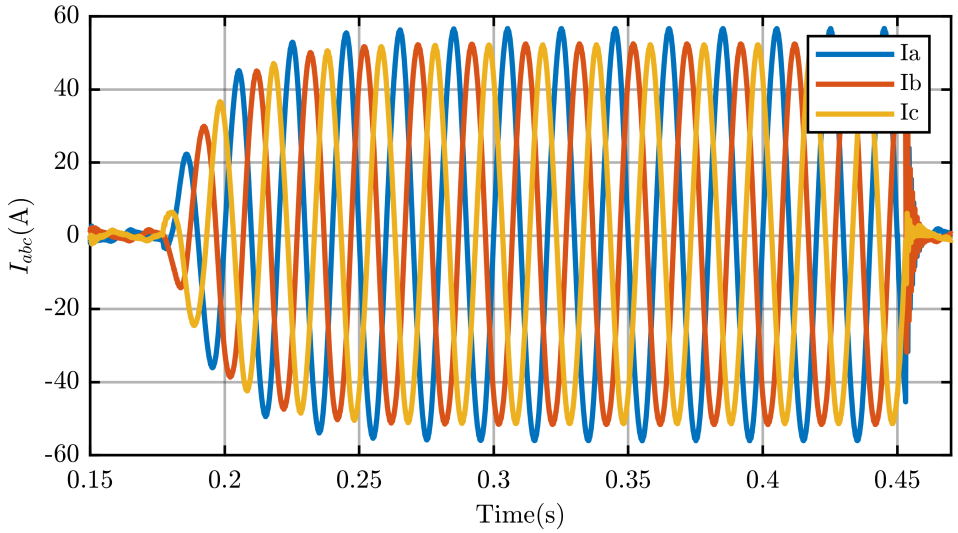

Figure 4.57: Phase currents during fault conditions.

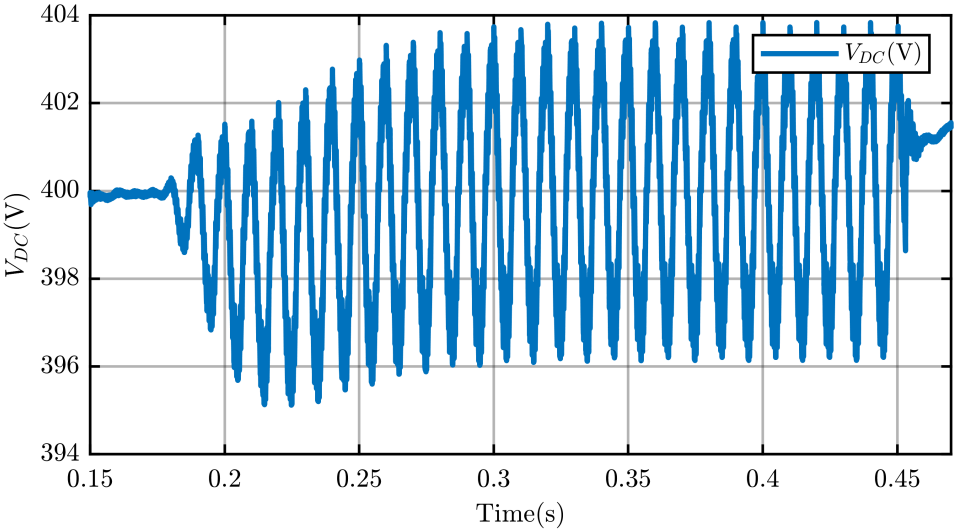

Figure 4.58: DC-link voltage during fault conditions.

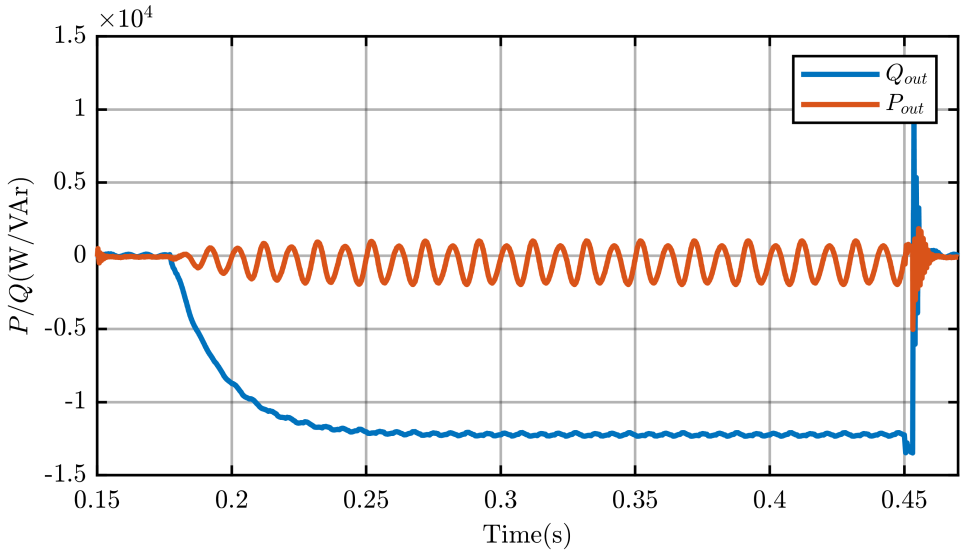

Figure 4.59: Active and reactive power during fault conditions.

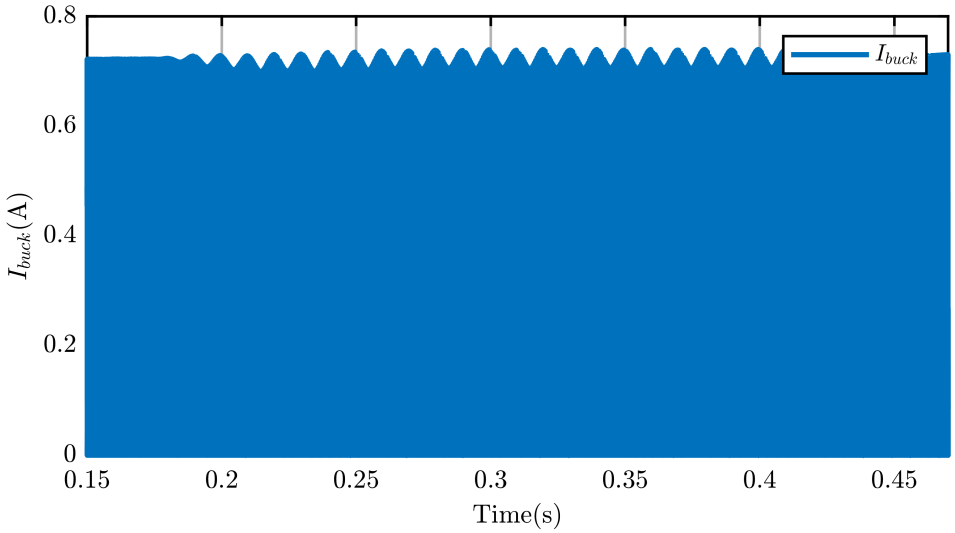

Figure 4.60: Buck current during fault conditions.

The last simulation represents an improper use of the PNSC technique, because it does not exploit the mathematical strategy to cancel the power oscillations, based on setting one of the two power reference to zero, as just seen. The simulation results absorbing either the active power and the reactive one are shown in the following figures.

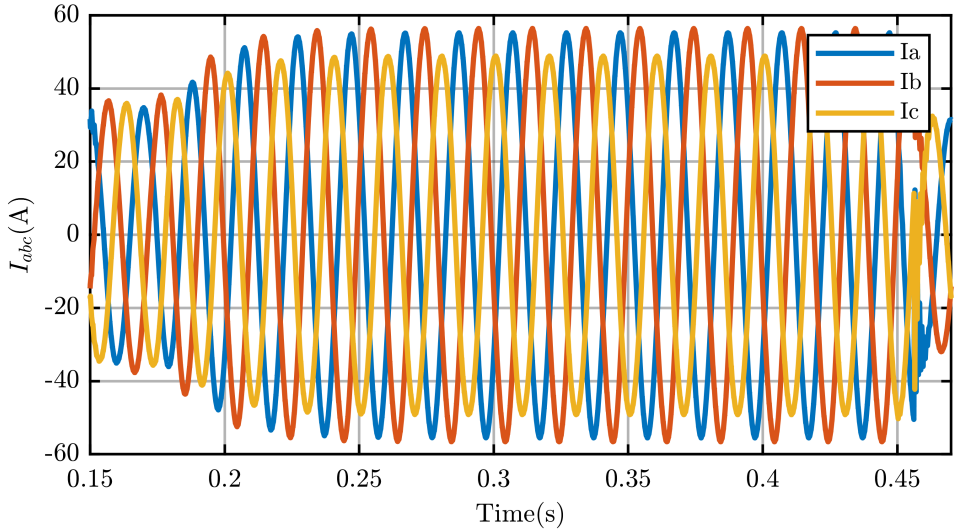

Figure 4.61: Phase currents during fault conditions.

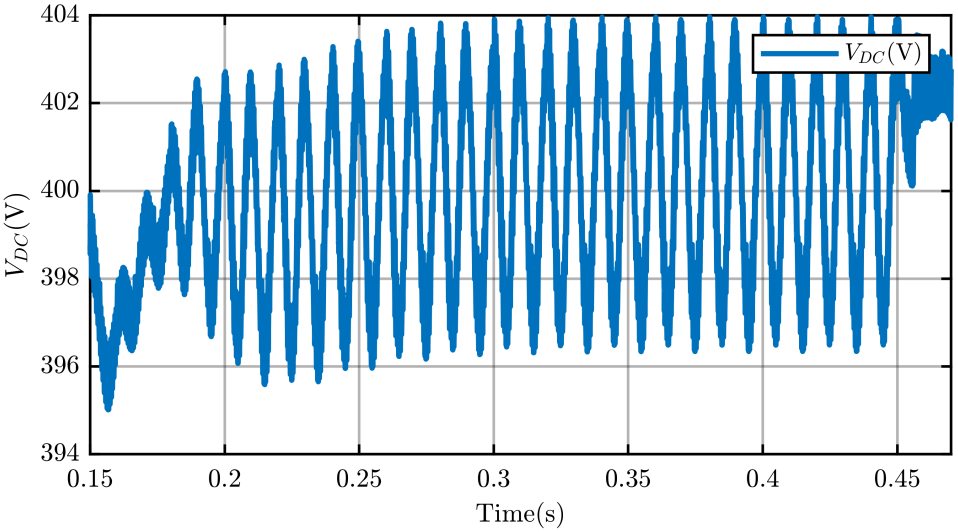

Figure 4.62: DC-link voltage during fault conditions.

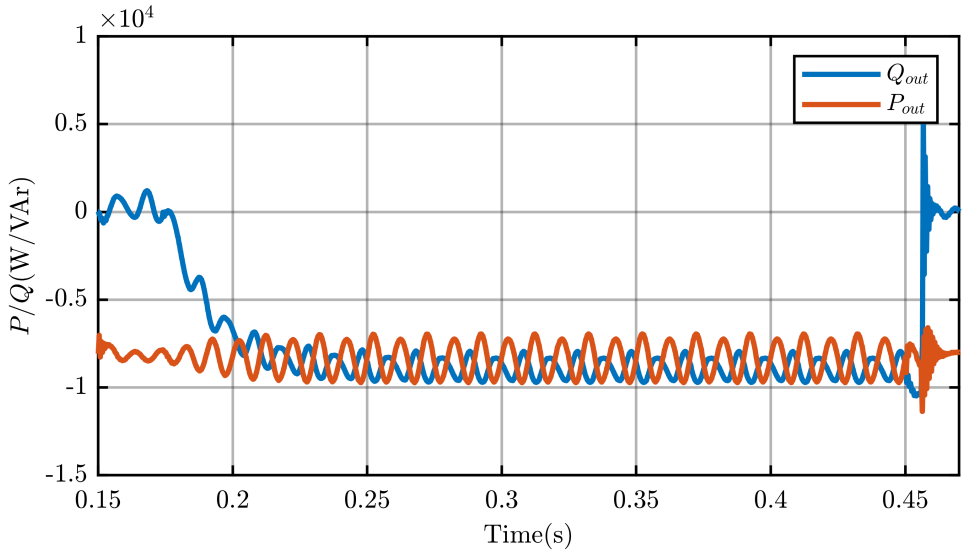

Figure 4.63: Active and reactive power during fault conditions.

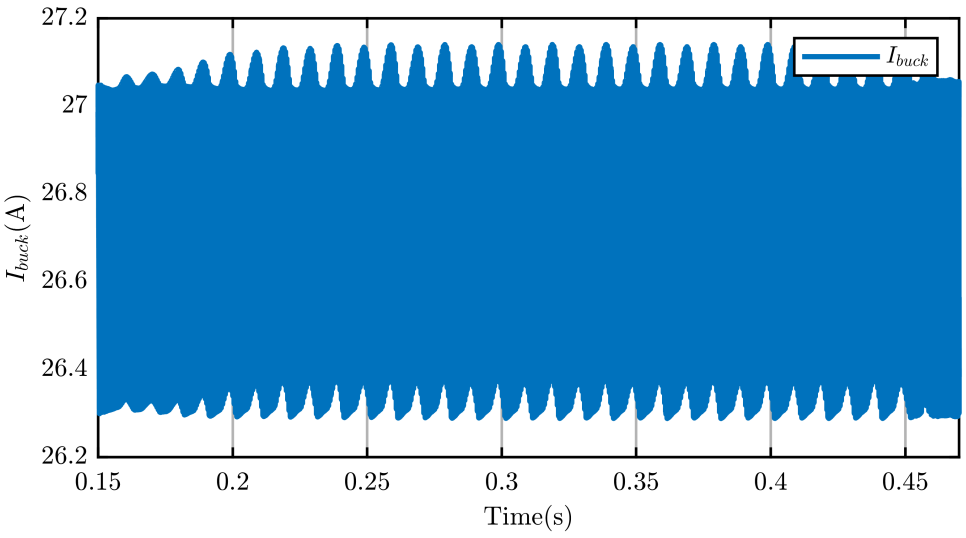

Figure 4.64: Buck current during fault conditions.

4.3.4 Simulation Results for AARC

Starting from absorbing only Active power, we obtain the following results.

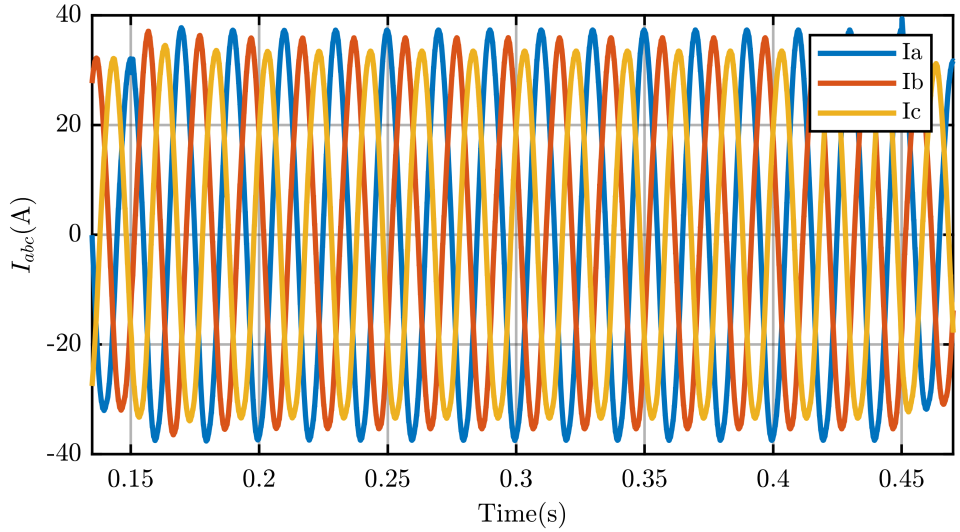

Figure 4.65: Phase currents during fault conditions.

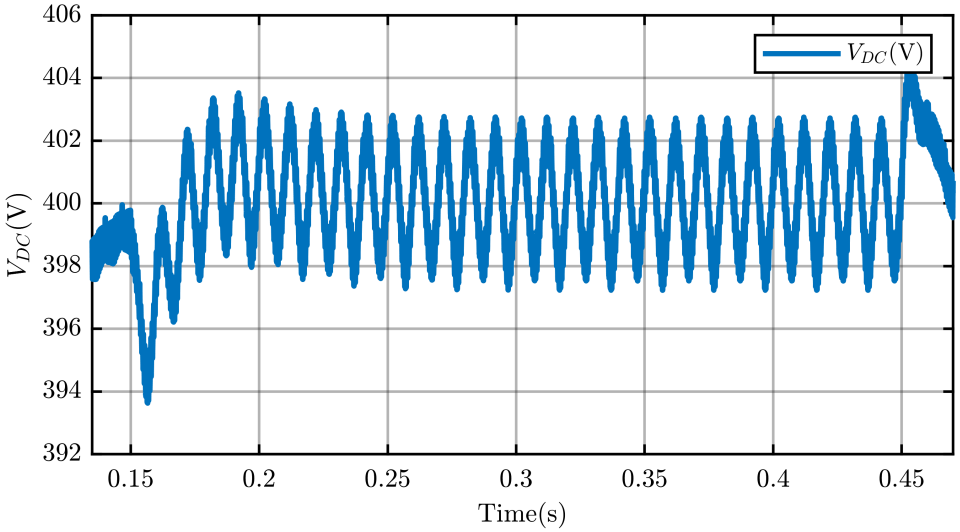

Figure 4.66: DC-link voltage during fault conditions.

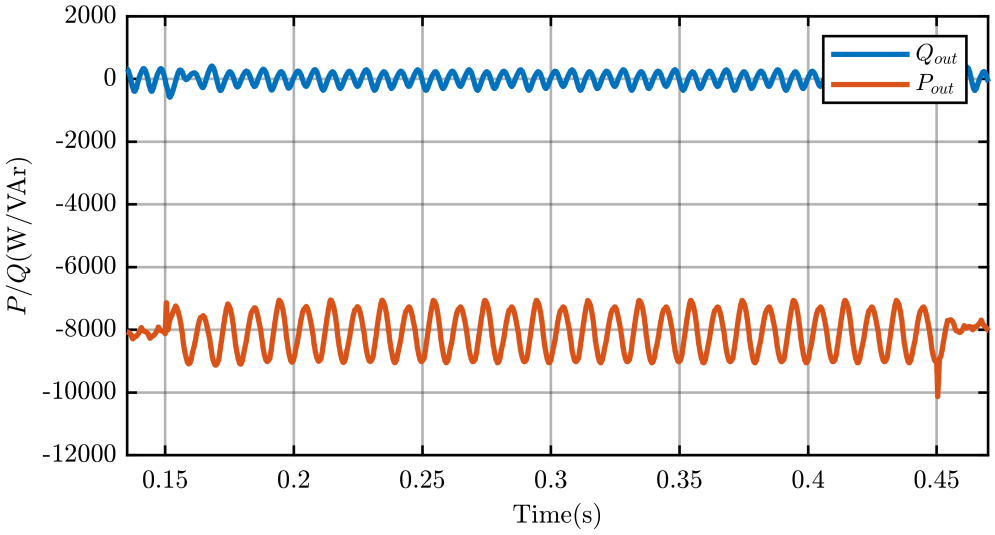

Figure 4.67: Active and reactive power during fault conditions.

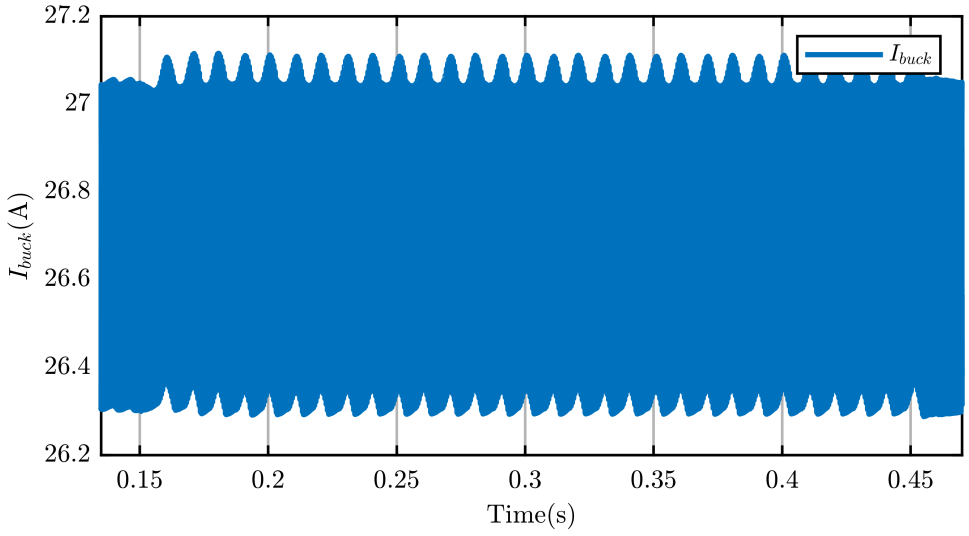

Figure 4.68: Buck current during fault conditions.

As we can see, Q is set to zero, and it keeps constant in time while P performs oscillations. In the following figures, instead, we can see the results of setting the active power reference to zero.

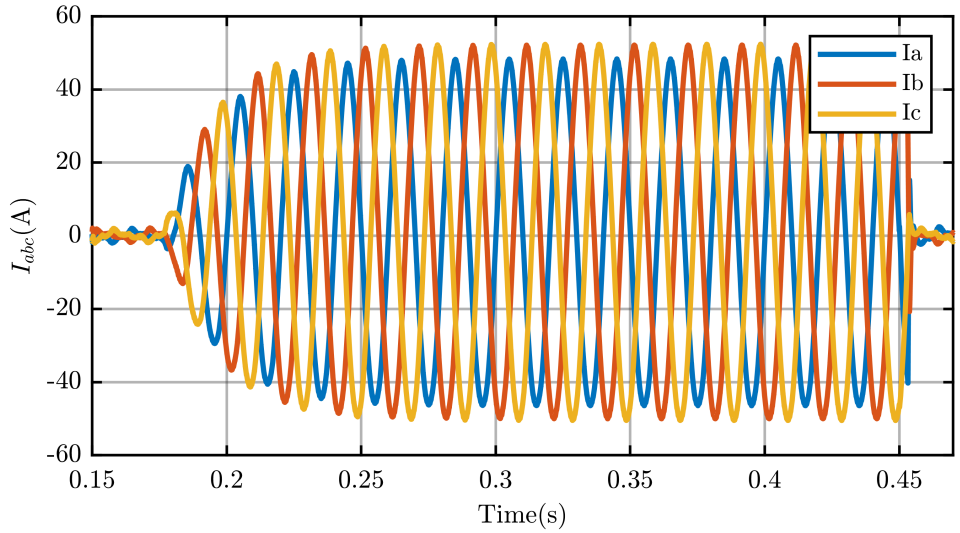

Figure 4.69: Phase currents during fault conditions.

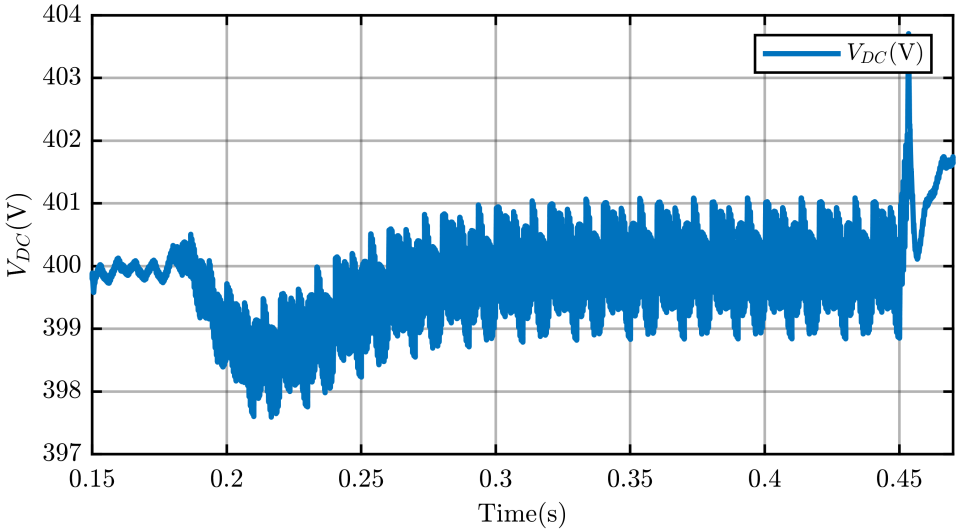

Figure 4.70: DC-link voltage during fault conditions.

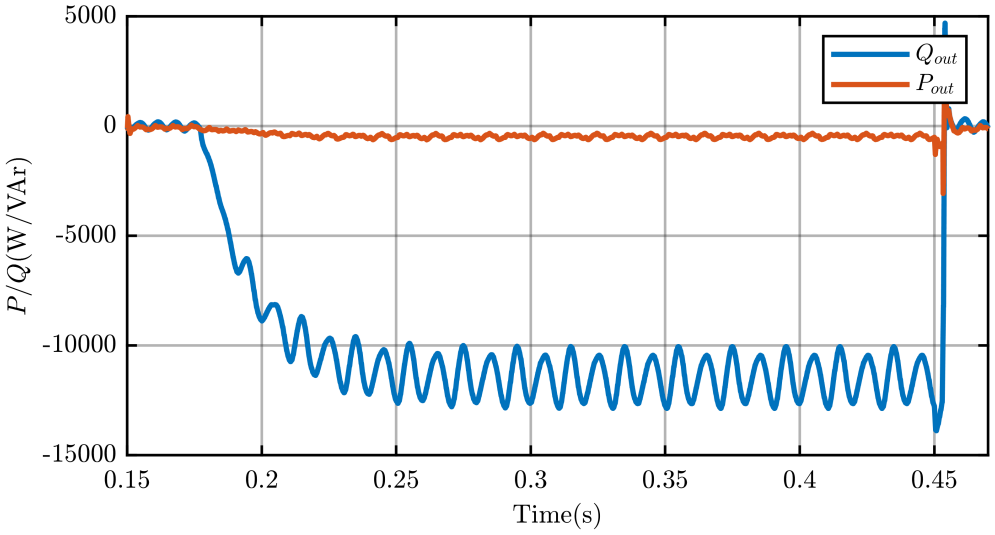

Figure 4.71: Active and reactive power during fault conditions.

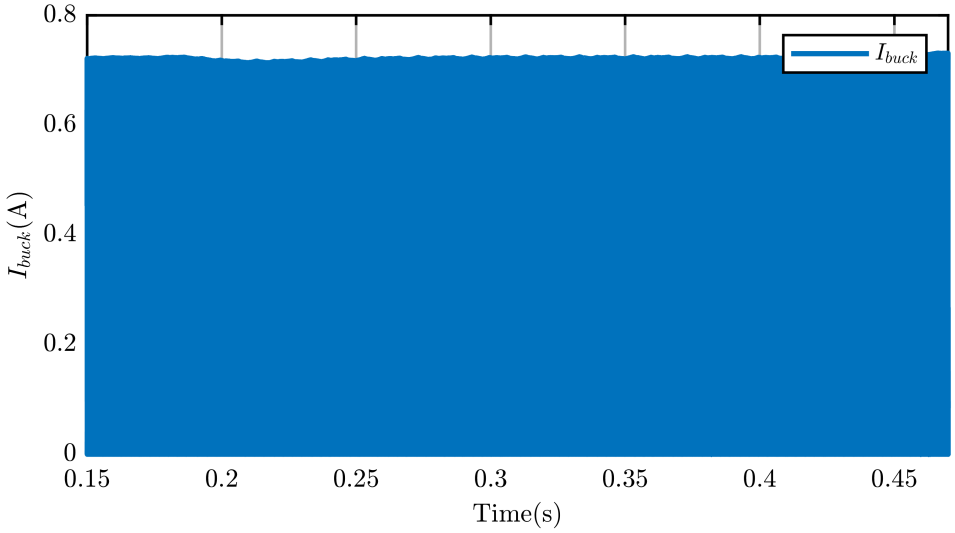

Figure 4.72: Buck current during fault conditions.

In this case, the reactive power is maximized but oscillating in respect to the PNSC, but the active power generation is wasted also if constant in time.

The last simulation represents an improper use of the AARC technique, because it does not exploit the mathematical strategy to cancel the power oscillations, based on setting one of the two power reference to zero, as just seen.

The simulation results in absorbing either the active power and the reactive one are shown in the following figures.

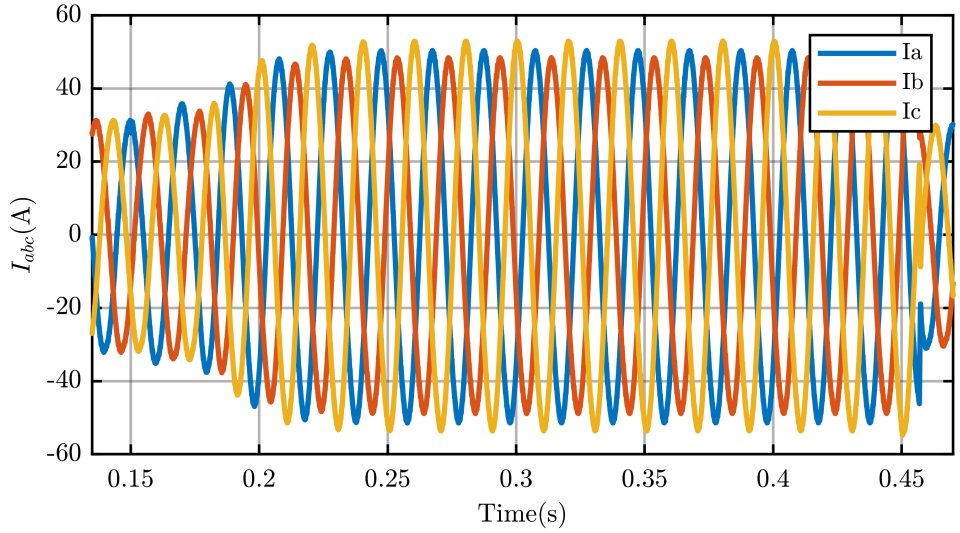

Figure 4.73: Phase currents during fault conditions.

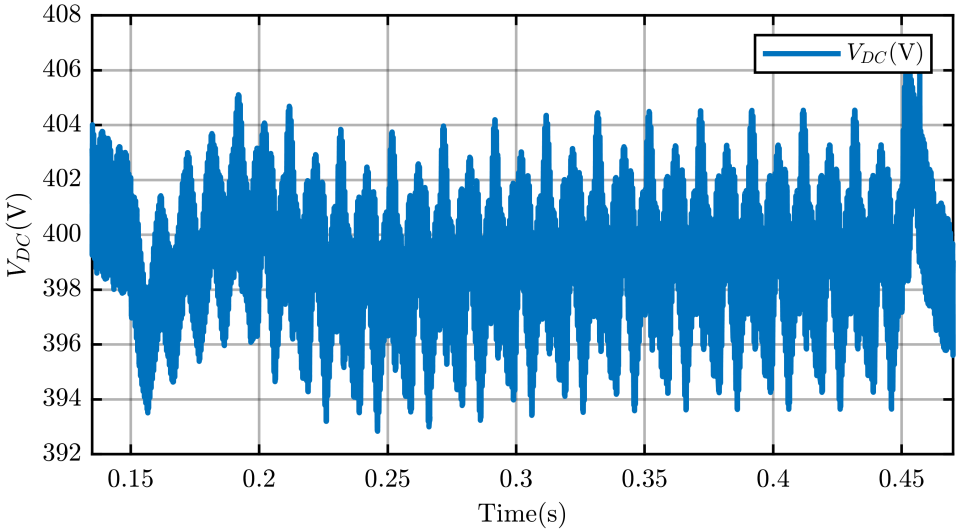

Figure 4.74: DC-link voltage during fault conditions.

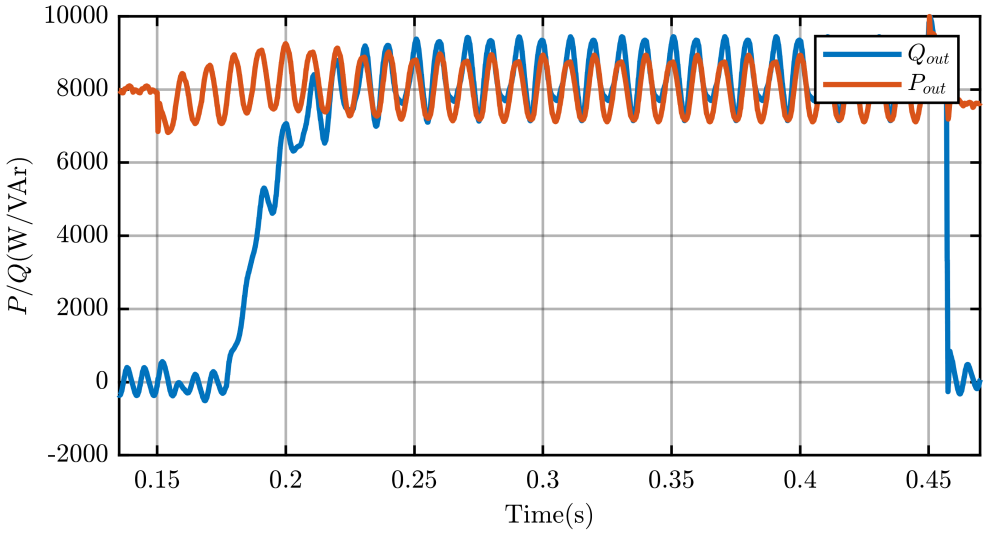

Figure 4.75: Active and reactive power during fault conditions.

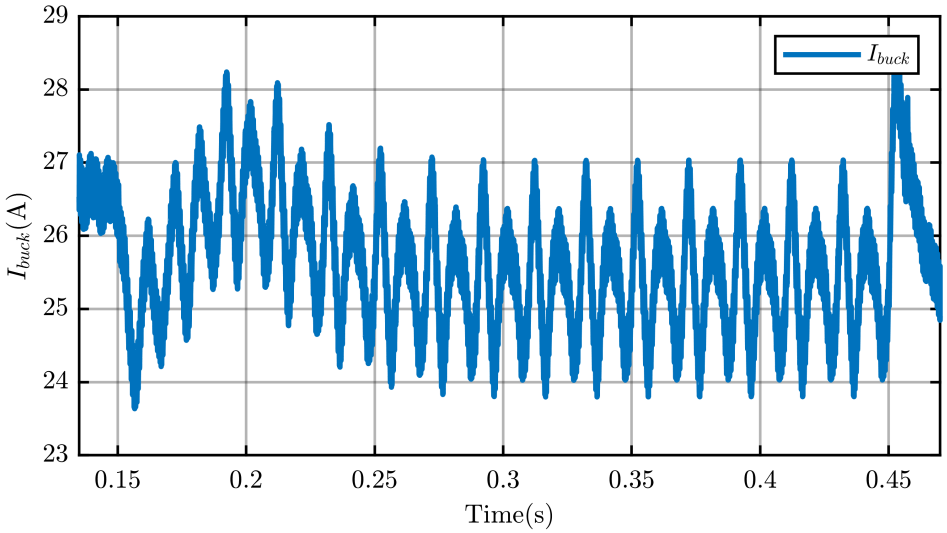

Figure 4.76: Buck current during fault conditions.

As we can see, the oscillations in power reference generate oscillations in Buck currents.

Chapter 5

Experimental Validations

5.1 Test bench

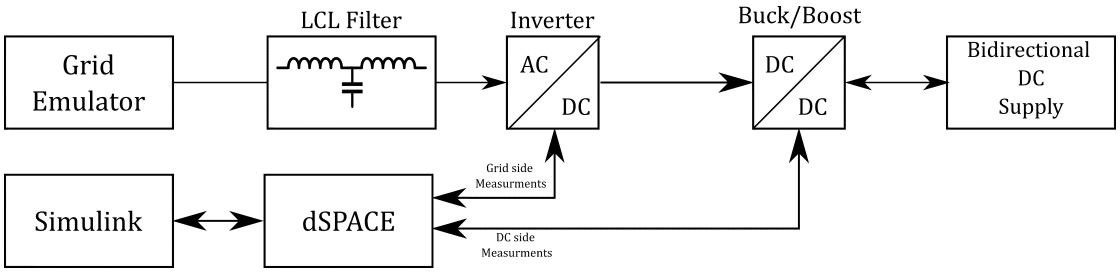

Figure 5.1: Bench test scheme setup.

The analyzed control techniques were validated experimentally. To do that, a test bench was build up at the Power Electronics Innovation Center (PEIC). The test bench consists of a grid simulator (see Fig.5.2a) to emulate the set of grid voltages and the fault, an inverter (Fig.5.2b) which is controlled according to the studied control techniques, and a bidirectional DC supply, acting as load or generator (Fig.5.3a). The control code was implemented in C-code running at 10 kHz on a dSPACE 1005 rapid prototyping system connected to the target inverter (Fig.5.3b).

(a)

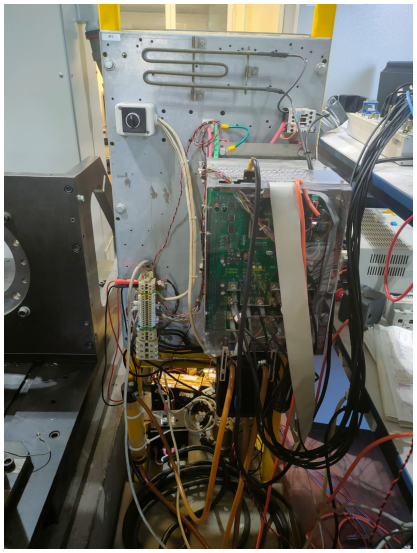

(b)

Figure 5.2: Grid emulator (a) and inverter (b).

(a)

(b)

Figure 5.3: Bidirectional dc supply (a) and dSPACE (b).

The setting parameters are the same used for the software simulations, as reported in Tab.4.6 of sec.4.2, emulating a bi-phase voltage dip, in which phase voltages were equal to $v_a = 1pu$, $v_b = 0.85pu$, $v_c = 0.85pu$.

5.1.1 Experimental Results

As already seen for the simulations, all technique can be divided in tree categories with different consequences on both the DC and AC side:

- Oscillating instantaneous active power.
- Constant instantaneous active power.
- Oscillating reactive power.

In case of Oscillating Instantaneous Active Power, the related problem is different if the AC/DC converter interfaces a generator or a load. In the first case (generator), low frequency power oscillations, at the frequency of 100Hz, directly influence the source current, as shown in the following figures. These oscillations contribute to a larger stress on the dc source. This is for example an issue when interfacing battery storage systems (stress on batteries) or solar production plants, where an oscillating power at the output also means a stress on the maximum power point tracking algorithms of the PV system.

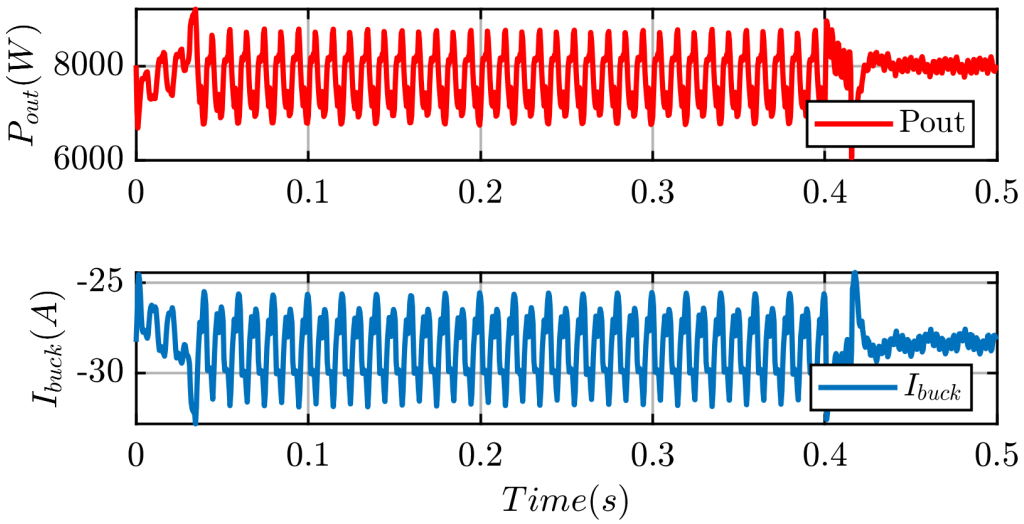

Figure 5.4: BPSC active power output, P_{out} and DC source current I_{buck}.

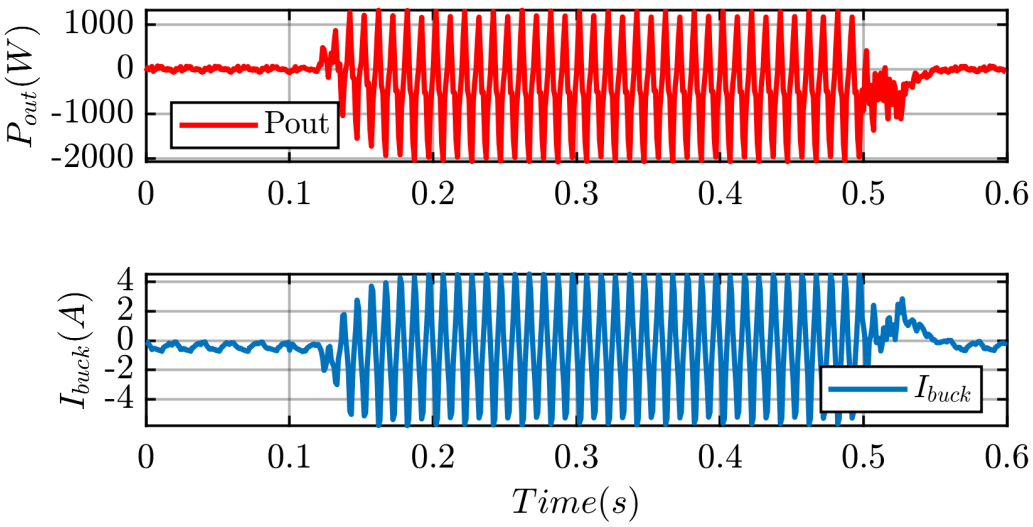

Figure 5.5: PNSC active power output, P_{out} and DC source current I_{buck}.

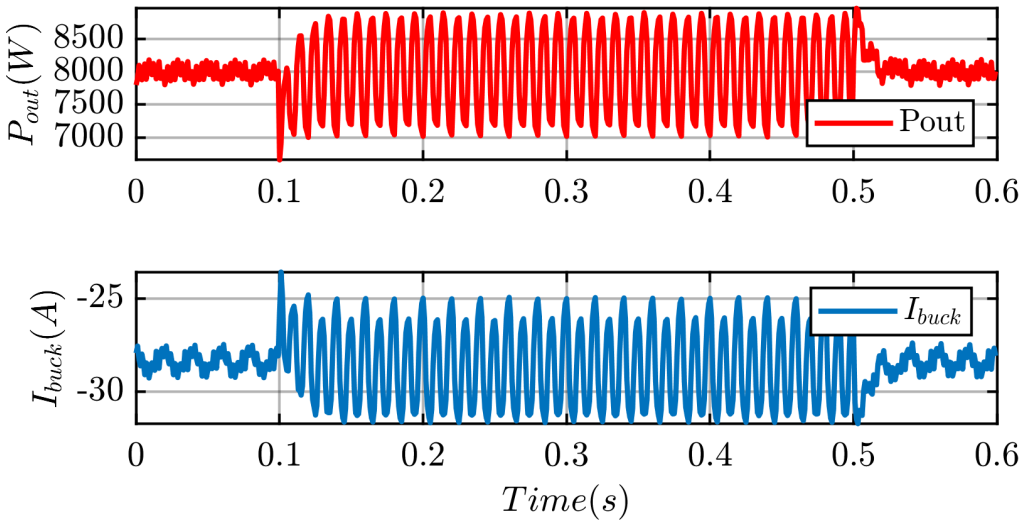

Figure 5.6: AARC active power output, P_{out} and DC source current I_{buck}.

In the second case (load), the power oscillation, influences the quality of the DC-link voltage, that gets worsen, stressing the DC-link capacitor, as shown in the following figures. Moreover, this voltage ripple could not be acceptable for some sensitive loads and applications.

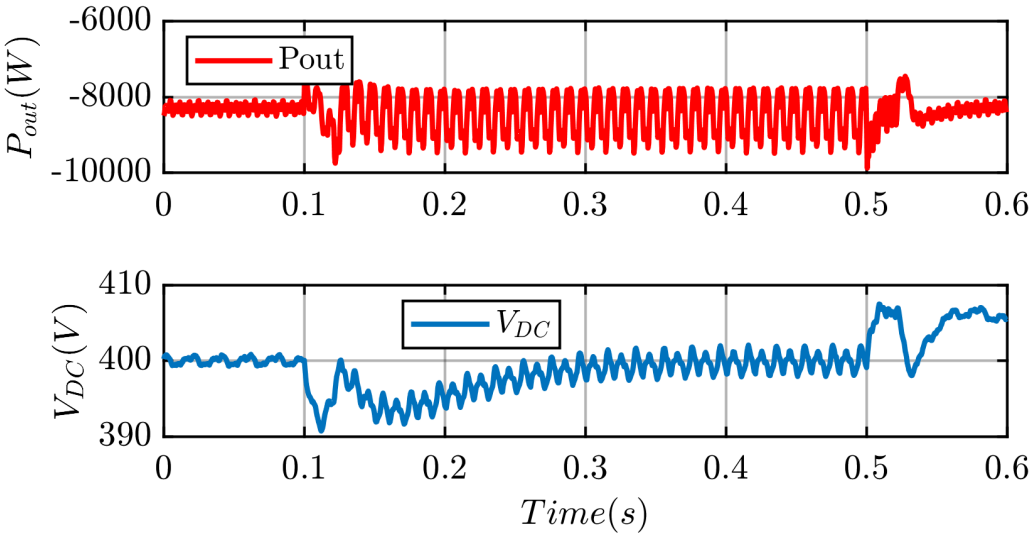

Figure 5.7: BPSC active power output, P_{out} and DC-link voltage V_{DC}.

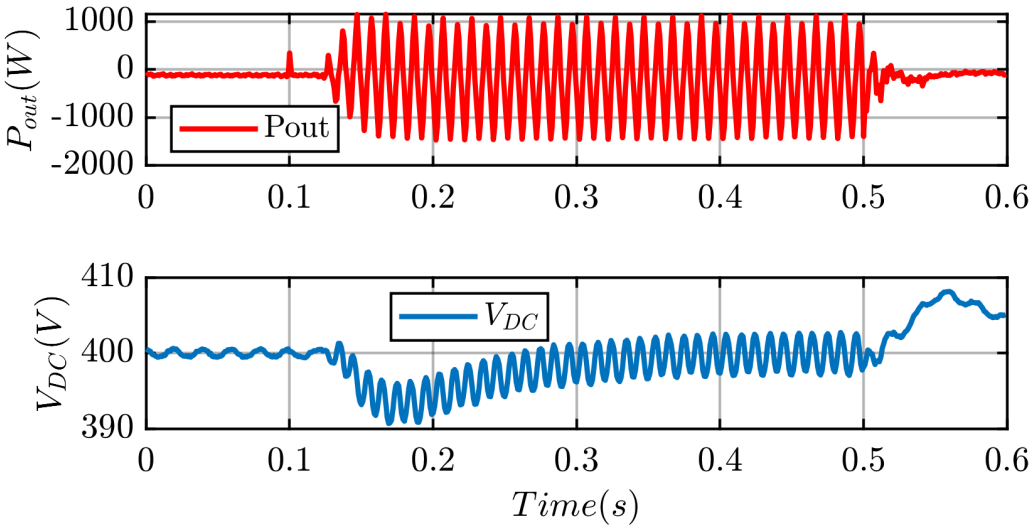

Figure 5.8: PNSC active power output, P_{out} and DC-link voltage V_{DC}.

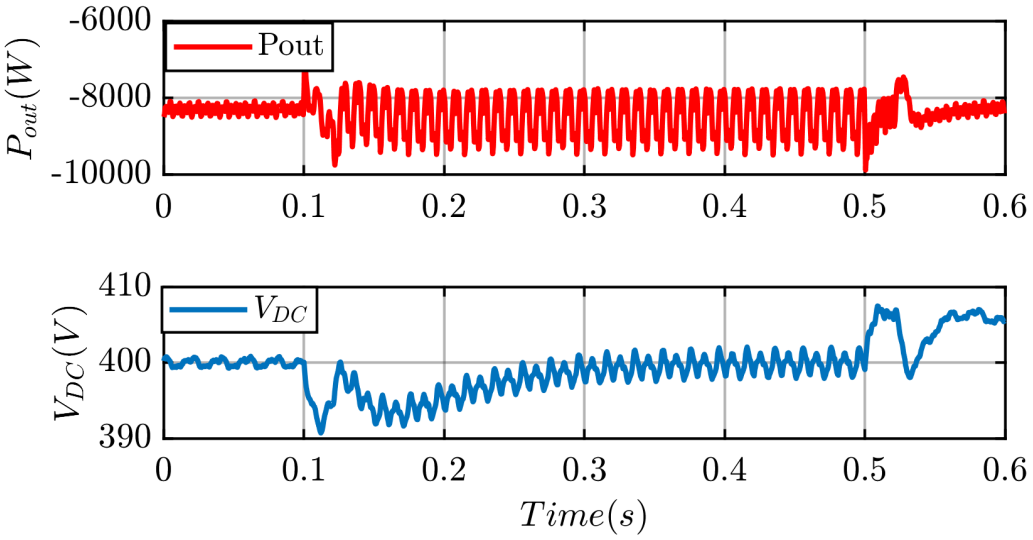

Figure 5.9: AARC active power output, P_{out} and DC-link voltage V_{DC}.

All the techniques also allow performing instantaneous active power too, except for the BPSC. Differently from the previous experimental results, this time the couple of active and reactive power are set in a definite way, which depends on the technique.
The IARC is the only technique which performs constant active and reactive power; this could be particular useful in case the ratio between active and reactive power was defined by grid codes or capability curves [5]. The power performances of the IARC are shown in Fig.5.10.

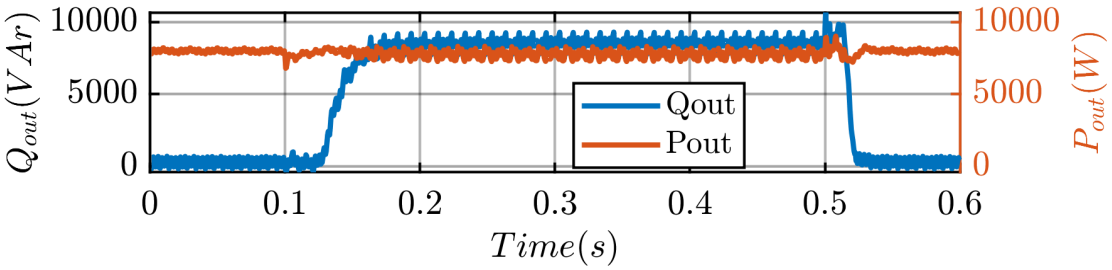

Figure 5.10: Active and reactive power for IARC technique.

Other techniques, PNSC and AARC, are able to perform constant active power too. For the PNSC, this feature can be achieved only by setting the reactive power reference to zero. It is useful in load case for remaining connected to the grid during the fault, but the limit is that a different reactive power reference from zero is not settable.

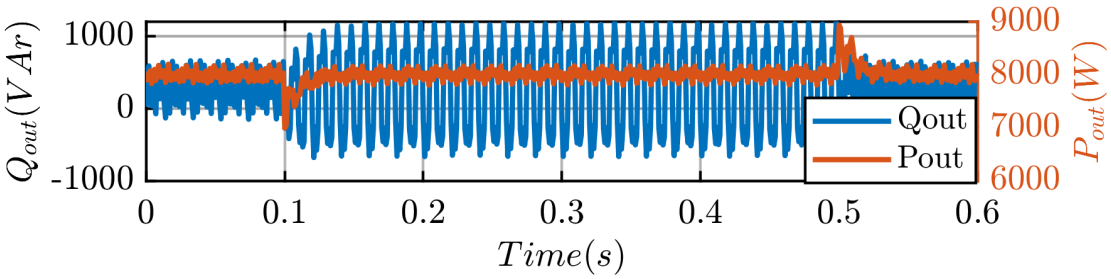

Figure 5.11: Active and reactive power for PNSC technique.

For the AARC the only way to keep constant the active power is setting the active power reference to zero. Doing that, the reactive power will be oscillating. For what just said, there are no particular applications for the AARC set this way and for this reason not reported.
For all the techniques, the control is based on injection of a certain amount of positive and negative sequence, so it could be interesting to see the evolution of the sequence injected to the fault, as shown in the following figures.

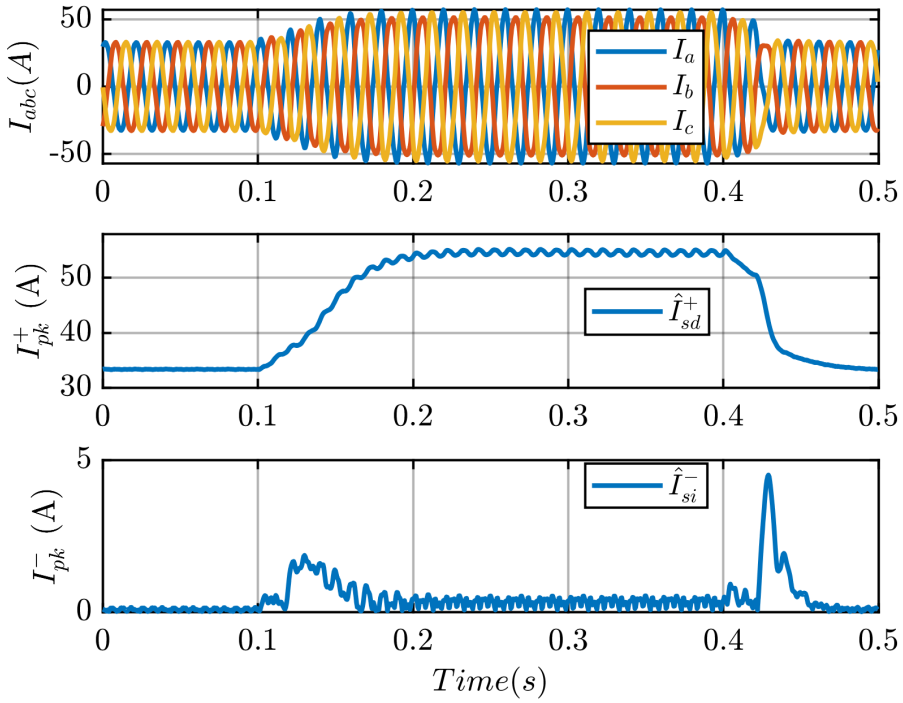

Figure 5.12: Grid side currents injected with IARC control technique and amplitude of positive and negative sequence injected.

The currents injected by the IARC control are shown in Fig.5.12. it is important to notice how the direct sequence amplitude is influence by a high frequency distortion.

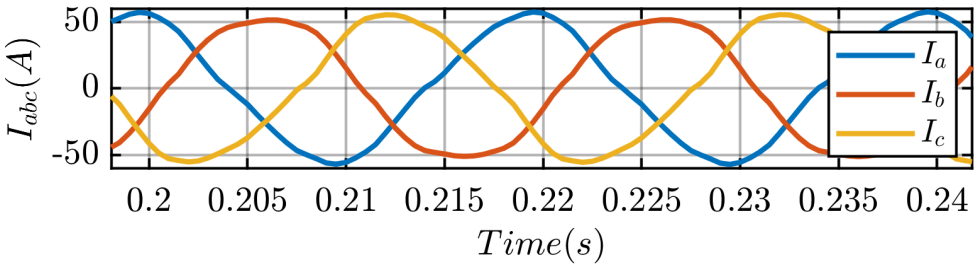

Figure 5.13: Grid side currents injected with IARC control technique.

Fig.5.13 shows how the amplitude distortion clearly influence the THD of the grid currents, that perform the influence of higher harmonics.

All the other techniques, differently from the IARC, future the influence of the negative sequence as Fig.5.14 shows. Also if the performance in the output powers is different for the PNSC and the AARC control technique, the influence of the negative sequence in the grid current is the same.

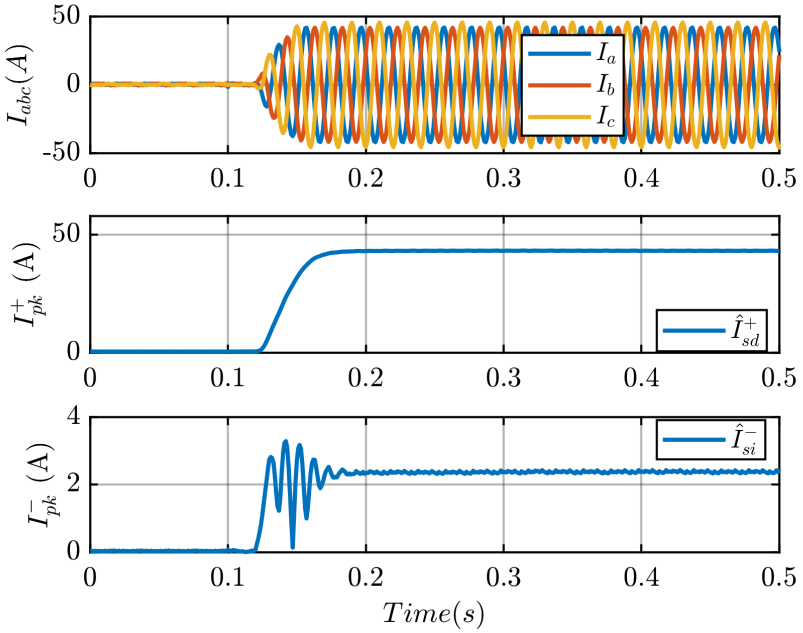

Figure 5.14: Grid side currents injected with PNSC and AARC control technique and amplitude of positive and negative sequence injected.

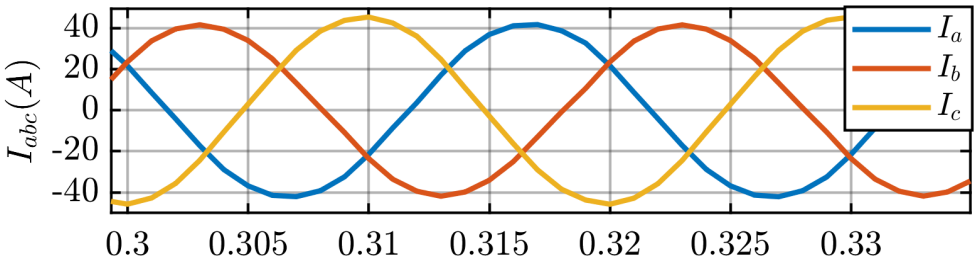

Figure 5.15: Grid side currents injected with PNSC and AARC control technique.

The figure below (Fig.5.15) is shown how the negative sequence influences the grid currents.

If the scope is to improve the THD during the fault, ignoring the performances of the output powers, that will be oscillating, the best technique is the BPSC, as shown in Fig.5.17 and Fig.5.16, because the grid side currents are sinusoidal and balanced.

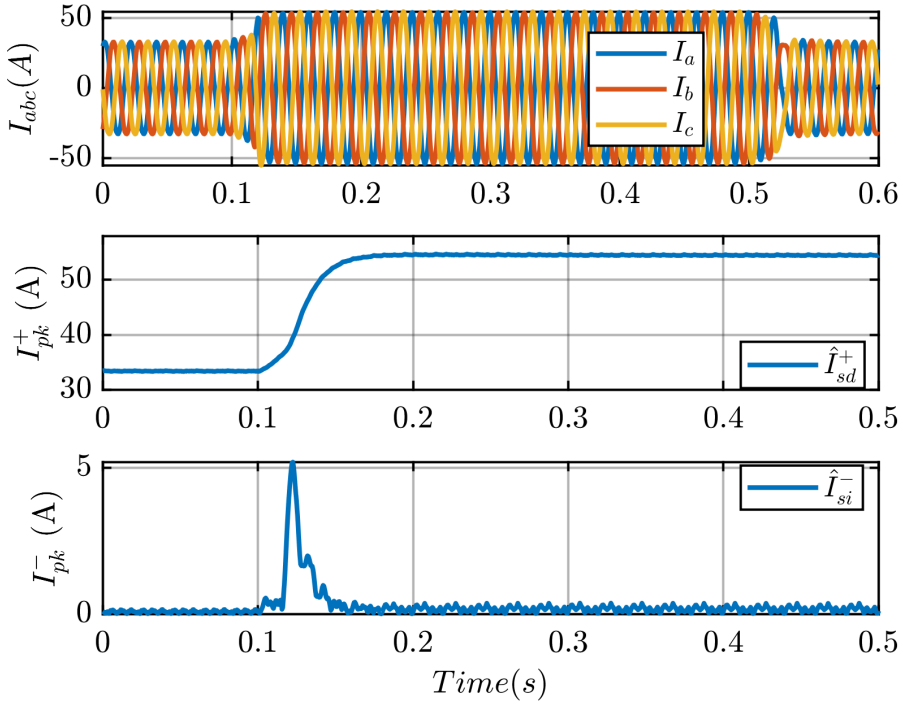

Figure 5.16: Grid side currents injected with BPSC control technique and amplitude of positive and negative sequence injected.

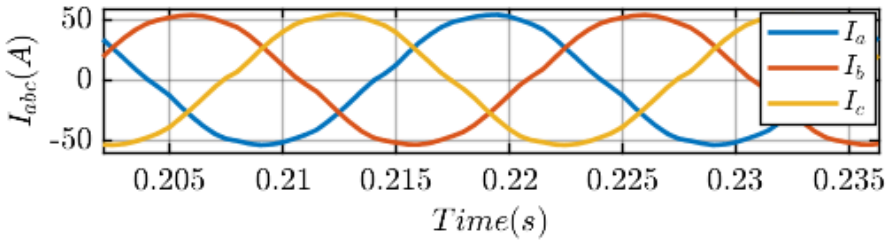

Figure 5.17: Grid side currents injected with BPSC control technique.

For the FPNSC, the difference is that the amount of positive and negative sequence can be controlled, setting k_1 and k_2. In the experimental validation, the FPNSC was controlled to generate constant active power with the scope to improve the source current in case the grid was connected to a generator or the DC-link voltage quality in case of a grid connected to a load. To do that, the amount of direct and inverse sequence current is the same, either for case generator and load, as shown in Fig.5.18.

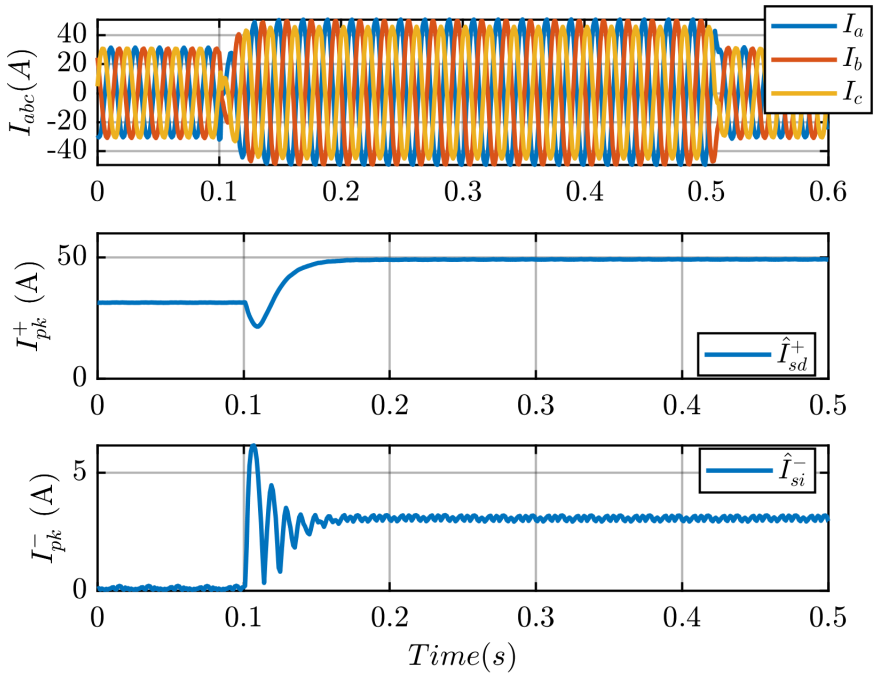

Figure 5.18: Grid side currents injected with FPNSC control technique and amplitude of positive and negative sequence injected.

Also in this case, the grid currents are influenced by the negative sequence, as

in Fig.5.15.

In terms of powers, the result in case generator and load are the following.

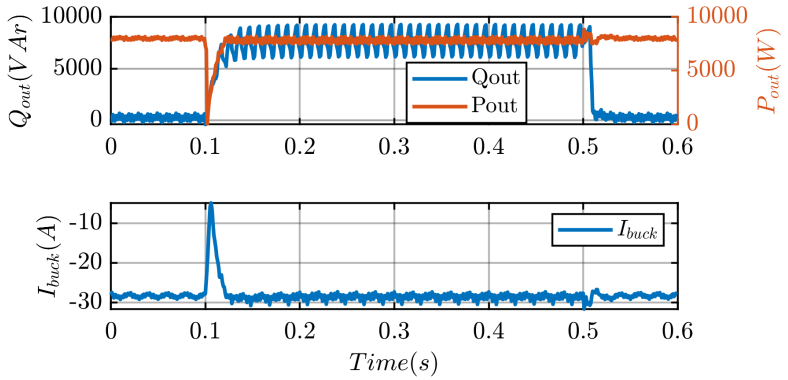

Figure 5.19: FPNSC active power output, P_{out} and DC source current I_{buck}. Case for k_1 and k_2 set to generate constant active power and oscillating reactive power.

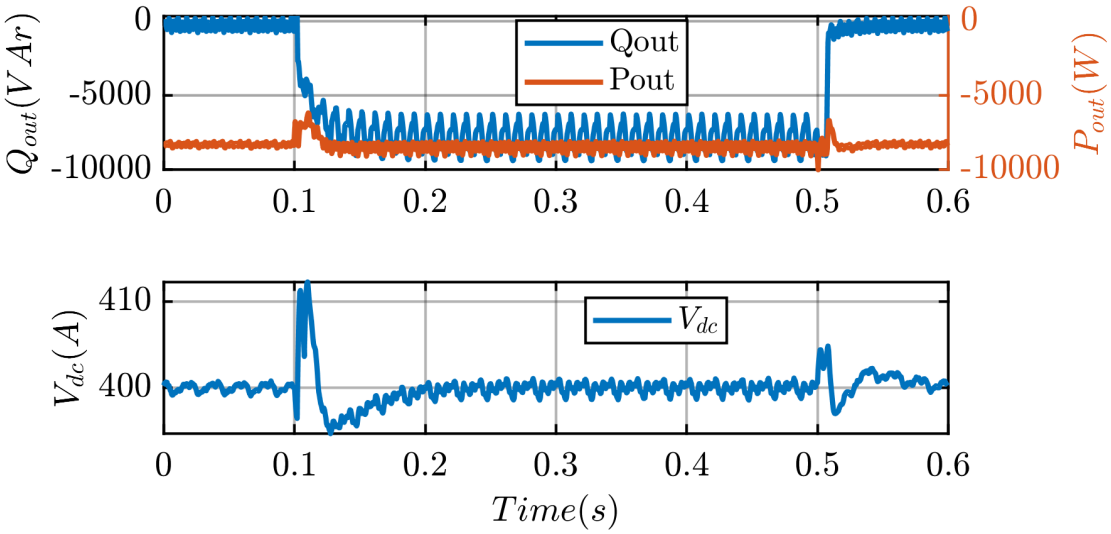

Figure 5.20: FPNSC active power output, P_{out} and DC-link voltage V_{DC}. Case for k_1 and k_2 set to generate constant active power and oscillating reactive power.

The previous figures, Fig.5.19 and Fig.5.20, show the performances of the FPNSC in case that k_1 and k_2 were set to impose constant instantaneous active power, generating oscillating reactive power. These features could be useful in case generator and load because it is possible to improve the source current, I_{buck} and the DC-link voltage quality, V_{dc}.

5.2 Conclusions

Controlling AC/DC converter interfaces load and generator to the grid is important to guarantee the reliability of the grid and the continuity of the service also improving the performance in the DC-side of the converter, such as oscillations in DC-link voltage and source current. Five control techniques has been studied and experimentally tested (IARC, BPSC, PNSC, AARC, FPNSC). The conclusion was that the right techniques to use depends on the goals, as reported in the table below.

	Settings		Current Sequence?		Goal		
	Q	P	+	−	Constant Active Power	Disadvantages	Advantages
IARC	$Q^*>0$	$P^*>0$	Y	N	Y	Harmonics in phase currents	Constant Powers P,Q
BPSC	$Q^*>0$	$P^*>0$	Y	N	N	Power oscillations	Balanced Sinusoidal Currents
PNSC	$Q^*=0$	$P^*>0$	Y	Y	Y	No Reactive injection	Constant Active Power
AARC	$Q^*>0$	$P^*=0$	Y	Y	Y	Null Active Power	No DC-side oscillations

Each technique performs advantages and disadvantages. In general, if the goal is to improve DC-side current and voltage DC-link, techniques whose perform constant active power are the best. If the goal is the THD minimization, the best techniques are the ones which inject a set of balanced sinusoidal currents (e.g. BPSC). If the grid codes impose to inject a certain amount of reactive power during a fault, the best technique is the IARC.The personal contributions to this work are summarized as:

- Research and analysis of the control techniques.
- Development of four current limitation algorithms.
- PLECS simulations and validation.
- Preparation of the test bench and experimental validation.

Future improvements could be the developing of a control algorithm that is able to select the best control techniques in base of the goals automatically and not ex ante.

Bibliography

[1] Dongliang Xie, Zhao Xu, Lihui Yang, Jacob Ostergaard, Yusheng Xue, and Kit Po Wong. «A Comprehensive LVRT Control Strategy for DFIG Wind Turbines With Enhanced Reactive Power Support». eng. In: *IEEE transactions on power systems* 28.3 (2013), pp. 3302–3310. ISSN: 0885-8950 (cit. on p. 2).

[2] Mohamed Elgenedy, A. Moussa, and Emad Negm. «Simulating Three Phase Induction Motor Performance During Different Voltage Sag Types». In: Dec. 2012 (cit. on p. 2).

[3] Remus Teodorescu, Marco Liserre, and Pedro Rodríguez. *Grid Converters for Photovoltaic and Wind Power Systems*. en. 1st ed. Wiley, Jan. 2011. ISBN: 978-0-470-05751-3 978-0-470-66705-7. DOI: 10.1002/9780470667057. URL: https://onlinelibrary.wiley.com/doi/book/10.1002/9780470667057 (visited on 03/15/2022) (cit. on pp. 2, 3, 8, 11, 23, 30, 32).

[4] Martin J. Heathcote. «Appendix 5 - Symmetrical components in unbalanced three-phase systems». eng. In: *J P Transformer Book*. Thirteenth Edition. Elsevier Ltd, 2007, pp. 848–870. ISBN: 9780750681643 (cit. on p. 8).

[5] Kamran Zeb, Saif Ul Islam, Imran Khan, Waqar Uddin, M. Ishfaq, Tiago Davi Curi Busarello, S.M. Muyeen, Iftikhar Ahmad, and H.J. Kim. «Faults and Fault Ride Through strategies for grid-connected photovoltaic system: A comprehensive review». en. In: *Renewable and Sustainable Energy Reviews* 158 (Apr. 2022), p. 112125. ISSN: 13640321. DOI: 10.1016/j.rser.2022.112125. URL: https://linkinghub.elsevier.com/retrieve/pii/S1364032122000533 (visited on 03/15/2022) (cit. on p. 80).